

7 AOF SRR 2013

The 7th Asia Oceania Forum for Synchrotron Radiation Research



September 21st-24th, 2013
Egret Himeji, Hyogo, JAPAN

Program and Abstracts Book

AOF
Synchrotron Radiation

AOFSRR 2013

The 7th Asia Oceania Forum for Synchrotron Radiation Research

September 21st-24th, 2013

Program and Abstracts Book

CONTENTS

Welcome Messages	ii
Committees	iv
Venue Floor Plan	vi
Program Timetable	viii
Program	xii
List of Posters	xvii
Abstracts - Oral Presentation -	1
Abstracts - Poster Presentation -	33
Exhibitors/Exhibit & Poster Floor Plan	119
Information	125

WELCOME MESSAGES

Message from the President of AOFSSRR



On behalf of the Asia-Oceania Forum for Synchrotron Radiation Research (AOFSSRR), I am very pleased to welcome you all to Himeji for the 7th AOFSSRR Workshop.

As you know well, the AOFSSRR was founded in 2006 in order to establish a general collaboration framework for the development of synchrotron radiation science and technology, to promote comprehensive cooperation, and to provide education and communication opportunities, which mutually benefits advancing research goals of all the parties in the Asia-Oceania region. To fulfill these missions, the AOFSSRR has annually been held since 2006 in Japan and then followed by the 2nd, 3rd, 4th, 5th and 6th one in Taiwan, Australia, China, Korea, and Thailand, respectively. This year, AOFSSRR return to the birth place, Japan. In addition, this year's Cheiron summer school, which is the 7th since 2007, will be held at SPring-8 in coming September (Sept. 24th to Oct. 3rd, <http://cheiron2013.spring8.or.jp/>). There will be around 25 lectures for the junior scientists that cover almost all about synchrotron light sources and sciences.

The 7th AOFSSRR Workshop held in Himeji will provide you all a good opportunity to meet old and new friends, as well as to discuss current activities and future on synchrotron light sources and sciences. Now it is the time for the entire synchrotron science community to synergistically address many challenges in advancing synchrotron sciences (including facilities) and key roles in science and technology in the 21st century. I hope that all participants enjoy this workshop and get great benefits from the exchange of knowledge, ideas and recent research developments. In addition, I believe that you will have really a good time enjoying the national treasures of modern and traditional cultural heritages of Japan especially those of HIMEJI.

Finally I deeply thank all the speakers and participants for their presentations and contributions to this workshop. Also I would like to thank very much the Japanese Society for Synchrotron Radiation Research (JSSRR), RIKEN, JASRI, KEK, SACLA, SPring-8 and staff members for hosting this special event and their endeavors and supports. The appreciation is also extended to organizing, program and local committee members of this workshop for their great efforts.

Finally, once more, welcome you all to the Himeji 7th AOFSSRR workshop.

Hongjie XU

President, Asia-Oceania Forum for Synchrotron Radiation Research

Message from the Organizing Chairman of AOFSSR2013

On behalf of the eight Synchrotron Radiation facilities in Japan, it is my distinct pleasure to welcome you to the 2013 workshop of the AOFSSR (Asia - Oceania Forum for Synchrotron Radiation Research). Thankfully, we are happy to be able to hold the workshop in Japan this year despite the devastating Tohoku earthquake that struck two years ago. We would like to again express our sincere appreciation of the kindness and warm support of our friends in the AOFSSR countries.



The objective of the AOFSSR is to promote comprehensive cooperation for the development of science and technology in the Asia Oceania region. As you know, the AOFSSR has developed a program with advanced Synchrotron Radiation technical experts and scientists to nurture the continued development of Synchrotron Radiation Research in the Asia Oceania region by a systematic sharing of Cheiron School activities among all the region's Synchrotron Radiation facilities, with the core Cheiron School based at SPring-8. I am very happy that this year the AOFSSR meeting will be immediately followed by the Cheiron School. As a consequence, all the young participants of the Cheiron School are also able to attend the AOFSSR, present their current activities, and discuss them with distinguished scientists from the Asia Oceania region. I am convinced that such an experience will have a big influence on their research activities in the future.

I strongly believe that this workshop will once again provide an opportunity for fruitful communication advancing the research goals of all parties. I look forward to seeing you all during September 21 - 24, 2013, in Himeji, a city which showcases the beautiful historical heritage of Japan.

Jun'ichiro Mizuki
Chairman, the AOFSSR2013 Organizing Committee &
President, The Japanese Society for Synchrotron Radiation Research

Asia Oseania Forum

Council Members

President: Hongjie Xu (China)

Members: Jun'ichiro Mizuki (Japan)
Mark Breese (Singapore)
Andrew Peele (Australia)
Shih-Lin Chang (Taiwan)
Moohyun Cho (Korea)
Sarawut Sujitjorn (Thailand)
P.D. Gupta (India)
Moonhor Ree (Korea)

Secretary-General :

Masaki Takata (Japan)

Secretary-Treasurer :

Richard Garrett (Australia)

Associate Members

Don Smith (New Zealand)
Swee Ping Chia (Malaysia)
Tran Duc Thiep (Vietnam)

Special Advisors to the President

Osamu Shimomura (Japan)
Herbert Moser (Germany)
Sunil K. Sinha (USA)
Keng Liang (Taiwan)
Prayoon Songsiriritthigul (Thailand)

Organizing Committee

Chair: Jun'ichiro Mizuki (JSSRR / KG Univ., Japan)

Members: Hongjie Xu (China)
Mark Breese (Singapore)
Andrew Peele (Australia)
Shih-Lin Chang (Taiwan)
Moo-hyun Cho (Korea)
Sarawut Sujitjorn (Thailand)
P.D.Gupta (India)
Masaki Takata (Riken / JASRI, Japan)

Program Committee

Chair: Jun'ichiro Mizuki (JSSRR / KG Univ., Japan)

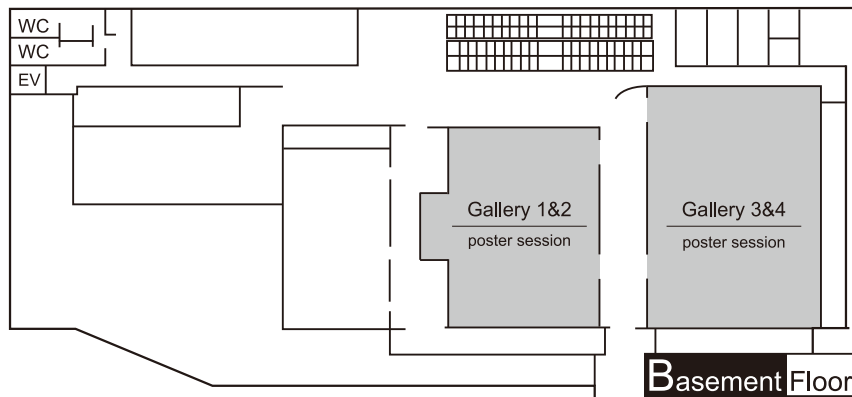
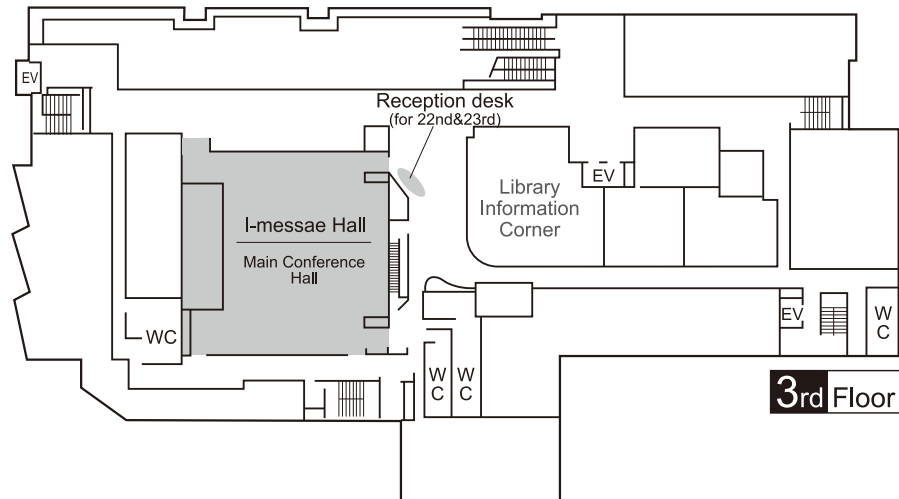
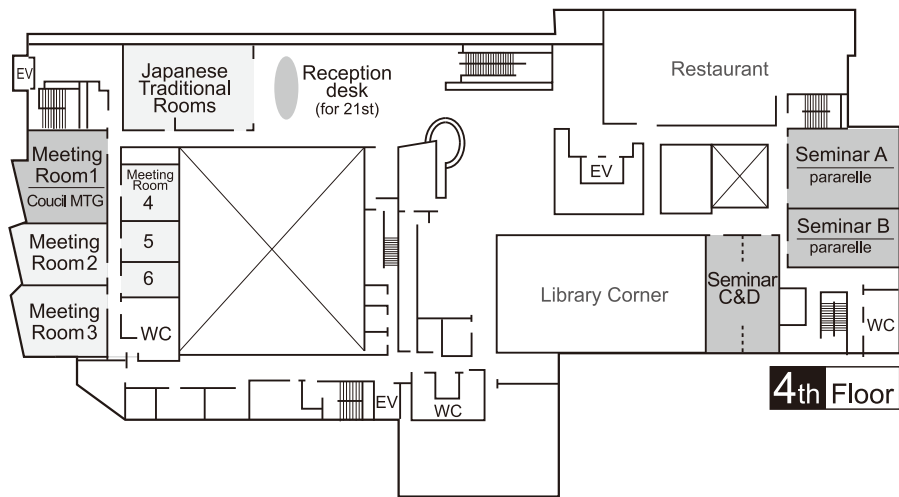
Members: Masaki Takata (Riken / JASRI, Japan)
Eiichiro Matsubara (JSSRR / Kyoto Univ., Japan)
Youichi Murakami (PF / KEK, Japan)
Masahiro Katoh (UVSOR, Japan)
Masashiro Sawada (Hiroshima Univ., Japan)
Kazushi Sumitani (Kyushu SR Center, Japan)

Local Organizing Committee

Chair: Hiroaki Kimura (JSSRR / JASRI)

Members: Iwao Matsuda (JSSRR / The Univ. of Tokyo)
Yoshihisa Harada (The Univ. of Tokyo)
James Harries (JAEA)
Shigeru Kimura (JASRI)
Masayo Suzuki (JASRI)
Mizuki Tada (JSSRR / Nagoya Univ.)
Masamitsu Takahashi (JAEA)
Kanji Tamasaku (JSSRR / Riken)

VENUE FLOOR PLAN



September 22nd (sun)

	I-messae Hall Main Conference Hall 3rd Floor	Gallery 1/2/3/4 Basement Floor	Meeting Room1 4th Floor
9:00			
	Opening Address Conference Photo	Vendor Exhibition	
11:00	AOFSRR Session New Perspective of Synchrotron Radiation Facility in AOF Region	Coffee Break	
13:00			
		Poster Session (light meals are available)	Council Meeting
15:00			
17:00	Oral Session I Recent Topics on Photon Science	Coffee Break	
19:00			

September 23rd (mon)

	I-messae Hall Main Conference Hall 3rd Floor	Seminar A 4th Floor	Seminar B 4th Floor	Seminar C&D 4th Floor
9:00				
	Oral Session II New Applications (Nano, Magnetism, Industry, etc.)			Coffee Break
11:00				
13:00				
	Oral Session III 1. Green, Environment, Material, etc.	Oral Session III 2. Advanced Data Acquisition	Oral Session III 3. Instruments, SR Tech., etc.	Coffee Break
15:00				
	General Assembly			
17:00	Closing Session			

PROGRAM TIMETABLE

21st September (sat)			
15:00 - 18:00	Registration		@4th floor
18:00 - 20:00	Welcome Party		@Koukoen
22nd September (sun)			
9:00 - 9:30	Registration		@3rd floor
Opening Address		@H-messae Hall, 3rd floor Chair: Masaki Takata (RIKEN/JASRI/SPRING-8, Japan)	
9:30 - 10:00	Special Welcome Address: Mr. Kisaburo Tokai Member of the House of Representatives, Chairman of the Special Committee on Promotion of Science and Technology, and Innovation		
	Welcome Address: Jun'ichiro Mizuki , Conference Chair		
	Welcome Address: Hongjie Xu , President of AOFSTR		
	Congratulatory Address: Mr. Sadayuki Tsuchiya Director-General, Science and Technology Policy Bureau, Ministry of Education, Culture, Sports, Science and Technology (MEXT)		
10:00 - 10:20	Conference Photo		
AOFSTR SESSION: New Perspective of Synchrotron Radiation Facility in AOF Region			
10:20 - 10:50	Global Trends of DLSR and XFEL Tetsuya Ishikawa (RIKEN SPRING-8 Center, Japan)	A1	@H-messae Hall, 3rd floor Chair: Andrew Peele (Australian Synchrotron, Australia)
10:50 - 11:20	Construction Progress and Future Research Opportunities of the Taiwan Photon Source Shih-Lin Chang (NSRRC, Taiwan)	A2	
11:20 - 11:30	BREAK (coffee available at Gallery A/B/C/D, Basement floor)		
Chair: Osamu Shimomura (JSPS, Japan)			
11:30 - 12:00	Current Status of PAL-XFEL Project In Soo Ko (PAL, POSTECH, Korea)	A3	
12:00 - 12:30	Progress and Plans of Synchrotron Radiation Facilities in China Hongjie Xu (SSRF, SINAP, CAS, China)	A4	
12:30 - 12:50	From Krabi's Initiatives to ASEAN Synchrotron: SLRI's Perspectives Sarawut Sujitjorn (SLRI, Thailand)	A5	
Lunch & Poster Session, Facility Posters/AOFSTR Council Meeting			
12:50 - 16:00	Poster Session, Facility Posters (light meal available at Gallery A/B/C/D, Basement floor)	@Gallery A/B/C/D, Basement floor	12:50 - 14:50 AOFSTR Council Meeting @Meeting Room 1, 4th floor

ORAL SESSION I. Recent Topics on Photon Science			@I-messae Hall, 3rd floor Chair: Naoto Yagi (JASRI/SPRing-8, Japan)
16:00 - 16:30	Non destructive imaging of Japanese Buddha statues Junji Sugiyama (Kyoto University, Japan)	B1	
16:30 - 17:00	In-situ and 3-dimensional Nano-Transmission X-ray Microscopy at NSRRC Yen-Fang Song (NSRRC, Taiwan)	B2	
17:00 - 17:20	BREAK (coffee available at Gallery A/B/C/D, Basement floor)		
Chair: Yoshiyuki Amemiya (The University of Tokyo, Japan)			
17:20 - 17:50	Advances in Small Angle Scattering for Soft Matter Stephan V. Roth (DESY, Germany)	B3	
17:50 - 18:20	KOTOBUKI-1 apparatus for cryogenic coherent X-ray diffraction imaging at SPRing-8 and SACLA Masayoshi Nakasako (Keio University, Japan)	B4	
RECEPTION @The Royal Classic Himeji			
18:40 -	Travelling from the Egret Himeji to the Reception venue		
19:00 - 21:00	Reception		
23rd September (mon)			
ORAL SESSION II. New Applications (Nano, Magnetism, Industry, etc.)			
9:30 - 10:00	What's new of PES in SRRF Shan Qiao (Shanghai Institute of Microsystem and Information Technology, CAS, China)	C1	@I-messae Hall, 3rd floor Chair: Richard Garrett (ANSTO, Australia)
10:00 - 10:30	Synchrotron radiation-based Fourier Transform Infra-Red micro-imaging in service of forensic science Agnieszka Banas (SSLS, NUS, Singapore)	C2	
10:30 - 10:50	BREAK (coffee available at Seminar C/D, 4th floor)		
Chair: Sudip K Deb (RRCAT, Indore, India)			
10:50 - 11:20	SAXS Studies of Leather Richard G. Haverkamp (Massey University, New Zealand)	C3	
11:20 - 11:50	Advances in SR diffraction techniques for magnetic and chiral materials Hiroyuki Ohsumi (RIKEN SPRing-8 Center, Japan)	C4	
11:50 - 13:00	LUNCH		

ORAL SESSION III. (parallel) Innovation in SR Science						
1. Green, Environment, Material, etc. @L-messae Hall, 3rd floor Chair: Tai Renzhong (SSRF, SINAP, CAS, China)		2. Advanced Data Acquisition @Seminar A, 4th floor Chair: Brendan J. Kennedy (The University of Sydney, Australia)		3. Instruments, SR Tech., etc. @Seminar B, 4th floor Chair: Mark Breese (SSLS, Singapore)		
13:00 - 13:20	Development of In Situ Grazing Incidence Small-Wide-angle X-ray Scattering for Bulk Heterojunction Thin-film Solar Cells at NSRRC U-Ser Jeng (NSRRC, Taiwan)	D1	Biomedical Applications of Synchrotron-based Infrared Microspectroscopy at NSRRC Yao-Chang Lee (NSRRC, Taiwan)	E1	Feasibility Studies of Single Molecule Scattering Analysis with X-Ray Free Electron Lasers Moonthor Ree (PAL, POSTECH, Korea)	F1
	The first collaborative team access beamline at SLRI (BL 5.2) Sukit Limpijumnong (Suranaree University of Technology, Thailand)	D2	The notable low tolerance of rat skin and bone marrow to synchrotron radiation: A bio-safety evaluation of single dose synchrotron radiation X-ray on young rat legs Guo-Yuan Yang (Shanghai Jiao Tong University, China)	E2	Development of Very Short Period Undulators Shigeru Yamamoto (KEK, Japan)	F2
13:40 - 14:00	BREAK (coffee available at Seminar C/D, 4th floor)		Development of X-ray 2D Detector for SACLA Takaki Hatsui (RIKEN SPring-8 Center, Japan)	E3	BREAK (coffee available at Seminar C/D, 4th floor)	
14:00 - 14:20	Resonant Photoemission studies of $Ti_{1-x}Fe_xO_{2-d}$ R. J. Choudhary (UGC DAE Consortium for Scientific Research, Indore, India)	D3	BREAK (coffee available at Seminar C/D, 4th floor)		Radiation Damage and Aging Accelerator Components at the SPring-8 Shigeki Sasaki (JASRI/SPring-8, Japan)	
			Chair: Ryotaro Tanaka (JASRI/SPring-8, Japan)			
14:20 - 14:40	Phase Decomposition and Valence Change during Delithiation in Olivine-type $LiFePO_4/FePO_4$ System - An Application of Simultaneous XRD and XAFS Measurements - Eiichiro Matsubara (Kyoto University, Japan)	D4	Soft x-ray nanoscopes at the PLS: application activities and status Hyun-Joon Shin (PAL, POSTECH, Korea)	E4	Multipole wiggler beamlines at the Siam Photon Laboratory Supagorn Rugmai (SLRI, Thailand)	
14:40 - 15:00			Real-time observation of surface chemical reaction at millisecond resolution by means of soft X-ray dispersive XAFS Kenta Anemiya (KEK, Japan)	E5	XAFS facility at INDUS-2 Synchrotron Radiation Source and Recent Results Shambhu Nath Jha (BARC, Mumbai, India)	

General Assembly		@I-messae Hall, 3rd floor Chair: Yoshihisa Harada (The University of Tokyo, Japan)
15:00 - 15:40	Council Report Masaki Takata (RIKEN/JASRI/SPring-8, Japan)	
	Overview of Cheiron School	
15:40 - 15:50	Overview Masaki Takata (RIKEN/JASRI/SPring-8, Japan)	
15:50 - 16:00	Young Scientist Presentation I Margie P. Olbinado (The University of Tokyo, Japan)	G1
16:00 - 16:10	Young Scientist Presentation II Xeniya Kozina (JASRI/SPring-8, Japan)	G2
16:10 - 16:30	Great Memories of the Cheiron School Brendan J. Kennedy (The University of Sydney, Australia)	G3
Closing Session		@I-messae Hall, 3rd floor Chair: Masaki Takata (RIKEN/JASRI, Japan)
16:30 - 16:50	Next AOFSTR: Shih-Lin Chang (NSRRC, Taiwan)	
16:50 - 17:00	Closing Remark: Jun'ichiro Mizuki , Conference Chair	
24th September (tue)		
SPring-8/SACLA Site Tour		
9:00 - 10:15	Travelling from JR Himeji Station to Spring-8/SACLA	
10:15 - 12:30	SPring-8/SACLA Site Tour	
12:30 - 13:30	LUNCH @ Spring-8 Cafeteria	
13:30 - 15:00	Travelling from Spring-8/SACLA to JR Himeji Station	

PROGRAM

21st September (sat)

- 15:00Registration (4th floor)
- 18:00**Welcome Party**

22nd September (sun)

- 9:00Registration (3rd floor)

<u>Opening Address</u>		I-messae Hall, 3 rd floor
Chair: Masaki Takata (RIKEN/JASRI/SPring-8)		
9:30	Special Welcome Address: Mr. Kisaburo Tokai, Member of the House of Representatives, Chairman of the Special Committee on Promotion of Science and Technology, and Innovation Welcome Address: Jun'ichiro Mizuki, Conference Chair Welcome Address: Hongjie Xu, President of AOFSSRR Congratulatory Address: Mr. Sadayuki Tsuchiya, Director-General, Science and Technology Policy Bureau, Ministry of Education, Culture, Sports, Science and Technology (MEXT)	
10:00	Conference Photo	

<u>AOFSSRR Session: New Perspective of Synchrotron Radiation Facility in AOF Region</u>		I-messae Hall, 3 rd floor
Chair: Andrew Peele (Australian Synchrotron)		
10:20	A-1 Global Trends of DLSR and XFEL Tetsuya Ishikawa (RIKEN SPring-8 Center)	2
10:50	A-2 Construction Progress and Future Research Opportunities of the Taiwan Photon Source Shih-Lin Chang (National Synchrotron Radiation Research Center)	3
11:20	<i>BREAK (Gallery 1/2/3/4, Basement floor)</i>	
Chair: Osamu Shimomura (JSPS)		
11:30	A-3 Current Status of PAL-XFEL Project In Soo Ko (Pohang Accelerator Laboratory, POSTECH)	4
12:00	A-4 Progress and Plans of Synchrotron Radiation Facilities in China	

	Hongjie Xu (Shanghai Synchrotron Radiation Facility, SINAP, CAS).....	5
12:30	A-5 From Krabi's Initiatives to ASEAN Synchrotron: SLRI's Perspectives Sarawut Sujitjorn (Synchrotron Light Research Institute)	6
12:50	Lunch & Poster Session, Facility Posters (Gallery 1/2/3/4, Basement floor)	

Oral Session I. Recent Topics on Photon Science

I-messae Hall, 3rd floor

Chair: Naoto Yagi (JASRI/SPring-8)

16:00	B-1 Non destructive imaging of Japanese Buddha statues Junji Sugiyama (Kyoto Univ.)	7
16:30	B-2 In-situ and 3-dimensional Nano-Transmission X-ray Microscopy at NSRRC Yen-Fang Song (National Synchrotron Radiation Research Center)	8
17:00	<i>BREAK (Gallery 1/2/3/4, Basement floor)</i>	
	Chair: Yoshiyuki Amemiya (The Univ. of Tokyo)	
17:20	B-3 Advances in Small Angle Scattering for Soft Matter Stephan V. Roth (Deutsches Elektronen-Synchrotron)	9
17:50	B-4 KOTOBUKI-1 apparatus for cryogenic coherent X-ray diffraction imaging at SPring-8 and SACLA Masayoshi Nakasako (Keio Univ.)	10
18:40	Travelling from the Egret Himeji to the Reception venue	
19:00	Reception	

23rd September (mon)

Oral Session II. New Applications (Nano, Magnetism, Industry, etc.)

I-messae Hall, 3rd floor

(Chair: Richard Garrett, ANSTO)

9:30	C-1 What's New of PES in SSRF Shan Qiao (Shanghai Institute of Microsystem and Information Technology, CAS)	11
10:00	C-2 Synchrotron radiation-based Fourier Transform Infra-Red micro-imaging in service of forensic science Agnieszka Banas (Singapore Synchrotron Light Source, NUS)	12

10:30	<i>BREAK (Seminar C&D, 4th floor)</i>	
	Chair: Sudip K Deb (Raja Ramanna Center for Advanced Technology, Indore)	
10:50	C-3 SAXS Studies of Leather Richard G. Haverkamp (Massey Univ.)	13
11:20	C-4 Advances in SR diffraction techniques for magnetic and chiral materials Hiroyuki Ohsumi (RIKEN SPring-8 Center)	14
11:50	<i>LUNCH</i>	

Oral Session III. (parallel): Innovation in SR Science

1. Green, Environment, Material, etc.

I-messae Hall, 3rd floor

Chair: Tai Renzhong (Shanghai Synchrotron Radiation Facility, SINAP, CAS)

13:00	D-1 Development of In Situ Grazing Incidence Small-/Wide-angle X-ray Scattering for Bulk Heterojunction Thin-film Solar Cells at NSRRC U-Ser Jeng (National Synchrotron Radiation Research Center)	15
13:20	D-2 The first collaborative team access beamline at SLRI (BL 5.2) Sukit Limpijumnong (Suranaree Univ. of Technology)	16
13:40	<i>BREAK (Seminar C&D, 4th floor)</i>	
	Chair: Youichi Murakami (KEK)	
14:00	D-3 Resonant Photoemission studies of Ti_{1-x}Fe_xO_{2-d} epitaxial films R. J. Choudhary (UGC DAE Consortium for Scientific Research, Indore)	17
14:20	D-4 Phase Decomposition and Valence Change during Delithiation in Olivine-type LiFePO₄/FePO₄ System - An Application of Simultaneous XRD and XAFS Measurements - Eiichiro Matsubara (Kyoto Univ.)	18

2. Advanced Data Acquisition

Seminar A, 4th floor

Chair: Brendan J. Kennedy (The Univ. of Sydney)

13:00	E-1 Biomedical Applications of Synchrotron-based Infrared Microspectroscopy at NSRRC Yao-Chang Lee (National Synchrotron Radiation Research Center)	19
13:20	E-2 The notable low tolerance of rat skin and bone marrow to synchrotron radiation: A bio-safety evaluation of single dose synchrotron radiation X-ray on young rat legs	

	Guo-Yuan Yang (Shanghai Jiao Tong Univ.)	20
13:40	E-3 Development of X-ray 2D Detector for SACLA Takaki Hatsui (RIKEN SPring-8 Center)	21
14:00	<i>BREAK (Seminar C&D, 4th floor)</i>	
	Chair: Ryotaro Tanaka (JASRI/SPring-8)	
14:20	E-4 Soft x-ray nanoscopes at the PLS: application activities and status Hyun-Joon Shin (Pohang Accelerator Laboratory, POSTECH)	22
14:40	E-5 Real-time observation of surface chemical reaction at millisecond resolution by means of soft X-ray dispersive XAFS Kenta Amemiya (KEK)	23

3. Instruments, SR Tech., etc.

Seminar B, 4th floor

Chair: Mark Breese (Singapore Synchrotron Light Source, NUS)

13:00	F-1 Feasibility Studies of Single Molecule Scattering Analysis with X-ray Free Electron Lasers Moonhor Ree (Pohang Accelerator Laboratory, POSTECH)	24
13:20	F-2 Development of Very Short Period Undulators Shigeru Yamamoto (KEK)	25
13:40	<i>BREAK (Seminar C&D, 4th floor)</i>	
	Chair: In Soo Ko (Pohang Accelerator Laboratory, POSTECH)	
14:00	F-3 Radiation Damage and Aging Accelerator Components at the SPring-8 Shigeki Sasaki (JASRI/SPring-8)	26
14:20	F-4 Multipole wiggler beamlines at the Siam Photon Laboratory Supagorn Rugmai (Synchrotron Light Research Institute)	27
14:40	F-5 XAFS facility at INDUS-2 Synchrotron Radiation source and recent results Shambhu Nath Jha (Bhabha Atomic Research Centre)	28

General Assembly

I-messae Hall, 3rd floor

Chair: Yoshihisa Harada (The Univ. of Tokyo)

15:00	Council Report Masaki Takata (RIKEN/JASRI/SPring-8)
	<i>Overview of Cheiron School</i>

15:40	Overview Masaki Takata (RIKEN/JASRI/SPring-8)	
15:50	G-1 Young Scientist Presentation I Margie P. Olbinado (The Univ. of Tokyo)	29
16:00	G-2 Young Scientist Presentation II Xeniya Kozina (JASRI/SPring-8)	30
16:10	G-3 Great Memories of the Cheiron School Brendan J. Kennedy (The Univ. of Sydney)	31

Closing Session

I-messae Hall, 3rd floor

Chair: Masaki Takata (RIKEN/JASRI/SPring-8)

16:30	Next AOFSRR Shih-Lin Chang (National Synchrotron Radiation Research Center)
16:50	Closing Remarks: Jun'ichiro Mizuki, Conference Chair

24th September (tue)

9:00	Travelling from JR Himeji Station to SPring-8/SACLA
10:15	SPring-8/SACLA Site Tour
12:30	Lunch at SPring-8
13:30	Leave SPring-8
15:00	Travelling from SPring-8/SACLA to JR Himeji Station

P1: Advances in Optics

P1-1	Stroboscopic approach for the quantitative X-ray phase imaging of periodic processes in soft materials using X-ray Talbot interferometry Marge P. Olbinado (The Univ. of Tokyo)	34
P1-2	The design of infrared beamline at SSRF Te Ji (Shanghai Institute of Applied Physics, CAS)	35
P1-3	Numerical Simulation of MLLs with Layer Displacement Error Keliang Liao (Institute of High Energy Physics, CAS)	36
P1-4	Micron X-ray Protein Crystallography Beamline Design Calculated in Phase Space Analysis Yi-Jr Su (National Synchrotron Radiation Research Center)	37

P2: Advances in Materials Science

P2-1	The meso-scale order structure of immiscible polymer blends Tsuyoshi Inoue (Tokyo Metropolitan Univ.)	38
P2-2	Multilayer structure of PbS/EuS nanocrystals revealed by combining of synchrotron small-angle X-ray scattering method and energy dispersive X-ray spectroscopy Hiroyasu Masunaga (JASRI/SPRING-8)	39
P2-3	Multi-scale surface and interface measurement system for soft-material films at SPRING-8. Hiroyuki Ogawa (JASRI/SPRING-8)	40
P2-4	Dynamics of Relaxor Materials of $(1-x)\text{Pb}(\text{Mg}_{1/3}\text{Nb}_{2/3})\text{O}_3$-$x\text{PbTiO}_3$ Studied by X-ray Scattering Daisuke Shimizu (Kwansei Gakuin Univ.)	41
P2-5	Designing new $n = 2$ Sillen-Aurivillius phases by lattice-matched substitutions in the halide and $[\text{Bi}_2\text{O}_2]^{2+}$ layer Samuel Yu Him Liu (Univ. of Sydney)	42
P2-6	Materials Science Research at RIKEN SPRING-8 via the Northeastern University-RIKEN co-op program Ahmed Sajjad (RIKEN SPRING-8 Center/Northeastern Univ.)	43
P2-7	Surface and interfacial morphology and crystallization in polymer light emitting devices Ajeong Kim (Sogang Univ.)	44
P2-8	Responsive polymer brushes grafted from conducting PEDOT Alissa Hackett (Univ. of Auckland)	45
P2-9	Temperature dependent formation of ion tracks in apatite and quartz studied using SAXS Daniel Schauries (The Australian National Univ.)	46
P2-10	Polymer materials studied by SAXS/WAXS at SSRF Feng Tian (Shanghai Institute of Applied Physics, CAS)	47
P2-11	Development of X-ray speckle visibility spectroscopy for breaking the limit of time resolution in X-ray Photon Correlation Spectroscopy Ichiro Inoue (The Univ. of Tokyo/RIKEN SPRING-8 Center)	48

P2-12	The Activation of E-H Bonds (E = H or C) by an Amido-Digermine with a Ge-Ge Single Bond Jiaye Li (Monash Univ.)	49
P2-13	Internal Deformation Field Distribution of Gold Nanoparticles and Zeolite Microcrystals by Coherent X-ray Diffraction Imaging Jinback Kang (Sogang Univ.)	50
P2-14	Efficiency improvement of electrodeposited <i>p-n</i> homojunction cuprous oxide solar cells by surface passivation and annealing Karannagoda Mudalige Don Charith Jayathilaka (Univ. of Colombo)	51
P2-15	Resonant photoemission study of multiferroic YMnO₃ thin film Manish Kumar (UGC-DAE Consortium for Scientific Research, Indore)	52
P2-16	Formation of Silicon Nanocrystallites on Amorphous Hydrogenated Silicon Thin Film Using Dense Plasma Focus Device Siew Kien Ngoi (Univ. of Malaya)	53
P2-17	Synthesis, Characterization, and Dielectric Properties of Y₂NiMnO₆ Ceramics Prepared by A Simple Thermal Decomposition Route Theeranun Siritanon (Suranaree Univ. of Technology)	54
P2-18	Hybrid polymer/quantum dot materials for optoelectronic applications Thitikorn Boonkoom (National Nanotechnology Center, NSTDA)	55
P2-19	Development of Convenient Experimental and Analytical Methods for Diffraction Anomalous Fine Structure Tomoya Kawaguchi (Kyoto Univ.)	56
P2-20	Resonant Multiple-Beam Diffraction Results of La_{0.5}Sr_{1.5}MnO₄ Wen-Chung Liu (National Tsing Hua Univ.)	57
P2-21	Octahedral Tilting in SrRuO₃ Films Studied by Half-Order Reflexions Wenlai Lu (National Univ. of Singapore)	58

P3: Advances in Life Science

P3-1	Coronary Microangiography System for Rat Heart Functional Imaging at SPring-8 Keiji Umetani (JASRI/SPring-8)	59
P3-2	Structural Basis of the γ-Lactone-ring formation in ascorbic acid biosynthesis by the Senescence Marker Protein-30/Gluconolactonase Ayaka Harada (KEK)	60
P3-3	Design and installation of Protein Complex Crystallography beamline at SSRF Kunhao Zhang (Shanghai Institute of Applied Physics, CAS)	61
P3-4	Crystal structure of pyridoxine 4-oxidase from <i>Mesorhizobium loti</i> Andrew Njagi Mugo (Kochi Univ.)	62

P4: FEL Science and Technology

P4-1	Operation Status of SACLA, the Japanese Compact XFEL facility XFEL Research and Development Division, RIKEN SPring-8 Center XFEL Utilization Division, JASRI/SPring-8	63
P4-2	Image reconstruction from diffraction patterns in coherent X-ray diffraction	

	imaging using the dark-field phase-retrieval method Amane Kobayashi (Keio Univ./RIKEN SPring-8 Center)	64
P4-3	Software suite “SHITENNO” for automatically processing diffraction patterns in coherent X-ray diffraction imaging experiments at SACLA Yuki Sekiguchi (Keio Univ./RIKEN SPring-8 Center)	65

P5: Industrial Applications

P5-1	Feasibility study on explosives using synchrotron radiation: Chemical fertilizers Pisutti Dararutana (The Royal Thai Army Chemical School)	66
P5-2	Fabrication of Metallic Microstructures using X-ray Lithography Process Rungrueang Phatthanakun (Synchrotron Light Research Institute)	67
P5-3	Synchrotron-Based Data-Constrained Modeling Analysis of Microscopic Mineral Distributions in Limestone Yudan Wang (Shanghai Institute of Applied Physics, CAS)	68

P6: Insertion Device Technology

N/A

P7: *in situ* Experiments

P7-1	Suitability of Hydrated Magnesium Carbonates as Hosts for Atmospheric Carbon Dioxide: An <i>In-Situ</i> Powder Diffraction Study Bree Morgan (Commonwealth Scientific and Industrial Research Organisation)	69
P7-2	Discriminative Separation of CO₂ and CH₄ Using a Novel “Molecular Trapdoor” Zeolite: Materials and Process Study Jin Shang (The Univ. of Melbourne)	70
P7-3	<i>In situ</i> X-ray and neutron studies to investigate proton conduction in proton exchange membranes for direct alcohol fuel cells Krystina Evelyn Lamb (Univ. of the Sunshine Coast)	71
P7-4	Synchrotron Light Brightening Research in Volcanology Marco Brenna (Massey Univ.)	72
P7-5	Nucleation and crystallization kinetics of a complex lithium disilicate glass: <i>in situ</i> and time-resolved synchrotron powder diffraction study Saifang Huang (The Univ. of Auckland)	73

P8: IR Applications

P8-1	The infrared beamline BL43IR at SPring-8: present status and recent studies Yuka Ikemoto (JASRI/SPring-8)	74
P8-2	Powder X-ray Diffraction Studies of the Betaine–ester Imidazolium-based Amphotropic Ionic Liquid Crystals: As Nano-ion Channel Networks and Organogelators Ching-Wei Tseng (National Dong-Hwa Univ.)	75
P8-3	Multivariate evaluation, feature extraction, classification and clustering of images and spectral data sets by using R environment Krzysztof Banas (Singapore Synchrotron Light Source, NUS)	76

P8-4	Identification of a cassava bacterial blight pathogen, <i>Xanthomonas axonopodis</i> pv. <i>manihotis</i> using FT-IR spectroscopy Natthiya Buensanteai (Suranaree Univ. of Technology)	77
P8-5	Infrared Spectroscopy and Imaging Beamline at the Siam Photon Laboratory Sirinart Srichan (Synchrotron Light Research Institute)	78

P9: Magnetism

P9-1	Long- and short-ranged structure of multiferroic $\text{Pb}(\text{Fe}_{0.5}\text{Nb}_{0.5})\text{O}_3$ Hasung Sim (Seoul National Univ.)	79
------	---	----

P10: Nano Science and Technology

P10-1	Release of encapsulated dye from monolayer of gold nanoparticles by using UV light and Glutathione Apiwat Chompoosor (Khon Kaen Univ.)	80
P10-2	Fate of Zinc Oxide Nanoparticles during Anaerobic Digestion of Wastewater and Post-Treatment Processing of Sewage Sludge Ehsan Tavakkoli (The Univ. of Adelaide)	81
P10-3	Enhanced Photoassisted Field Emission of AuNPs Ligated by Alkanethiols Fei Wang (Shanghai Institute of Applied Physics, CAS)	82
P10-4	The origin of the intraband plasmons on Au/Si(5512) surface Jin Gul Kim (Pohang Univ. of Science and Technology)	83
P10-5	Topotactic synthesis of mesoporous ZnS and ZnO nanoplates and their Photocatalytic Activity Jum Suk Jang (Pohang Accelerator Laboratory, POSTECH)	84
P10-6	RGO-TiO₂ nanocomposite with highly exposed {001} facets for photoelectrochemical performance and electrochemical determination of dopamine Gregory Thien Soon How (Univ. of Malaya)	85
P10-7	SSRF XIL beamline BL08U1-B introduction Jun Zhao (Shanghai Institute of Applied Physics, CAS)	86
P10-8	Evidence of ultraviolet transparency of graphene on SrTiO₃ induced by excitonic Fano anti-resonance Pranjal Kumar Gogoi (National Univ. of Singapore)	87
P10-9	Structural properties of mixed magnetic oxide determined from synchrotron powder diffraction Tien Quoc Tran (Vietnam Academy of Science and Technology)	88
P10-10	CuO/TiO₂ - Low cost semiconductor photocatalysts for solar hydrogen production Wan-Ting Chen (The Univ. of Auckland)	89
P10-11	Small Angle X-ray Scattering and Fluorescence Spectroscopy of Lanthanide Binding Peptide Complexes Jessica Veliscek-Carolan (Australian Nuclear Science and Technology Organisation)	90
P10-12	Gap state tuning at the organic/metal interface by quantum-size effects Meng-Kai Lin (National Tsing-Hua Univ.)	91

P11: New Developments in Detectors

P11-1	Introduction to X-Ray Diffraction at RIKEN SPring-8 Jordan DeWitt (RIKEN SPring-8 Center/Northeastern Univ.)	92
-------	--	----

P12: New Facilities

P12-1	BL5S1: A new hard X-ray XAFS Beamline at the Aichi Synchrotron Radiation Center Hiroyuki Asakura (Nagoya Univ.)	93
P12-2	Current Status of Scanning Transmission X-ray Microscopy Beamline at UVSOR Takuji Ohgashi (UVSOR Facility, Institute for Molecular Science)	94
P12-3	Performance of two Public Beamlines with insertion devices at SAGA Light Source Kazushi Sumitani (Kyushu Synchrotron Light Research Center)	95
P12-4	Development of X-ray imaging beamline at INDUS-2 synchrotron source, India Balwant Singh (Bhabha Atomic Research Centre, Mumbai)	96
P12-5	Development of High- and Low-Energy Scanning Transmission X-ray Microscope (STXM) for Bacterial Samples Hiroki Suga (Hiroshima Univ.)	97
P12-6	The status of hard x-ray microfocusing at Shanghai Synchrotron Radiation Facility (SSRF) Shuai Yan (Shanghai Institute of Applied Physics, CAS)	98

P13: Radiation Damage Management

N/A

P14: Storage Ring Technology

P14-1	Status of UVSOR-III Light Source Kenji Hayashi (UVSOR Facility, Institute for Molecular Science)	99
P14-2	Present Status of the SPring-8 Storage Ring and the Performance Improvements Accelerator Division, JASRI/SPring-8	100
P14-3	Accelerators of Aichi Synchrotron Radiation Center Naoto Yamamoto (Nagoya Univ.)	101

P15: SR Experiments under Extreme Conditions

N/A

P16: Time Resolved Applications

P16-1	Chronology of Carriers at Semiconductor Surfaces Studied by Time-Resolved Photoemission Spectroscopy Iwao Matsuda (The Univ. of Tokyo)	102
-------	--	-----

P16-2	Development of Sub-picosecond Ultrafast X-ray Diffraction and Research of Ultrafast Photoinduced Strain Bingbing Zhang (Beijing Synchrotron Radiation Facility, Institute of High Energy Physics, CAS)	103
P16-3	Gelation Mechanism and Hierarchical Structure of P3HT/PCBM in Xylene Solution Kuei-Yu Kao (National Tsing-Hua Univ.)	104

P17: VUV Instrumentation and Applications

P17-1	Synchrotron based VUV spectroscopy in gas and matrix isolated phase Param Jeet Singh (Bhabha Atomic Research Centre, Mumbai)	105
P17-2	Electron Injection Enhancement in OLEDs with Interfacial Chemical Reactions between 8-hydroxyquinolatolithium and Aluminum Young Mi Lee (Pohang Accelerator Laboratory)	106

P18: Others

P18-1	Current status of UVSOR beam-lines Fumitsuna Teshima (UVSOR Facility, Institute for Molecular Science)	107
P18-2	A Floor Deformation of SACLA Building Hiroaki Kimura (RIKEN SPring-8 Center/JASRI/SPring-8)	108
P18-3	Optical design of an undulator based ARPES beamline on Indus-2 Kiran Baraik (Raja Ramanna Centre for Advance Technology, Indore)	109
P18-4	Low-cost, high-performance electrocatalysts for polymer electrolyte membrane fuel cells Kug-Seung Lee (Pohang Accelerator Laboratory)	110
P18-5	Capacitive coupled RF discharge plasma for cleaning of carbon contaminated Optics Praveen Kumar Yadav (Raja Ramanna Centre for Advance Technology, Indore)	111
P18-6	Fabrication of OSAKA MIRROR for Synchrotron Application Shota Matsuyama (JTEC Corporation)	112
P18-7	QXAFS system modified by IK220 card for the SSRF XAFS station Songqi Gu (Shanghai Institute of Applied Physics, CAS)	113
P18-8	MeV-Ion Beam Analysis of Atomic Layer-Deposition Ultra-Thin Oxide Films Teerasak Kamwanna (Khon Kaen Univ.)	114
P18-9	Studies of Phtonuclear Reactions Induced by Bremstrahlungs with End-point Energies above the Dipole Resonance Region Thanh Tien Kim (Vietnam Academy of Science and Technology)	115
P18-10	Monitoring Arsenic in Particulate Matter Travis Abel Ancelet (GNS Science)	116
P18-11	Metal sulfides-catalyzed hydrodeoxygenation of phenol and triglycerides Vorranutth Itthibenchapong (National Nanotechnology Center, NSTDA)	117

ABSTRACTS
-ORAL PRESENTATION-

Global Trends for DLSR and XFEL

Tetsuya Ishikawa

*RIKEN SPring-8 Center
Kouto 1-1-1, Sayo, Hyogo 678-5148, Japan*

When SASE XFELs were first conceived of decades ago, they faced stiff opposition from scientists favoring linac-based straight light sources which offered a greater number of beamlines. Light sources based on Energy Recovery Linac (ERL) technology capable of accommodating multiple beamlines were proposed as an alternative, partly because of the misconception that conventional storage ring technology had already reached its limits.

However, various new concepts have recently enabled the design of high performance light sources based on storage ring technology, which in most cases have exceeded the light source performance attainable using ERL technology. Inspired by the innovative design of the MAX-IV facility in Sweden, many major light sources including ESRF, SPring-8 and APS began making upgrade plans based on storage rings with <100 pm.rad emittance. In addition, ambitious new light source projects based on this next-generation storage ring technology are underway. Since these storage rings have emittance close to the diffraction limits of hard X-rays, they are often referred to as Diffraction Limited Storage Rings (DLSRs). The new concepts, when applied to larger scale storage rings as PEP, and possibly PETRA and TRISTAN, will provide new capabilities for ring-type soft-X-ray FELs.

X-ray free electron lasers (XFELs) based on self-amplified spontaneous emission (SASE) offer several advantages. Following the two existing operational facilities, LCLS and SACLA, the Euro-XFEL will come on line in 2015. The Swiss XFEL and Pohang XFEL will follow thereafter. There are opposing trends for future XFELs: compact or huge multi-user. Both types address the continued increasing demands of users wanting access to XFELs. Given typical constraints for new development, it is generally more feasible to build multiple compact XFELs, since they require less space, lower construction costs, and much shorter construction periods. On the contrary, though XFELs based on superconducting linac technology can support many FEL lines with a single linac with a very high repetition rate, they require enormous amounts of space, budget, and time for construction.

Co-location of XFEL and SR facilities, exemplified by SACLA and SPring-8, can serve as a model for future light source facilities. The processing of the huge amounts of data produced by these facilities will be critical in the near future. Standardization of data formats and/or processing software, preferably based on inter-facility collaboration, would facilitate data sharing and analysis.

Construction Progress and Future Research Opportunities of the Taiwan Photon Source

Shih-Lin Chang

National Synchrotron Radiation Research Center

101 Hsin-Ann Road, Hsinchu Science Park, Hsinchu, 30076 Taiwan, R.O.C.

The status of the 3 GeV Taiwan Photon Source (TPS) currently under construction for the establishment of a high brightness and low emittance mid-energy storage ring will be presented. The progress on the civil construction, manufacturing of machine components, as well as the opportunity of using low emittance synchrotron source and phase I beamlines at TPS will be mentioned. The future planning of phase II beamlines and related research will be sketched. Future developments will be also briefly outlined.

Current Status of PAL-XFEL Project

In Soo Ko

*Pohang Accelerator Laboratory
POSTECH*

San 31, Hyoja-Dong, Pohang 790-784 Korea

PAL-XFEL project is aiming to produce 0.1-nm coherent X-ray laser to photon beam users. In order to produce such photons, there are 10-GeV electron linac based on S-band normal conducting accelerating structures and a 150-m long out-vacuum undulator system. The project is already started in April 2011, and the 1,110-m long building is expected to be completed by November 2014. The injector test facility (ITF) which is the first 139-MeV section of the main linac has been installed and is under commissioning in newly added corner of old PLS linac building. In this talk, I will introduce the project in general, performances of ITF, and domestic developments of subsystems such as 200-MW modulator, high power RF components, precision low power RF systems, and undulators and the vacuum chambers.

Figure



Fig. 1. Artist concept of PAL-XFEL building along with existing PLS facilities

Progress and Plans of Synchrotron Radiation Facilities in China

Hongjie Xu

SSRF, SINAP, CAS

239 Zhang Heng Road, Pudong New District, Shanghai 201204, P. R. China

There are three synchrotron radiation facilities in China: Beijing Synchrotron Radiation Facility (BSRF), Hefei Light Source (HLS) and Shanghai Synchrotron Radiation Facility (SSRF). Recent progress and plans of the three SRs are illustrated here.

BSRF is the first synchrotron radiation facility in china. Currently, there are 3 experimental halls, 5 insertion devices, 14 beamlines and 15 endstations at BSRF. Institute of High Energy Physics (IHEP) are planning to build a 5GeV synchrotron radiation facility, Beijing Advanced Photon Source (BAPS) in the future. BAPS is a high-energy and low-emittance synchrotron radiation facility, to provide high brilliance hard X-ray, for requirement of industrial application, and also better support to fundamental research. Recently, R&D project of BAPS is proposed, to overcome difficulties in the technique for this machine, including the accelerator, beamlines and experimental stations.

HLS is the first dedicated synchrotron radiation facility in China. HLS is on upgrade from 2012 to 2013. There are 14 beamlines and endstations in HLS before upgrade. The performance of HLS will be notably improved after upgrade. Storage ring structure of HLS will be changed from $4 \times \text{TBA}$ to $4 \times \text{DBA}$. Straight section will be changed from $3.36\text{m} \times 4$ to $4.0\text{m} \times 4 + 2.3\text{m} \times 4$. Injection energy will increase from 200MeV to 800MeV. Seven Bending Magnets and Six Straight sections are available for beamline construction. Five ID Beamlines will be operated in the end of 2013. The project for upgrading the storage ring will push HLS into an excellent vacuum ultraviolet light source.

SSRF, a third-generation light source, was constructed from 2004 to 2009 with a 3.5 GeV storage ring and 7 beamlines (8 endstations) in project Phase-I. Over 1000 beamtime proposals were approved in 2012. After project Phase-I accomplished, additional 6 beamlines sponsored by users are under construction from 2010 to 2013, include 5 beamlines (6 endstations) on protein science and one photoemission spectroscopy beamline. Project Phase-II on SSRF, a new project with 16 advanced beamlines and auxiliary system, is proposed recently, with a 6 years period and 1.68 billion RMB budget. Project Phase-II will aim at research field as energy science (4 beamlines), material science (4 beamlines), environment science (3 beamlines), life science (2 beamlines), and industrial applications (3 beamlines). These beamlines would have their unique characteristic respectively, such as beamlines-combinative, extremely high-performance, multi-functional, in-situ and dynamic instrumentations, etc. Auxiliary system constructing plan include machine upgrading, user experiments supporting facility, beamline techniques supporting facility and utilities. With achieving project phase-II, SSRF would possess capacity for providing more than 10000 shifts to more than 5000 users annually.

From Krabi's Initiatives to ASEAN Synchrotron: SLRI's Perspectives

Sarawut Sujitjorn

Director, Synchrotron Light Research Institute, Thailand

ASEAN Economic Community (AEC) is one of the three polars of ASEAN, whilst being AEC in 2015 is approaching. For many years, ASEAN have coined their two objectives of being AEC, i.e. single market, and to reduce poverty and development gaps among ASEAN nations through collaborations and assistances. In 2010, the Ministry of Science and Technology, Thailand, proposed many salient programs for ASEAN collaborations, later referred to as Krabi's Initiatives. Among those, research collaborations in synchrotron science and technology were introduced. Later, an idea of using facility at SLRI, Thailand, as ASEAN synchrotron was proposed.

This short presentation will brief audiences on ASEAN COST and Krabi's Initiatives. These lead to an existence of Ad-hoc Working Group on Synchrotron Science and Technology of ASEAN. The Working Group have come-up with recommendations for use, and research fields of interests for ASEAN scientists to work together at SLRI-site. Presentation will cover introduction to SLRI synchrotron facility (originally donated by SORTEC of Japan) with some selected research results, recommendations for ASEAN use, research fields of ASEAN interests, and past activities with ASEAN.

Non destructive imaging of Japanese Buddha statues

Junji Sugiyama

Research Institute for Sustainable Humanosphere,

Kyoto University

Uji, Kyoto 611-0011, Japan

In Japan and in Korea separately, there is two statues: one was made from wood and the other was made of bronze. The first registered national treasure, Hokanmiroku at Koryu-ji temple is unique as it is made from Akamatsu wood (*Pinus densiflora*). In Asuka era, Kusunoki, *Cinnamomum camphora* and Kaya, *Torreya nucifera* have been mainly used for such statues. Later, Hinoki (*Chamaecyparis obtusa*) has been used for the same purpose. Who made and where it was made have been long debated.

In an old document, there is a record of a statue brought from Silla in 623, and the statue was handed down in Koryu-ji temple. This statue is supposed to be the present Houkenmiroku. Its appearance is also nearly identical to the bronze statue handed down in Korea (Korean National Treasure #83). Therefore it seems likely that the statue was brought from Silla.

Generally, in order to prevent crack formation on the face, body of the Buddha statue, hidden skills are there. The sculptor's invention is to carve inside for releasing internal stress of wood. This advanced technique was introduced from Silla. It was so well done but the cover is made of *Cinnamomum camphora*, which grows only in the limited area of Korean peninsular, southern most coast and Jeju island, but grows mainly in Japan.

Thus, who, where, and when it was made is still uncovered. As such, knowing wood species of important cultural artifacts is of great importance as an evidence for correct understanding of our history.

In the case of samples from national treasure or cultural assets, however, only non-destructive analysis is allowed. Even during restoration, sampling on purposely is strictly regulated. This is in such a situation that the samples are often too small to apply conventional microscopic technique even when samples became available unexpectedly.

SR-microCT technique provides resolution enough to resolve species-specific anatomical feature from such a precious sample and thus allowed us to identify wood species[1]. Some examples will be given in the presentation.

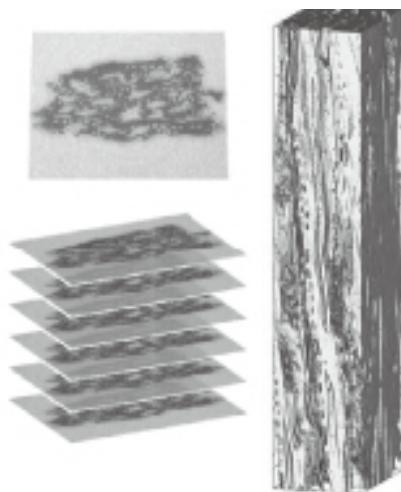


Fig.1 An example of wood fragment observed by SR-microCT technique.

[1] S. Mizuno, R. Torizu, J. Sugiyama, J. Archeol. Sci 37, 2842 (2010).

In-situ and 3-dimensional Nano-Transmission X-ray Microscopy at NSRRC

Yen-Fang Song, Chun-Chieh Wang and Cheng-Cheng Chiang

National Synchrotron Radiation Research Center, 101 Hsin-Ann Road, Hsinchu Science Park, Hsinchu 30076, Taiwan, R.O.C.

Transmission X-ray microscopy is an efficient instrument in in-situ and interior 3-dimensional structural observation of material in nano- to sub-micron scale owing to its large penetration depth and superior spatial resolution. The nano-transmission X-ray microscopy (TXM) at beamline BL01B [1,2] of the Taiwan Light Source (TLS) provides two-dimensional imaging and three-dimensional tomography at energy 8-11 keV with a spatial resolution of 50-60 nm, and with the Zernike-phase contrast capability for imaging light materials such as biological specimen. TXM allows aqueous specimen due to no vacuum requirement. This beamline now carries out successfully the researches that prefer a non-destructive probe, for example, (1) in-situ observation of the sulfidation process of nano cubes, supercrystal formation process and energy storage Li-ion battery (2) the characterization of porous material such as earthquake fault gauge, paleontological fossil and clay mineral in aqueous environment (3) the analysis of the failure mechanism in micro-electronic device. Furthermore, this X-ray microscopy can be applied in the research of cells in life science. With labeling contrast agents, such as immuno nano-gold or osmium tetroxide, imaging for specific cellular function is feasible.

In this presentation, I will demonstrate the applications utilizing transmission X-ray microscopy at NSRRC: (1) In-situ observation of the sulfidation process of Cu_2O nano-particle [3]. (2) Formation of polyhedral gold supercrystals [4]. (3) Study on the interior microstructures of working metal or SnSb particle electrode of Li-ion batteries [5]. (4) 3-dimensional interior structure of geological specimen [6].

-
- [1] Gung-Chian Yin, Mau-Tsu Tang, Yen-Fang Song, Fu-Rong Chen, Keng S. Liang, Frederick W. Duewer, Wenbing Yun, Cheng-Hao Ko, and Han-Ping D. Shieh, *Appl. Phys. Lett.*, **88**, 241115 (2006)
 - [2] Y. F. Song, C. H. Chang, C. Y. Liu, S. H. Chang, U-Ser Jeng, Y. H. Lai, D. G. Liu, J. F. Lee, H. S. Sheu, M. T. Tang, K. L. Tsang, and K. S. Liang, *J. of Synchrotron Rad.* **14**, 320 (2007)
 - [3] Chun-Hong Kuo, Yi-Ting Chu, Yen-Fang Song, and Michael H. Huang, *Adv. Funct. Mater.* **21**, 792 (2011)
 - [4] Ching-Wen Liao, Yeh-Sheng Lin, Kaushik Chanda, Yen-Fang Song, and Michael H. Huang, *J. Am. Chem. Soc.* **135**, 2684-2693(2013)
 - [5] Sung-Chieh Chao, Yen-Fang Song, Chun-Chieh Wang, Hwo-Shuenn Sheu, Hung-Chun Wu and Nae-Lih Wu, *J. Phys. Chem. C* **115**, 22040-22047 (2011).
 - [6] Yu-Min Chou, Sheng-Rong Song, Charles Aubourg, Teh-Quei Lee, Anne-Marie Boullier, Yen-Fang Song, En-Chao Yeh, Li-Wei Kuo, & Chien-Ying Wang, *Geology* **40** 551-554 (2012).

Advances in Small Angle Scattering for Soft Matter

Stephan V. Roth

Deutsches Elektronen-Synchrotron (DESY)

Notkestr. 85

D-22607 Hamburg, Germany

Small-angle X-ray scattering (SAXS) is a very powerful tool in modern materials science. Its field of application ranges from biological relevant samples, e.g. proteins, to hard and soft condensed matter. This is due the fact that SAXS allows for quantitatively extracting the structural and morphological length scales in nanomaterials [1]. After a general introduction, I will review recent and future developments by presenting explicit examples, including the combination with tomographic methods, micro- and nanofocused x-ray beams as well as grazing incidence. Especially the domain of high-time resolution in kinetic investigations will be addressed, elucidating in-situ microfluidic and deformation processes, thus allowing for establishing the structure-function relation in such processes [2,3].

-
- [1] C.C. Egger, C. du Fresne, V. I. Raman, V. Schädler, T. Frechen, S. V. Roth and P. Müller-Buschbaum, *Langmuir* **24**, 5887 (2008)
 - [2] M.Trebbin, D. Steinhauser, J. Perlich, A. Buffet, S. V. Roth, W. Zimmermann, J. Thiele, and S. Förster, *PNAS* **110**, 6706 (2013).
 - [3] K. Brüning, K. Schneider, S. V. Roth, and G. Heinrich, *Macromolecules* **45**, 19 (2012).

KOTOBUKI-1 apparatus for cryogenic coherent X-ray diffraction imaging at SPring-8 and SACLA

Masayoshi Nakasako^{1,2}, Yuki Takayama^{1,2}, Tomotaka Oroguchi^{1,2},
Yuki Sekiguchi^{1,2}, Amane Kobayashi^{1,2}, Keiya Shirahama¹,
Masaki Yamamoto², Takaaki Hikima², Koji Yonekura², Saori Maki-Yonekura²,
Yoshiki Kohmura², Yuichi Inubushi²,
Yukio Takahashi^{2,3}, Akihiro Suzuki^{2,3},
Sachihiro Matsunaga⁴, Yayoi Inui⁴,
Kensuke Tono⁵, Takashi Kameshima⁵, Yasumasa Joti⁵,
Takahiko Hoshi⁶

¹*Department of physics, Faculty of Science and Technology, Keio University, 3-14-1 Hiyoshi, Kohoku-ku, Yokohama 223-8522, Japan.* ²*RIKEN SPring-8 Center, RIKEN Harima Institute, 1-1-1 Kouto, Sayo, Hyogo 679-5148, Japan.*

³*Department of Precision Science and Technology, Graduate School of Engineering, Osaka University, 2-1 Yamadaoka, Suita, Osaka 565-0871, Japan.* ⁴*Department of Applied Biological Science Faculty of Science and Technology, Tokyo University of Science, 2641 Yamazaki, Noda, Chiba 278-8510, Japan.* ⁵*Japan Synchrotron Radiation Research Institute, 1-1-1 Kouto, Sayo, Hyogo 679-5198, Japan.* ⁶*Kohzu Precision Co., Ltd., 2-6-15 Kurigi, Aso-ku, Kawasaki, Kanagawa 215-8521, Japan.*

We have developed an experimental apparatus named KOTOBUKI-1 for use in coherent X-ray diffraction imaging experiments of frozen-hydrated non-crystalline particles at cryogenic temperature. We here use a cryogenic pot cooled by the evaporation cooling effect by liquid nitrogen as a cryogenic specimen stage with small positional fluctuation for a long exposure time of more than several minutes. To bring specimens stored in liquid nitrogen to the specimen stage in vacuum, a loading device and miscellaneous devices are developed. Biological specimens are prepared in frozen-hydrated state using a humidity controlled specimen preparation chamber [1]. The apparatus allows diffraction data collection for frozen-hydrated specimens at 66 K with a positional fluctuation of less than 0.4 μm , and provide an experimental environment to easily exchange specimens from liquid nitrogen storage to the specimen stage. The apparatus was used in diffraction data collection of non-crystalline particles with dimensions of micron from material and biological sciences, such as metal colloid particles and chloroplast, at BL29XU of SPring-8. Very recently, the apparatus has been utilized for single-shot diffraction data collection of non-crystalline particles with dimensions of sub-micron using X-ray free electron laser at BL3 of SACLA. A program suite SHITENNO has been developed for automatic data processing and phase retrieval calculations [2] of collected diffraction data.

[1] Y. Takayama, and M. Nakasako, *Rev. Sci. Instrum.* **83**, 054301 (2012).

[2] T. Oroguchi, and M. Nakasako, *Phys. Rev. E* **87**, 022712 (2013).

What's new of PES in SSRF

Shan Qiao

*Shanghai Institute of microsystem and information technology,
Chinese academy of sciences, 865 changning road,
Shanghai 200050, P. R. China*

An VUV beamline with minimum photon energy of 7 eV will be constructed in Shanghai Synchrotron Radiation Facility (SSRF) for photoelectron spectroscopy. The heat load problem is a fatal problem to generate low energy photons in such a 3.5 GeV ring. To resolve this problem, a knot undulator which can suppress the heat load for almost 100 times was proposed for electrical undulator [1, 2]. To decrease the energy consume, undulator with permanent magnets is more favorite. The APPLE-8 undulator has been proposed to overcome the heat load problem for undulator to generate polarized photons with permanent magnets. I will discuss the problem of APPLE-8 undulator and report the idea of revised knot undulator for permanent magnets. An APPLE-Knot structure is proposed and its perfect performance will be shown. Also, the design considerations of the related beamline and end station will be discussed.

-
- [1] S. Qiao, Dewei Ma, Donglai Feng, S. Marks, R. Schlueter, S. Prestemon and Z. Hussain, Rev. Sci. Instrum. 80, 085108(2009).
[2] J. Yan and S. Qiao, Rev. Sci. Instrum. 81, 056101(2010).

Synchrotron radiation-based Fourier Transform Infra-Red micro-imaging in service of forensic science

A. Banas¹, K. Banas¹, M. B. H. Breese^{1,2}, J. Loke³, S.K. Lim³ and H.O. Moser⁴

¹ *Singapore Synchrotron Light Source, National University of Singapore, 5 Research Link, Singapore 117603*

² *Physics Department, National University of Singapore, 2 Science Drive 3, Singapore 117542*

³ *Forensic Management Branch, Criminal Investigation Department, Police Cantonment Complex 391 New Bridge Road #20-04, Tower Block C, Singapore 088762*

⁴ *Network of Excellent Retired Scientists (NES) and Institute of Microstructure Technology (IMT), Karlsruhe Institute of Technology (KIT), Postfach 3640, D-76021 Karlsruhe, Germany*

Synchrotron radiation-based Fourier Transform Infra-Red (SR-FTIR) micro-imaging has been developed as a rapid, direct and non-destructive technique. This method, taking advantage of synchrotron light brightness and a small effective source size, is capable of exploring the molecular chemistry within the microstructures of microscopic particles without the destruction of inherent structures at ultraspatial resolutions. This is in contrast to traditional “wet” chemical methods, which, during processing for analysis, often caused destruction of original samples.

In the present study, we demonstrate the potential of SR-FTIR micro-imaging as an effective way to identify accurately microscopic particles deposited within latent fingerprints. These particles are present from residual amounts of materials left on a person’s fingers after handling such materials. Fingerprints contaminated with various types of powders, creams, medications and high explosive materials (3-nitrooxy-2,2-bis(nitrooxymethyl)propyl nitrate (PETN), 1,3,5-trinitro-1,3,5-triazinane (RDX), 2-methyl-1,3,5-trinitrobenzene (TNT)) deposited on various - daily used - substrates have been analysed herein without any further sample preparation. Non-destructive method for the transfer of contaminated fingerprint from hard to reach areas of the substrates to the place of analysis was also presented.

This method potentially could have a significant impact on forensic science and could dramatically enhance the amount of information that can be obtained from the study of fingerprints.

SAXS Studies of Leather

Richard G. Haverkamp[†], Katie H. Sizeland[†], Melissa M. Basil-Jones[†], Hannah Wells[†], Hanan Kayed[†], Richard L. Edmonds[‡], Nigel Kirby[§], Adrian Hawley[§]

[†]School of Engineering and Advanced Technology, Massey University, Private Bag 11222, Palmerston North, New Zealand 4442; [‡]Leather and Shoe Research Association of New Zealand, PO Box 8094, Palmerston North, New Zealand 4446; [§]Australian Synchrotron, Melbourne, Australia.

Leather is a fibrous collagen material. Leathers from different animals have different physical properties. High strength leather has much greater commercial value than weak leather, therefore understanding the basis of the strength is an important goal. Other collagen based materials are important in medical applications. We used small angle X-ray scattering to characterise the structure of leather and other fibrous collagen materials. The two dimensional small angle scattering pattern provides information on the internal fibril structure and the fibril arrangement. Leathers from different animals were characterized. It is shown that greater collagen alignment in the plane of the leather leads to stronger material. The structural response to dynamic loads varies between strong and weak material. Under tension fibrils reorient at low strain then individual fibrils stretch at higher strain. Stronger material has more uniform strain throughout the thickness and greater extension of fibrils is achieved. Processing treatments affect the response of these tissues to strain. Cross linking influences the fibril orientation. These studies provide an insight into the structural basis of strength in leather and the behaviour of these materials under stress.

Advances in SR diffraction techniques for magnetic and chiral materials

Hiroyuki Ohsumi¹ and Taka-hisa Arima^{1,2}

¹*RIKEN SPring-8 Center, Sayo, Hyogo 679-5148 (Japan)*

²*Department of Advanced Materials Science, University of Tokyo, Kashiwa 277-8561 (Japan)*

X-rays interact with electron charge and spin through its oscillating electric and magnetic field, respectively. However, the amplitude of magnetic scattering relative to charge scattering is quite small. For investigation of magnetic structure, it is essential to discriminate magnetic scattering from charge scattering. The most distinct difference between the ordinary charge scattering (Thomson scattering) and magnetic scattering appears in the dependence on x-ray polarization. Therefore, polarization control and analysis techniques are quite important in x-ray magnetic diffraction experiments.

In this talk we present our recent works using circularly polarized x-rays. Right- and left-handed circular polarizations are not superposable on each other and being mirror images of one another. Using these chiral x-rays one can specify the handedness of helical magnetic structures. MnWO_4 and DyMnO_3 exhibit ferroelectricity induced by magnetic order. The origin of multiferroic behaviors was confirmed to be of the same type of TbMnO_3 [1] by observing the correspondence of spin chirality to the direction of poling field [2]. Similarly, one can distinguish enantiomers using chiral x-rays. CsCuCl_3 has a chiral crystal structure and its handedness were readily identified using a screw axis ATS reflection (here ATS represents the anisotropy of the tensor of susceptibility)[3]. In addition, we developed a scanning x-ray microscope using the Kirkpatrick-Baez mirrors and visualized chirality domain distribution in this compound (see figure 1). This technique is applicable even though a specimen is opaque. Furthermore, control of the penetration depth enables us to analyze a depth profile of the chirality near crystal growth front[4]. Finally, a perspective of SR x-ray magnetic diffraction techniques is discussed from the point of view of x-ray polarization.

These works were partly supported by a Grant-in-Aid for Scientific Research from MEXT, Japan, and by Funding Program for World Leading Innovative R&D on Science and Technology (FIRST) on “Quantum Science on Strong Correlation” from JPSJ.

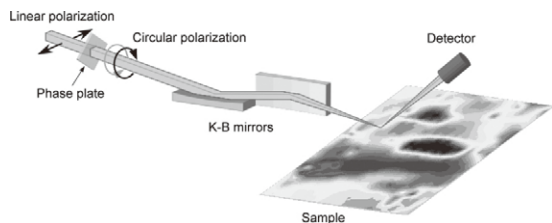


Figure 1. Scanning x-ray microscope.

Linearly polarized x-rays are converted to circular polarization by the diamond phase plate and then are focused by the K-B mirrors.

[1] T. Kimura *et al.*, *Nature* **426**, 55 (2003).

[2] H. Sagayama, H. Ohsumi, T. Arima *et al.*, *J. Phys. Soc. Jpn* **79**, 043711 (2010).

[3] Y. Kousaka, H. Ohsumi, T. Arima *et al.*, *J. Phys. Soc. Jpn* **78**, 123601 (2009).

[4] H. Ohsumi, T. Arima *et al.*, *Angew. Chem. Int. Ed.* in press.

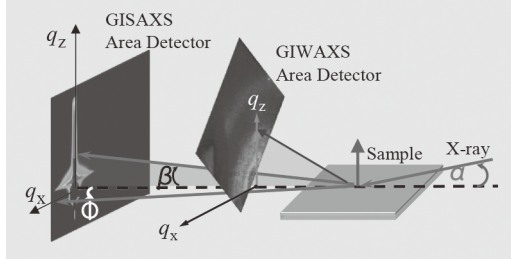
Development of In Situ Grazing Incidence Small-/Wide-angle X-ray Scattering for Bulk Heterojunction Thin-film Solar Cells at NSRRC

U-Ser Jeng, Chun-Jen Su, Yi-Qi Yeh, Wei-Ru Wu; Wen-Bin Su, Kuei-Fen Liao, Chun-Yu Chen, and Jhih-Ming Lin

National Synchrotron Radiation Research Center, 101 Hsin-Ann Road, Hsinchu Science Park, Hsinchu City 30076, Taiwan

At the National Synchrotron Radiation Research Center (NSRRC), the recent upgrade of the 23A SWAXS endstation with a Pilatus 1M-F (133 Hz) and a Mythen-3K (472 Hz) detectors has advanced synchronized small- and wide-angle X-ray scattering (SAXS/WAXS) measurements for structural kinetics into millisecond resolution. Together with an additional flat panel area detector CMOS-9728DK (3.3 Hz), the integrated detecting system covers a wide-range of X-ray scattering angle with several different modes of operation, including transmission (T), grazing incidence (GI), and anomalous (A) SAXS/WAXS. Particularly, a solvent-vapor controlled chamber with a heating stage has been developed allowing observation of time-resolved, simultaneous grazing incidence SAXS/WAXS (GISAXS/GIWAXS) upon drying, heating, or isothermal annealing of organic thin films for bulk heterojunction (BHJ) photovoltaic solar cells comprising, in general, binary mixtures of conjugate polymers and fullerene derivatives. Crystallization behavior including kinetics (crystalline orientation and size) of the polymer in organic BHJ solar cells can be studied with GIWAXS, whereas aggregation behavior (from several to several tens nm) of the fullerene derivatives and hierarchical large grain size spacing (several hundreds of nm) can be observed with GISAXS. The GISAXS/GIWAXS performance is illustrated via a concomitant observation of [6,6]-phenyl-C₆₁-butyric acid methyl ester (PCBM) aggregation and poly(3-hexylthiophene) (P3HT) crystallization in bulk heterojunction (BHJ) thin film (ca. 85 nm) solar cells. With a time and spatial resolutions (5 s/frame; minimum $q \approx 0.004 \text{ \AA}^{-1}$), synchrotron GISAXS has captured in detail the fast growth in size of PCBM aggregates from 7 to 18 nm within 100 s of annealing at 150 °C. Simultaneously observed is the enhanced crystallization of P3HT into lamellae oriented mainly perpendicular but also parallel to the substrate. An Avrami analysis of the observed structural evolution indicates that the faster PCBM aggregation follows a diffusion-controlled growth process, whereas the slower development of crystalline P3HT nanograins is characterized by constant nucleation rate.

Figure 1. Schematic for the simultaneous, grazing incidence small- and wide-angle X-ray scattering at 23A SWAXS beamline of NSRRC.



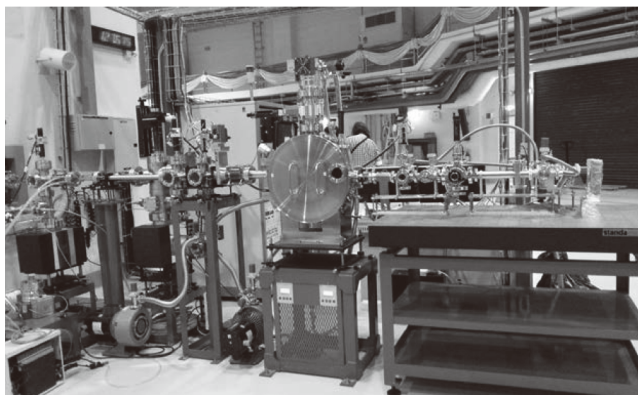
- [1] W.-R. Wu, U. Jeng, C.-J. Su, K.-H. Wei, M.-S. Su, M.-Y. Chiu, C.-Y. Chen, W.-B. Su, C.-H. Su, and A.-C. Su, *ACS Nano*, **5**, 6233 (2011).
- [2] H.-J. Liu, U. Jeng, N. L. Yamada, A.-C. Su, W.-R. Wu, C.-J. Su, S.-J. Lin, K.-H. Wei and M.-Y. Chiu, *Soft Matter*, **7**, 9276, (2011).

The first collaborative team access beamline at SLRI (BL 5.2)

Sukit Limpijumnong

School of Physics and NANOTEC-SUT Center of Excellence on Advanced Functional Nanomaterials, Suranaree University of Technology, Nakhon Ratchasima 30000, Thailand

On 1st August 2011 three institutes in Thailand, namely, Suranaree University of Technology (SUT), National Nanotechnology Research Center (NANOTEC) and Synchrotron Light Research Institute (SLRI) signed an agreement to evenly co-support the establishment of the *SUT-NANOTEC-SLRI Joint Research Facility*, where the members and associates from the three institutes can jointly utilize the facility, with the budget totaled at 45 million Baht (roughly \$1.5 million). The main propose of the project is to promote the utilization of synchrotron techniques for nanotechnology research. The planned flagship project of the facility was to build the first collaborative team access beamline at SLRI (BL 5.2) and its station. The beamline was designed for the XAS technique, which is the most heavily utilized synchrotron technique in Thailand. The beamline was completed and opened for use on 19th October 2012. The formal opening ceremony was graciously presided by HRH Princess Maha Chakri Sirindhorn – the crown princess of Thailand. The three institutes are evenly allocated the beamtime to be used by their members or their associates according to their own criteria. The technical detail of the beamline, the challenge and benefit of the collaborative team access scheme, and examples of research being carried out, will be presented.



The SUT-NANOTEC-SLRI XAS beamline (BL 5.2) at SLRI.

Resonant Photoemission studies of $\text{Ti}_{1-x}\text{Fe}_x\text{O}_{2-d}$ epitaxial films

R. J. Choudhary,* Komal Bapna and D. M. Phase

*UGC DAE Consortium for Scientific Research, Khandwa Road, Indore-01,
India.*

Abstract

We have investigated the structural and electronic properties of the epitaxial thin films of Fe doped (4 at. %) and undoped anatase TiO_{2-d} deposited pulsed laser deposition. The films reveal room temperature magnetic hysteresis behavior. We have examined the electronic environment of Ti and Fe using photoelectron spectroscopy measurements, which reveal the ionic state of Fe in TiO_2 , excluding the possibility of Fe metal clusters. Valence band spectra of these films mainly involve O-2p derived state. In Fe doped film, Fe derived state is also observed. Resonance photoelectron spectroscopy studies indicate that Fe ions are hybridized with the oxygen vacancy induced Ti 3p defect states. Our study reveals the formation of local magnetic moment and finite density of states at the Fermi level indicating its metallic (degenerate semiconducting) behavior in both the films, leading to magnetic ordering at room temperature and a Kondo minimum in resistivity behavior. Present work suggests that there is a competition between magnetic ordering mechanism by J_{RKKY} and moment screening mechanism by J_{Kondo} .

*Corresponding author: ram@csr.res.in

Phase Decomposition and Valence Change during Delithiation in Olivine-type $\text{LiFePO}_4/\text{FePO}_4$ System

- An Application of Simultaneous XRD and XAFS Measurements -

Eiichiro Matsubara¹, Kazuya Tokuda¹, Tomoya Kawaguchi¹,
Katsutoshi Fukuda², Masatsugu Oishi¹ and Tetsu Ichitsubo¹

¹ Dept. Mater. Sci. & Eng., Kyoto University, Kyoto 606-8501, Japan

² SACI, Kyoto University, Kyoto, 615-8520, Japan

The olivine-type lithium iron phosphate (LiFePO_4) [1] has been attracted great attention for positive electrodes of Li-ion batteries by largely improving its electron conductivity by carbon coating [2]. This material is characterized by the two-phase reaction of LiFePO_4 (LFP) and FePO_4 (FP). These two phases have the same structure symmetries with different lattice parameters. There is about 6.8% volume change between these two phases. Thus, the battery reaction is affected by large coherent strain, which is yielded due to the phase change.

In the present study, we experimentally determined the valence change from Fe(II) to Fe(III), and the phase decomposition from LFP to FP during delithiation by the simultaneous in situ XANES and resonant X-ray diffraction (XRD) measurements. The present measurements were carried out at the beam line BL-28XU (the Kyoto University-NEDO RISING beam line), SPring8. By simultaneously measuring the information on valence and structure in the same location of the sample by XANES and XRD, respectively, we can reveal a change of active materials inherent in the battery reaction without being affected by the reaction inhomogeneity due to various causes in batteries. The experimental relations between the volume fractions of Fe(II) and LFP, and Fe(III) and FP in Fig. 1 were determined from the experimental time dependence of the volume fractions of Fe (II) and Fe(III) by XANES and those of LFP and FP by XRD.

The relation in Fig. 1 provides us a new insight into the structure transition from LFP to FP under the influence of the large coherent strain. Namely, at the initial stage of the phase decomposition, the nucleation and growth of the FP phase in the LFP matrix is suppressed due to the large coherent strain. At a point (E in Fig. 1) where the volumes of the LFP phase and the FP phase are equal, the influence of the strain energy on the phase decomposition is reversed and the growth of the FP phase is accelerated at the latter stage. In our presentation, we also introduce the battery reaction analysis by the combination of XANES and resonance X-ray powder diffraction.

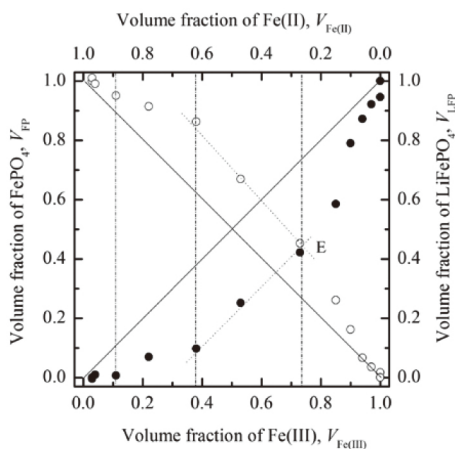


Fig. 1. Changes of the volume fractions of LFP (V_{LFP}) and FP (V_{FP}) vs. the volume fraction of Fe(III) ($V_{\text{Fe(III)}}$).

[1] A. K. Padhi, K. S. Nanjundaswamy, and J. B. Goodenough, J. Electrochem. Soc. 144, 1188 (1997).

[2] A. Yamada, S. C. Chung, and K. Hinokuma, J. Electrochem. Soc. 148, A224 (2001).

Biomedical Applications of Synchrotron-based Infrared Microspectroscopy at NSRRC

Yao-Chang Lee, Pei-Yu Huang and Ching-Iue Chen

National Synchrotron Radiation Research Center

No. 101 Hsin-Ann Road, Hsinchu Science Park, Hsinchu 30076, Taiwan

The end-station of synchrotron-based infrared microspectroscopy (SR-IMS) at BL14A1 of NSRRC in Taiwan is equipped with an infrared microspectroscopic bench of Fourier-transform infrared (FT-IR) spectrometer coupled with an infrared confocal microscope using infrared synchrotron radiation as light source. The unapertured focused infrared beam size of NSRRC synchrotron radiation at full width at half maximum (FWHM) of NSRRC is about $10 \times 13 \mu\text{m}^2$ for giving ultrahigh spatial resolution in FT-IR imaging acquisition, being utilized for the detection at diffraction limited sample area. Based on the advantage of ultrahigh spatial resolution of infrared synchrotron radiation, end-station of SR-IMS is able to be employed for acquiring ultrahigh spatially-resolved spectral image of functional group of bio-components within biological sample [1, 2]. In this study, we successfully demonstrated an innovative method of wax physisorption kinetics (WPK) for fast discriminating malignancy from normal for oral cavity cancer using N-alkanes of C22-C34 frame and beeswax ($\text{C}_{46}\text{H}_{92}\text{O}_2$) as diagnostic wax agents, and relative amount of residual wax onto cell surface was measured by using FT-IR imaging shown in the Fig. 1 [3]. Moreover, paraffin ($\text{C}_{25}\text{H}_{52}$) and beeswax are potential diagnostic wax agents and work excellently for screening colorectal cancer, gastric cancer, cervical cancer, and prostate cancer. The relative amount of residual wax adhering onto cell surface was employed as a signpost for differentiating malignancy from normal according to the variance of wax physisorption of membrane polarizability between normal and cancer cell. We proposed that oligosaccharides of residual glycoprotein within cell membrane play a crucial role of physisorption with wax agent during the treatment of acid-catalyzed hydrolysis and deglycosylation of PNG_{ase} F. Furthermore, bias-assisted wax physisorption kinetics (BA-WPK) was developed for establishing a new standard to define cancer grade of oral cavity cancer using breakdown bias of oligosaccharides of residual glycoprotein within cancer cell surface as applying external bias on cancer cells. Therefore, WPK-based cancer diagnosis could be a potential method for fast cancer screening and grading in the future clinic applications.

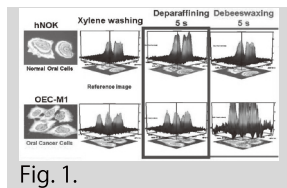


Fig. 1. The results of wax physisorption kinetics of normal and cancer human oral cavity cells showed a variant physisorption capability between paraffin and beeswax.

- [1] S.-E. Peng*, C.-S. Chen, Y.-F. Song, H.-T. Huang, P.-L. Jiang, W.-N. U. Chen, L.-S. Fang and Y.-C. Lee*, Biol. Lett. **8**(3), 434(2012)
- [2] R. R. Reisz*, T. D. Huang, E. Roberts, S.-R. Peng, C. Sullivan, K. Stein, A. LeBlanc, D.-B. Shieh, R.-S. Chang, C.-C. Chiang, C.-W. Yang, S.-M. Zong, Nature, 496, 210 (2013)
- [3] L.-F. Chiu, P.-Y. Huang, W.-F. Chiang, T.-Y. Wong, S.-H. Lin, Y.-C. Lee*, D.-B. Shieh*, Anal. Bioanal. Chem. **405**, 1995 (2013)

The notable low tolerance of rat skin and bone marrow to synchrotron radiation: A bio-safety evaluation of single dose synchrotron radiation X-ray on young rat legs

Yifan Lu, Guanghui Tang, Peng Miao, Xiangming Zhang, Xiaojie Lin, Yongting Wang, and Guo-Yuan Yang

Neuroscience and Neuroengineering Centre, Med-X Research Institute and School of Biomedical Engineering, Shanghai Jiao Tong University, Shanghai 200030, China

Synchrotron Radiation (SR) imaging *in vivo* is a novel experimental technique owing to its excellent imaging resolution and sensitivity. Since SR X-ray has high intensity, high collimation and monochromaticity, the tolerance of tissues to SR X-ray is unknown. In this study, we used SR X-ray to treat limb of rats to explore the tolerance of SR X-ray and to establish the safety threshold dose of SR X-ray *in vivo*.

Male Sprague-Dawley (SD, 5 weeks old) rats were randomly divided into 6 groups, which respectively subjected to 0, 0.1, 0.5, 1, 5 and 20 Gy single irradiation dose on left tibia and femur metaphyseal. The irradiation was performed in BL13W beam line at Shanghai Synchrotron Radiation Facility (SSRF). The number of red blood cell, white blood cell and platelet in circulating blood was examined up to 3 months. The responses of bone marrow and skin to SR X-ray were determined up to 6 months.

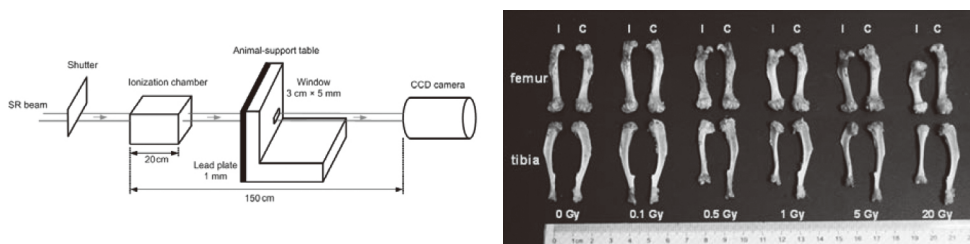


Fig.1 left was the illustration of irradiation device, right showed the discrepancy of femur and tibia length between ipsilateral and control lateral after 3 months of SR X-ray irradiation.

We found that 20 Gy treated group showed an acute decrease of lymphocytes and platelet at 2 days compared to the control ($n=14$, $p<0.05$) and it recovered after 7 days. Visible morphology changes including hair loss, moist desquamation and inhibition of bone growth were detected in 0.5, 1.5 and 20 Gy group, but not in 0.1 Gy treated group ($p<0.001$). Joint deformity could occur in 0.5, 1 and 5 Gy treated group while it was absent in 20 Gy treated group whose bone growth was quickly ended by severe ionizing radiation injury. Moreover, tumor formation was not observed in any groups up to 6 months.

We concluded that the safety threshold dose of SR X-ray for the skin and the bone marrow of young SD rats is between 0.1 Gy and 0.5 Gy. The reduction of lymphocytes and platelet occurred after local 20 Gy SR X-ray treatment, suggesting 20 Gy local irradiation can cause an influence at whole-body level.

Development of X-ray 2D Detector for SACLA

Takaki Hatsui

RIKEN Spring-8 Center

1-1-1 Kouto, Sayo-cho, Sayo-gun, Hyogo 679-5148

X-ray Free-Electron laser (XFEL) facilities are now enabling a new era of X-ray science owing to their high-peak intensity, pulse width down to a few femto-second, and full spatial coherence. In most of the XFEL experiments, samples are destroyed upon single pulse irradiation, and hence X-ray image data should be stored shot-by-shot. This experimental scheme gives also the opportunity to correlate the pulse characteristics, such as pulse intensity, pulse position, arrival time, etc., which are generally not stable with current XFEL generation technology.

These shot-by-shot data acquisition demands dedicated X-ray 2D detectors. Since the statistics of the data from the single shot cannot be improved by accumulating multiple shot data due to sample damage, data quality of each frame is the most important performance. Therefore one of the common requirements are (1) single photon detection, and (2) high peak signal. Furthermore, (3) x-ray radiation hardness more than 30 Mrad, and (4) frame rate matching the XFEL pulse period are mandatory. In order to meet these requirements, a multi-port charge-coupled device (MPCCD) detector has been developed. In this talk, MPCCD sensor and readout system is outlined.

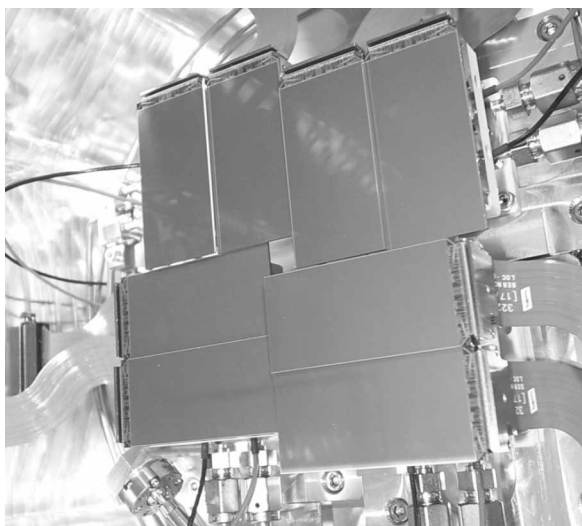


Fig. 1. Multi-port Charge-Coupled device (MPCCD) developed for SACLA. 8 sensors are arrayed to form imaging area of 100 mm x 100 mm. At the center, a rectangular hole with variable size is installed in order to avoid direct illumination of XFEL pulses.

Soft x-ray nanoscopes at the PLS: application activities and status

Hyun-Joon Shin, Jaeyoon Baik, and Jun Lim

*Pohang Accelerator Laboratory, Pohang University of Science and Technology,
Pohang, Kyungbuk, 790-784, Korea
shj001@postech.ac.kr*

In this presentation, current status of Pohang Light Source's soft-x-ray-based three nanoscopes and their activities will be introduced.

(1) Scanning photoelectron microscope (SPEM) has been operational for the past ~10 years and has been utilized in order to investigate local chemical states and electronic structures on the surface and interfaces. The space resolution is 500 ~ 1000 nm and usable photon energy range is about 400 ~ 1100 eV. The schematic and basic specifications of the SPEM and its application examples, such as investigation of phase separated diluted magnetic semiconductors and functionally modified graphene surfaces, will be provided.

(2) A compact transmission x-ray microscope (TXM) has been developed. This TXM has no dedicated beamline but is easily mountable to any beamline and is efficient in alignment. Sample is placed in air. The space resolution is around 30 nm at the photon energy of 500 eV and data acquisition time is typically 1 ~ 10 sec with a bending magnet beamline radiation. With this TXM, nano-particles and bio samples in solution are intensively being investigated.

(3) A scanning transmission x-ray microscope (STXM) is under construction at an elliptically polarized undulator beamline. The STXM is expected to be commissioned from this autumn. The expected space resolution is in the range of 20 ~ 50 nm at the photon energy range of 250 eV ~ 1500 eV, with spectral resolving power ($E/\Delta E$) of 3000 ~ 5000.

Real-time observation of surface chemical reaction at millisecond resolution by means of soft X-ray dispersive XAFS

Kenta Amemiya,¹ Yuka Kousa,² Shuichi Nakamoto,² Taiga Harada,² Shogo Kozai,² Masaaki Yoshida,² Hitoshi Abe,^{1,2} Ryohei Sumii,¹ Masako Sakamaki,¹ Kazuma Suzuki,² Hiroshi Kondoh,² Tsuneharu Koide,¹ Kenji Ito,¹ Kimichika Tsuchiya,³ Kentaro Harada,³ Hiroyuki Sasaki,³ Tomohiro Aoto,³ Tatsuro Shioya,³ Takashi Obina,³ Shigeru Yamamoto¹ and Yukinori Kobayashi³

¹*Institute of Materials Structure Science, High Energy Accelerator Research Organization, 1-1 Oho, Tsukuba, 305-0801 Ibaraki, Japan*

²*Department of Chemistry, Faculty of Science and Technology, Keio University, 3-14-1 Hiyoshi, Kohoku-ku, 223-8522 Yokohama, Japan*

³*Accelerator Laboratory, High Energy Accelerator Research Organization, 1-1 Oho, Tsukuba, 305-0801 Ibaraki, Japan*

A dispersive XAFS technique in the soft X-ray region has been developed, as illustrated in Fig. 1, to realize the real-time observation of surface chemical reactions at one event, and a time resolution of 33 ms [1] or faster has been achieved. The observation of the CO oxidation reaction on Ir(111) surface is shown in Fig. 2 as an example. The coverage of each species at the surface during the reaction is quantitatively estimated from a series of XAFS spectra. Moreover, the observation of the changes in the molecular orientation within one reaction has been also achieved [2] by combing the dispersive XAFS technique with polarization switching [3] between the horizontal and vertical linear polarizations.

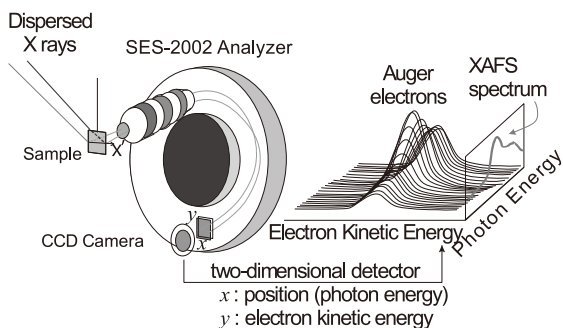


Fig. 1. Schematic layout for dispersive XAFS measurement. The position, x' , on the sample surface corresponds to the photon energy. The Auger electrons emitted at x' after X-ray absorption are separately corrected at x on the two-dimensional detector, yielding the XAFS spectrum.

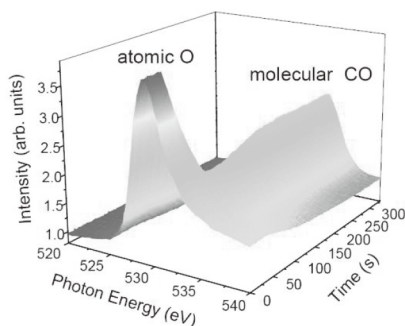


Fig. 2. Three-dimensional plot of O K-edge XAFS spectra taken at every 33 ms during the exposure of O/Ir(111) surface to 4×10^{17} Torr CO at 400 K.

[1] K. Amemiya *et al.*, Appl. Phys. Lett. **99**, 074104 (2011).

[2] K. Amemiya *et al.*, Appl. Phys. Lett. **101**, 161601 (2012).

[3] K. Amemiya *et al.*, J. Phys.: Conf. Ser. **425**, 152015 (2013).

Feasibility Studies of Single Molecule Scattering Analysis with X-ray Free Electron Lasers

Kyungtae Kim¹, Heesoo Kim^{*2}, Tai-Hee Kang³, Moonhor Ree^{*1,3}

¹*Department of Chemistry, Division of Advanced Materials Science, Center for Electro-Photo Behaviors in Advanced Molecular Systems, Polymer Research Institute, and BK School of Molecular Science, Pohang University of Science and Technology (POSTECH), Pohang, 790-784, Republic of Korea*

²*Department of Microbiology, Dongguk University College of Medicine, Gyeongju 780-714, Republic of Korea*

³*Pohang Accelerator Laboratory (PAL), Pohang University of Science and Technology, Pohang, 790-784, Republic of Korea*

The feasibility of single molecule elastic scattering analysis with the X-ray free electron laser (XFEL) sources in operation and under construction around the world was investigated for various biological and synthetic materials (pepsin, polyethylene, poly(4,4'-oxydiphenylene pyromellitimide), and ferric oxide). This study found that existing XFEL facilities provide coherent pulse X-ray beams with the required energies (8.3–12.4 keV) but their fluxes are too low for single molecule elastic scattering experiments to determine the three-dimensional structures of such molecules; for single molecule scattering, the XFEL facilities need to improve their beam flux density to 2×10^{15} to 7×10^{18} photons pulse⁻¹μm⁻² depending on the beam energy. However, the existing XFEL facilities' sources were found to enable the elastic scattering analysis of pepsin and the synthetic polymers in sample sizes of 1–60 μm as well as of ferric oxide in sample sizes ≥80 nm. These criteria for the sample size can be extended to other soft (biological, organic, and polymer molecules) and hard (molecules containing heavy metals) materials. In addition, the inelastic scattering, absorption, and radiation damage characteristics of the chosen materials when exposed to the XFEL sources were examined.

Development of Very Short Period Undulators

Shigeru Yamamoto

*Photon Factory, Institute of Materials Structure Science,
High Energy Accelerator Research Organization, KEK
Oho, Tsukuba, Ibaraki 305-0801, Japan*

*Department of Materials Structure Science,
The Graduate University for Advanced Studies
Oho, Tsukuba, Ibaraki 305-0801, Japan*

The energy of photons from undulators is inversely proportional to the period length of the undulator field and proportional to the square of the electron-beam energy. Hard x-ray radiation was usually generated with in-vacuum undulators with period lengths of several cm installed in electron storage rings with 6-8GeV energies[1, 2]. Construction of newer sources has recently been planned and partly realized in compact 3rd generation light sources with in-vacuum undulators of period lengths around 20mm [3]. This was preceded by the construction of three in-vacuum-type undulators at the Photon Factory (PF), High Energy Accelerator Research Organization, KEK. It proved that these short gap undulators were very useful as hard x-ray sources in the 2.5-GeV storage ring [4, 5].

As the next step, we have been exploring a method to fabricate very short period undulators. Here, “very short period” means periods one order-of-magnitude shorter than the ordinary period of several cm. We are developing a plate-type magnet some 100mm long with a period length of 4mm in the longitudinal direction. We selected 4-mm period since we can generate 12-keV radiation with the first harmonic of this undulator in the 2.5-GeV storage ring. The very short period undulators operate in a gap one order-of-magnitude shorter than that of ordinary undulators. Thus these undulators are very useful when they are combined with very low emittance storage rings and linacs.

A multi-pole magnetizing method was applied to magnetizing this plate: a periodic undulator field (of 4-mm period in this case) was generated by pulsed electro-magnets, and was transcribed into the plate. The magnetization procedure allows the undulator field to be obtained in a very short gap between the pair of opposing plates [6]. Here we report the magnetization method to obtain a very short period and present the test results. The spectrum calculation of the radiation from the measured undulator field compares well with that from an ideal magnetic field in the region of the fundamental radiation, and the radiation from 10 to 15keV was found to be useful for synchrotron radiation experiments in case of 2.5-GeV energy of the electron beam.

-
- [1] S. Yamamoto, X. Zhang, H. Kitamura, T. Shioya, T. Mochizuki, H. Sugiyama and M. Ando, J. Appl. Phys. **74**, 500 (1993).
 - [2] e.g. <http://www.esrf.eu/>, <http://www.aps.anl.gov/> and <http://www.spring8.or.jp/>.
 - [3] e.g. <http://www.psi.ch/sls/>, <http://www.bnl.gov/ps/nsls2/about-NSLS-II.asp> and <http://www.lunduniversity.lu.se/research-and-innovation/max-iv-and-ess>.
 - [4] S. Yamamoto, K. Tsuchiya and T. Shioya, AIP Conf. Proc. **879**, 384 (2007).
 - [5] S. Yamamoto, K. Tsuchiya, H. Sasaki, T. Aoto and T. Shioya, AIP Conf. Proc. **1234**, 599 (2010).
 - [6] S. Yamamoto, Journal of Phys.: Conf. Ser. **425** 032014 (2013).

Radiation Damage and Aging Accelerator Components at the SPring-8

Shigeki Sasaki

SPring-8/JASRI

Sayo1-1-1, Hyogo 679-5198, Japan

We encountered degradations caused by the radiation damages or aging of the accelerator components, during more than 16 years of operation of SPring-8 accelerator complex. Some of them invoked beam aborts during the user time. Others were found in the occasion of the regular inspections during annual maintenance periods, and had no effects on the user time, but countermeasures or cures were required. Some cases of these experiences will be presented.

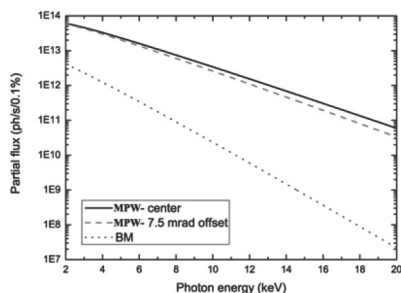
Examples of the degradations are pneumatic tube breaks, corrosion of water cooling pipes by chemicals in the cooling water, chemical reactions induced by synchrotron radiation in the absorber cooling water path, radiation damage on the rubber hoses for magnet cooling water, etc. Some of them were caused by inadequate usage condition, while the others occurred even under normal usage conditions. Causes of these phenomena will be described. Countermeasures including such as shielding of the components from the scattered X rays, modification of the structure of the absorbers will be also presented.

Multipole wiggler beamlines at the Siam Photon Laboratory

P. Chirawatkul, S. Tancharakorn, S. Soontaranon, J. Chairapa and S. Rugmai

*Synchrotron Light Research Institute (Public Organization), P.O. Box 93,
Nakhon Ratchasima 30000 Thailand*

A 2.4 Tesla multipole wiggler (MPW) is being installed in the straight section number one of the Siam Photon Source (SPS) [1] at SLRI. The MPW is on loan from ASTEC, UK, and is the world's highest field permanent magnet wiggler [2,3]. Three branched x-ray beamlines are under construction to utilize the MPW radiation. BL1.1W, jointly funded by SLRI and Khon Kaen University, will be a multi-technique x-ray beamline, having capability of performing X-ray Absorption Spectroscopy (XAS), X-ray Diffraction (XRD), X-ray Fluorescence (XRF) and X-ray Scattering (SAXS/WAXS), with the priority given to XRD and XAS and the coupling of the two techniques. BL1.2W is an imaging beamline planned for X-ray Imaging, X-ray Tomography and micro-beam X-ray Fluorescence. The beamline is primarily aimed at biomedical, environmental and archaeological applications. BL1.3W is a dedicated SAXS beamline which will be transferred, with some modification, from the existing SAXS beamline BL2.2 [4]. The three beamlines are expected to have the photon flux around two orders of magnitude higher than the bending magnet source of the SPS in the photon energy range of 5-20 keV. The SAXS beamline, BL1.3W, will be in operation at the end of 2013, while BL1.1W and BL1.2W are planned to be completed and operational at the beginning of 2015.



The figure shows calculated partial flux from the center beamline for BL1.2W (solid line), the 7.5 mrad branches for BL1.1W and BL1.3W (dashed line), compared to the bending magnet source (dotted line).

-
- [1] P. Klysubun et. al., Nucl. Instr. Meth. Phys. Res. **A582**, 18 (2007).
 - [2] J. Clarke et. al., Proceeding of Particle Accelerator Conference, 2656 (1999).
 - [3] F. Hannon, ASTeC-ID-002, November 2002.
 - [4] S. Soontaranon and S. Rugmai, Chinese J. Phys. **50**, 204 (2012)

XAFS facility at INDUS-2 Synchrotron Radiation source and recent results.

Shambhu Nath Jha, Dibyendu Bhattacharyya, Ashwini Kumar Poswal, Ankur Agrawal, Sohini Basu, Ashok Kumar Yadav, Chandrani Nayak and Naba Kishore Sahoo

Atomic & Molecular Physics Division, Bhabha Atomic Research Centre, Trombay, Mumbai-400 085, India.

X-ray absorption fine structure (XAFS) spectroscopy is a well established materials characterisation technique for studying the local structure around selected elements that are contained within a material. The technique can be applied to any type of material viz. amorphous, crystalline, polycrystalline, surfaces, thin films, liquid, and solution.

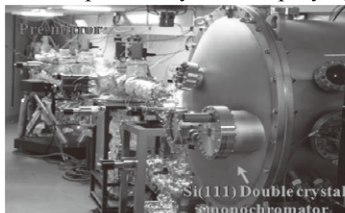


Fig. 1. A view of scanning XAFS beamline
Fig. 1. A view of scanning XAFS beamline



Fig. 2. A view of dispersive XAFS beamline

Atomic and Molecular Physics Division, BARC has over the last few years developed a comprehensive XAFS measurement facility at INDUS-2 Synchrotron Radiation Source, RRCAT, Indore, India to cater the needs of the scientists and researchers of India. The above facility consists of two beamlines namely: i) Energy Dispersive EXAFS beamline and ii) Energy Scanning EXAFS beamline. Both of these beamlines are based on bending magnet source. The Dispersive EXAFS beamline [1], which had been set up at the BL-8 port of INDUS-2, and is operational for last few years, uses a bent crystal polychromator and a position sensitive CCD detector and works in the dispersive mode in the energy range of 5 -20keV. The second beamline viz., energy scanning type EXAFS beamline uses a double crystal monochromator and a collimating pre-mirror and focussing post-mirror based optical system. This beamline, which has been setup at BL-9 port of INDUS-2, has been commissioned recently. The beamline operates in the energy range of 4 to 25 keV.

Efforts have been made over the last few years to widen the scope of XAFS experiments by introducing low temperature, high temperature and high pressure facilities in the above beamlines. In this presentation, the current status of the XAFS beamlines, including their optical layout, operational parameters and the instrumentation available for the users along with future up-gradation plan will be discussed. Highlights of recent results will be utilised to demonstrate the beamline capabilities.

[1] Bhattacharyya D, Poswal A K, Jha S N, Sangeeta and Sabharwal S C 2009 Nuclear Instruments and Methods in Physics Research A 609 286.

Stroboscopic approach for the quantitative X-ray phase imaging of periodic processes in soft materials using X-ray Talbot interferometry

Margie P. Olbinado^{*}, Patrik Vagovič¹, Wataru Yashiro¹ and Atsushi Momose¹

Dept. of Advanced Materials Science, Graduate School of Frontier Sciences, The University of Tokyo, 5-1-5 Kashiwanoha, Kashiwa, Chiba 277-8561, Japan

¹*Institute of Materials Research for Advanced Materials, Tohoku University, 2-1-1 Katahira, Aoba-ku, Sendai, Miyagi 980-8577, Japan*

X-ray phase imaging is a valuable tool for non-destructive visualization of soft materials such as biological tissues and polymers. Because it is a non-invasive imaging technique, x-ray phase imaging is a very good candidate for the investigation of many dynamic processes in soft materials [1]. However, the realization of quantitative X-ray phase imaging with a good temporal and spatial resolution remains a challenge [2-5]. A demonstration of the new time-resolved imaging technique called the stroboscopic X-ray Talbot interferometry that is applicable for the visualization of periodic processes in soft materials will be presented. X-ray phase imaging was performed via the phase stepping technique in which each moiré image was obtained by repeatedly acquiring an image of a specific phase of a motion in which an object was captured “frozen in time”. This technique achieves a quantitative X-ray phase imaging, which was not easily achieved by the recent reports using propagation-based and analyzer-based methods. A microsecond temporal resolution was achieved in contrast with the previously reported millisecond temporal resolution using non stroboscopic X-ray Talbot interferometry with white synchrotron radiation [5]. Figure 1 shows the X-ray differential phase image of a PMMA sphere moving at 1.4 ms/ captured stroboscopic with a camera exposure time of 8 μ s in comparison with a non-stroboscopic image captured at 0.3 ms.

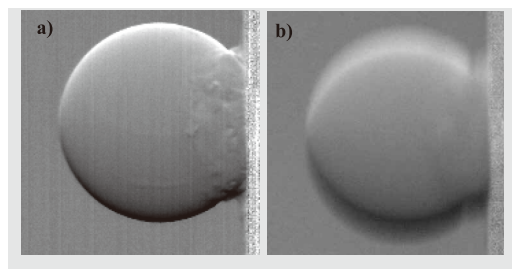


Fig. 1. X-ray differential phase images of a PMMA sphere ($\phi = 3.2\text{mm}$) attached at the edge of a disk rotating at 5 rev/s. The sphere was moving at 1.4 m/s downward and captured: (a) stroboscopic with 8 μ s exposure time, and (b) non-stroboscopic with 0.3 ms exposure time.

- [1] A. Momose: Jpn. J. Appl. Phys. **44** (2005) 6355.
- [2] S. Dubsky, S. B. Hooper, K. K. W. Siu, and A. Fouras: J. R. Soc. Interface **9** (2012) 2213.
- [3] M. J. Kitchen¹, D. M. Paganin, K. Uesugi, B. J. Allison, R. A. Lewis, S. B. Hooper and K. M. Pavlov: Phys. Med. Biol. **56** (2011) 515.
- [4] T. Takeda, A. Yoneyama, J. Wu, Thet-Thet-Lwin, A. Momose and K. Hyodo: J. Synchrotron Rad. **19** (2012) 252.
- [5] A. Momose, W. Yashiro, S. Harasse, and H. Kuwabara: Opt. Express **19** (2011) 8423.

Xeniya Kozina

Japan Synchrotron Radiation Research Institute (JASRI)
SPring-8

This presentation will give a short overview of the experience and valuable knowledge gained as a participant of the 6th Cheiron School held at Spring-8 in September 2012.

Aiming to provide useful and basic knowledge as well as perspectives of synchrotron radiation science and technology and promoting the cooperation between young researchers in the field of synchrotron radiation the school might be very useful not only for graduate students but also for postdoctoral fellows.

Clear and at the same time informative lectures and site tours at Spring-8 facilities give an opportunity to learn about a wide range of experimental methods in a variety of research areas based on synchrotron radiation. Meeting the experts allowed detailed discussions in the selected fields giving a deep understanding of techniques and methods of interest. Very well organized beamline practical provide a unique chance to be exposed to a real beamtime experiment obtaining the necessary understanding of the method of choice and information that can be obtained with particular measurements as well as the details of beamline and experiment setup. All this, being quite encouraging, motivating for one's own research, serves as useful base for the step forward in one's research career inspiring and giving ideas for the perspective experiments.

With my personal research realization I would like to express my deepest gratitude to the organizers for providing such useful and helpful opportunities in the area of synchrotron radiation technologies.

Great Memories of the Cheiron School

Brendan J. Kennedy

School of Chemistry, The University of Sydney, Sydney, NSW 2006 Australia

One of the most important activities of the AOFSSRR is the annual Cheiron School which is now in its seventh year. The main aim of the Cheiron School is to introduce young researchers, working in the Asia-Ocenia region, who are interested in pursuing a career using synchrotron radiation to the fundamentals of the production and applications of synchrotron radiation. The School consists of a series of lectures and practical exercises. Since forming networks throughout the region is an important goal of the Cheiron School the students are also presented with a number of social events.

In this presentation I shall reflect upon the last six Cheiron Schools, starting with the first school held in 2007.

Cheiron2007

The 1st AOFSSRR Summer School

The 7th AOFSSRR

**Cheiron
School
2013**

**SPRING-8, Japan
Sept 24th - Oct 3rd**



ABSTRACTS - POSTER PRESENTATION -

Abstracts with the image of Cheiron " are presented by the participants of the Cheiron School 2013.

Stroboscopic approach for the quantitative X-ray phase imaging of periodic processes in soft materials using X-ray Talbot interferometry

Margie P. Olbinado^{*}, Patrik Vagović¹, Wataru Yashiro¹ and Atsushi Momose¹

Dept. of Advanced Materials Science, Graduate School of Frontier Sciences, The University of Tokyo, 5-1-5 Kashiwanoha, Kashiwa, Chiba 277-8561, Japan

¹*Institute of Materials Research for Advanced Materials, Tohoku University, 2-1-1 Katahira, Aoba-ku, Sendai, Miyagi 980-8577, Japan*

X-ray phase imaging is a valuable tool for non-destructive visualization of soft materials such as biological tissues and polymers. Because it is a non-invasive imaging technique, x-ray phase imaging is a very good candidate for the investigation of many dynamic processes in soft materials [1]. However, the realization of quantitative X-ray phase imaging with a good temporal and spatial resolution remains a challenge [2-5]. A demonstration of the new time-resolved imaging technique called the stroboscopic X-ray Talbot interferometry that is applicable for the visualization of periodic processes in soft materials will be presented. X-ray phase imaging was performed via the phase stepping technique in which each moiré image was obtained by repeatedly acquiring an image of a specific phase of a motion in which an object was captured “frozen in time”. This technique achieves a quantitative X-ray phase imaging, which was not easily achieved by the recent reports using propagation-based and analyzer-based methods. A microsecond temporal resolution was achieved in contrast with the previously reported millisecond temporal resolution using non stroboscopic X-ray Talbot interferometry with white synchrotron radiation [5]. Figure 1 shows the X-ray differential phase image of a PMMA sphere moving at 1.4 ms/ captured stroboscopic with a camera exposure time of 8 μ s in comparison with a non-stroboscopic image captured at 0.3 ms.

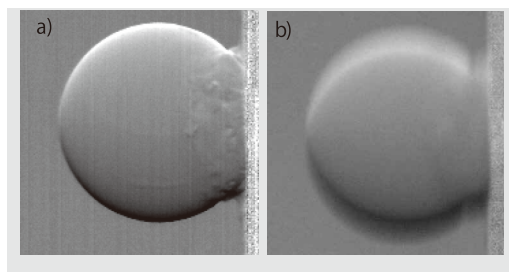


Fig. 1. X-ray differential phase images of a PMMA sphere ($\varphi = 3.2\text{mm}$) attached at the edge of a disk rotating at 5 rev/s. The sphere was moving at 1.4 m/s downward and captured: (a) stroboscopic with 8 μ s exposure time, and (b) non-stroboscopic with 0.3 ms exposure time.

-
- [1] A. Momose: Jpn. J. Appl. Phys. **44** (2005) 6355.
 - [2] S. Dubsky, S. B. Hooper, K. K. W. Siu, and A. Fouras: J. R. Soc. Interface **9** (2012) 2213.
 - [3] M. J. Kitchen, D. M. Paganin, K. Uesugi, B. J. Allison, R. A. Lewis, S. B. Hooper and K. M. Pavlov: Phys. Med. Biol. **56** (2011) 515.
 - [4] T. Takeda, A. Yoneyama, J. Wu, Thet-Thet-Lwin, A. Momose and K. Hyodo: J. Synchrotron Rad. **19** (2012) 252.
 - [5] A. Momose, W. Yashiro, S. Harasse, and H. Kuwabara: Opt. Express **19** (2011) 8423.



The design of infrared beamline at SSRF

Te Ji, Min Chen

*Shanghai Institute of Applied Physics, Chinese Academy of Sciences,
NO.2019 JiaLuo Road, Jiading District, Shanghai, 201800, China*

The infrared (IR) beamline (BL01B) at the third generation Shanghai Synchrotron Radiation Facility (SSRF) will be opened to users at the end of 2013. The designed IR beamline project concerns two end stations at SSRF, one dedicated to time resolved IR spectroscopy, and another dedicated to IR microspectroscopy.

The optical schematic for IR beamline layout is shown at Fig. 1. The first optical component of the beamline is the plane mirror M1 with slot size of 2.6mm. It deflects the photon beam by 90° in the horizontal direction. The second flat mirror M2, directs the photon beam vertically, to a toroidal mirror T1. The beam will be directly outwards, and converges to CVD diamond window. The toroidal mirror T2 provides collimated beam and downwards turns the beam 90° . Two active feedback systems are installed after the toroidal mirror T2 to reduce the noise level of the beamline. Then the collimated IR light enters into the endstations (not shown in Fig. 1).

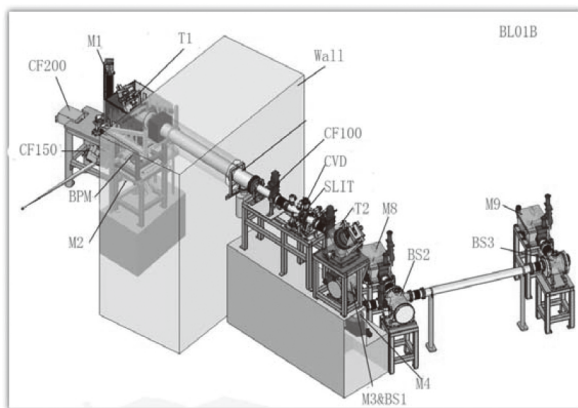


Fig. 1. The layout of IR beamline. (M: Flat Mirror; T: Toroidal mirror; BS: Beam splitter)



Numerical Simulation of MLLs with Layer Displacement Error

Keliang Liao

Weifan Sheng

Institute of High Energy Physics Chinese Academy of Science

15#

Beijing Synchrotron Radiation Facility

Institute of High Energy Physics

Chinese Academy of Sciences

P. O. Box 918, 100049 Beijing

R. P. China

The influences of the displacement error of each layers in tilted Multilayer Laue Lens(MLLs) is simulated by Beam Propagation method(BPM)^[1]. We investigate the convergence of BPM in our cases , then compare the wave field distributions in the output plane and focal plane with the results calculated by Takagi-Taupin description(TTD) of dynamical diffraction theory^[2]. The two methods coincidence very well. After adding the layer displacement error in the MLLs , the input wave field is propagated through MLLs and to the focal plane. The FWHM and focusing efficiency of the focal spot is presented.

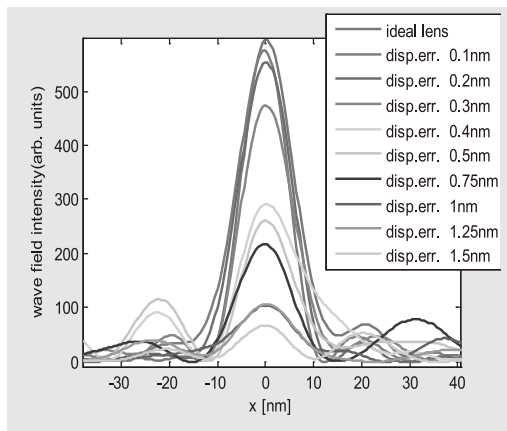


Fig. 1.Wave field intensity distribution in the focal plane. The main parameters of the tilted MLL are: $E=19.5\text{keV}$, Si/WSi_2 , $x_{\text{max}}=30\mu\text{m}$, $f=4.72\text{mm}$, $\text{tilt_angle}=1.6\text{mrad}$

A sequence of displacement error is added to layers in the MLLs. After getting the wave field distribution in the output plane of the focusing lens, We employ Fresnel-Kirchhoff integral^[3] to calculate the intensity distribution near the focal plane. As expected, the displacement error of layers leads to the decrease of focusing efficiency and a broadening of the focal spot. As the displacement error

can be measured by scanning electron microscope(SEM), We plan to use this simulation method to calculate the wave field distribution behind a real tilted MLL with imperfections.

[1]Thylén. L, Optical and Quantum Electronics ,15(5) (1983).

[2] H. F. Yan, J. Maser, A. Macrander, Q. Shen, S. Vogt, G. B. Stephenson, and H. C. Kang, Phys. Rev. B **76**, 115438 (2007).

[3] M. Born and E. Wolf, *Principles of Optics*, 7th ed. (Cambridge University Press, Cambridge, 1999).



Micron X-ray Protein Crystallography Beamline Design Calculated in Phase Space Analysis

Yi-Jr Su, Din-Goa Liu, Shih-Chun Chung, and Chien-Hung Chang

101 Hsin-Ann Road, Hsinchu Science Park, Hsinchu 30076, Taiwan

X-ray crystallography is a powerful method to define the arrangement of atoms. This technique enables us to observe protein structures and their interaction with other molecules or enzymes. Moreover, it can help to develop the new cures for diseases and the designs of novel drugs. Hence, it is importance to develop the micron x-ray protein crystallography beamline. Phase space analysis (PSA) is a useful approximate method to estimate the performance of beamline designs in synchrotron radiation x-ray optics. This analytic method in position-angle-wavelength space concisely represents widths, angular divergences, and intensities of the x-ray beam. All acceptance functions of the optical components are based on the approximation of Gaussian distribution. The parameters of an x-ray beam can be defined simultaneously in the horizontal and vertical plane by matrix algebra. The intensity of an x-ray source is represented by its brilliance [1-3] and the mathematical form is given by $I(x, x', z, z', \lambda) = I(0, 0, 0, 0, \lambda) I_x(x, x') I_z(z, z') I_\lambda(\Delta\lambda/\lambda)$, where $I_x(x, x') = \exp\{-(1/2)[x^2/\sigma_x^2 + x'^2/\sigma_{x'}^2]\}$, $I_z(z, z') = \exp\{-(1/2)[z^2/\sigma_z^2 + (z' - \Gamma z)^2/\sigma_{z'}^2]\}$, and $I_\lambda(\Delta\lambda/\lambda) = \exp\{-(1/2)[(\Delta\lambda/\lambda)^2/\sigma_\lambda^2]\}$. $I(0, 0, 0, 0, \lambda)$ is the brilliance at the center of the beamline source. The parameters of σ_x , $\sigma_{x'}$, σ_z , and $\sigma_{z'}$ are the standard deviations of the source size and the divergence in both perpendicular to the optical axis, and λ is the x-ray wavelength. The parameter of Γ is zero and σ_λ depends on the use of beamlines for an undulator source. The coordinate transformation in the phase space from source to sample is described by $M_{source}(x, x', \Delta\lambda/\lambda) = T_1 T_2 \dots T_N M_{sample}(x, x', \Delta\lambda/\lambda)$ [1-3], where T_i is the inverse of the transformation matrix of the i th optical component. Here, the parameters of σ_x , $\sigma_{x'}$, σ_z , $\sigma_{z'}$, and σ_λ are 0.12 mm, 18 μ rad, 4.92×10^{-3} mm, 8.59 μ rad, and 3.94×10^{-3} , respectively. In this study PSA is used to calculate the parameters of the micron x-ray protein crystallography beamline and the beam size (HxV, FWHM) and divergence (HxV, FWHM) in the sample position are $51.9 \times 3.9 \mu\text{m}^2$ and $68 \times 250 \mu\text{rad}^2$, respectively.

[1] J. S. Pedersen and C. Riekel, J. Appl. Crystallogr. **24**, 893–909 (1991).

[2] D.-M. Smilgies, Appl. Opt. **47**, E106–E115 (2008).

[3] C. Ferrero, D.-M. Smilgies, C. Riekel, G. Gattaa, and P. Dalyc, Appl. Opt. **47**, E116–E124 (2008).

The meso-scale order structure of immiscible polymer blends

Junhyeok JANG¹, Tsuyoshi INOUE¹, Hirohisa YOSHIDA¹, Masayuki KAWAZOE²

¹Graduate School of Urban Environmental Science, Tokyo Metropolitan University, 1-1 Minamiosawa, Hachioji-si Tokyo 192-0397, Japan,

²Yokoham Rubber Co. Ltd., Oiwake, Hiratsuka, Kanagawa 254-8651, Japan

¹Tel: +81-426-77-2844 Fax: +81-426-77-2821

E-mail:inoue-tsuyoshi@ed.tmu.ac.jp

Various nano-scale order structures formed by the micro phase separation of block copolymers are reported. On the other hand, the macro phase separation of immiscible polymer blends scarcely forms the order structure. We have reported the two dimensional hexagonally packed sphere structures in meso-scale based on the macro phase separation obtained by solvent casting from immiscible polymer blend solution ¹⁾.

Styrene butadiene rubber (SBR, Nihon Zeon Nipol 1502, styrene content ratio 23.5 % , Mw = 4.2×10^5) and acrylonitrile butadiene rubber (NBR, Nihon Zeon Nipol 1042 acrylonitrile content ratio 33.5 % , Mw = 4.5×10^5) were solved in Toluene and THF (3 wt %) with various blend contents. Within 3 days, the solution was separated to two phase. Subsequently, the solution was cast on Si wafer at room temperature. The obtained thin film was investigated by AFM (E-sweep, SII) and GISAXS (SPRing-8, FSBL03XU)

Two dimensional hexagonally packed sphere structures were obtained by solvent casting from the SBR-rich layer of equilibrium phase separated NBR/SBR toluene solution. The diameter and the thickness of sphere domain was about 1~3 μm and about 40 ~ 100 nm, respectively. The thickness of thin film was about 7 μm , thus the sphere domain was rather flat. The diameter of sphere and the distance between spheres depended on NBR fraction of NBR/SBR solution. From the AFM phase image analysis of the order structure, the spheres consisted of NBR shell and NBR rich core. Figure 1 show GISAXS profile of the thin film casting from equilibrium SBR rich phase in toluene solution. The sharp diffraction arc was

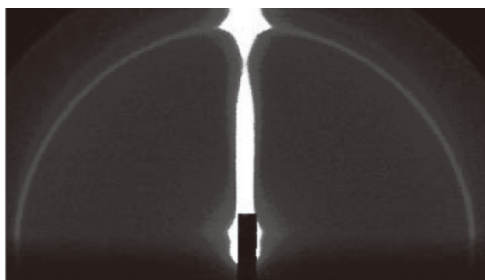


Fig. 1. 2D GISAXS image of NBR/SBR blend thin film

observed at $q = 2.4 \text{ nm}^{-1}$, which assigned to the order structure in acrylonitrile sequence of NBR. The azimuth profile of the diffraction at 2.4 nm^{-1} , two maximums at 38 and 143° were observed. GISAXS profile indicated that the stacked structure of acrylonitrile sequence existed in the NBR shell of sphere. At the early stage of phase separation from NBR/SBR toluene solution, NBR aggregated on the interface of NBR rich phase, acrylonitrile sequences had an important role of meso-scale order structure.

[1] J. H. Jang, T. Inoue, M. Kawazoe and H. Yoshida, Polym. Prepr. Jp., **61**, 1234 (2013).

Multilayer structure of PbS/EuS nanocrystals revealed by combining of synchrotron small-angle X-ray scattering method and energy dispersive X-ray spectroscopy

Hiroyasu Masunaga, Hiroki Ogawa, Sono Sasaki, Takaaki Hikima, Masaki Takata, Takuya Nakashima, Tsuyoshi Kawaid

*Japan Synchrotron Radiation Research Institute(JASRI)
1-1-1, Sayo, Sayo, Hyogo, 679-5198, Japan*

Multilayer nanostructure analysis has been carried out for core-shell PbS/EuS NCs by the combination of the synchrotron SAXS measurement and EDS-TEM observation. Structure information on the PbS/EuS NCs was obtained from EDS-TEM images to construct their initial structure models for SAXS intensity analyses. With statistically high precision, structure of the PbS/EuS NCs was successfully analyzed using a trilayer-cubic core-shell structure model by combining different techniques of SAXS and EDS-TEM. SAXS measurement of NCs carried out at BL45XU in the SPring-8 (RIKEN SPring-8 Center, Japan). Fig. 1a shows a transmission electron microscopic (TEM) image of PbS NCs, which is core particles. It was found that the shape of the PbS NCs was a quasi-cube with a narrow size distribution. An electron density profile, $\rho(r)$, of this spherical structure was indicated in Fig. 1b. If cubes orient in the statistically random direction in the solvent, their electron density distribution can be regarded approximately as that of a core-shell electron density distribution model. The electron density of the core with a radius of L is defined as ρ_1 . Here, ρ_1 denotes the electron density of PbS crystal. Also, L means half the side length of a cubic particle. Fig. 1c show SAXS profiles of PbS NCs measured for their hexane solution, and simulated scattering profiles on the basis of electron density models of randomly-rotating spherical and cubic structures. L of a reasonable cubic structure was determined as 4.6 nm in average so as to minimize a difference in the peak position around q equal to 1.0 nm^{-1} and 2.2 nm^{-1} between measured and simulated profiles.

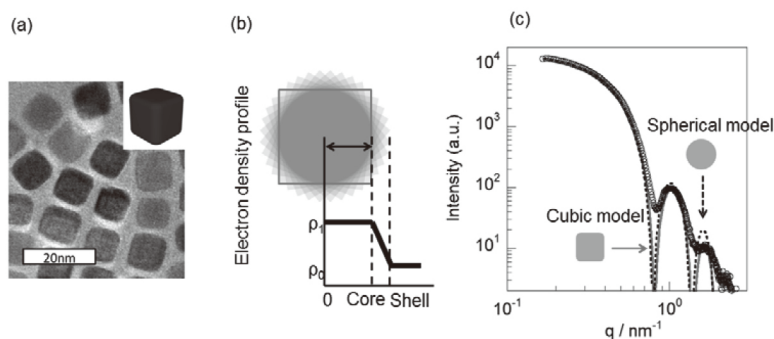


Fig. 1 A TEM image of PbS NCs. The shape of PbS NCs was a quasi-cube with a side length of 9.7 nm with a narrow size distribution (a). An electron density profile of a randomly-rotating cubic model in a solvent (b), scattering profiles measured for the PbS NCs (open circle) and simulated ones using spherical and cubic structures (lines) (c).

Multi-scale surface and interface measurement system for soft-material films at SPring-8.

H. Ogawa¹, K. Yamamoto², A. Fujiwara¹, N. Yagi¹, M. Takata¹, A. Takahara², K. Sakurai², T. Kanaya², T. Takeda³ and H. Matsuda³

¹Japan Synchrotron Radiation Research Institute (JASRI/SPring-8), 1-1-1 Kouto, Sayo, Hyogo 679-5198, Japan

²Representatives of the academic members of FSBL, 1-1-1 Kouto, Sayo, Hyogo 679-5198, Japan

³Representatives of the industrial members of FSBL, 1-1-1 Kouto, Sayo, Hyogo 679-5198, Japan

A new experimental system has been launched by coupling with the measurement techniques, which include grazing incidence small/wide angle X-ray scattering (GISWAXS) and grazing incidence X-ray diffraction (GIXD), as well as X-ray reflectivity (XR), at the BL03XU beamline of SPring-8 [1].

In the GISWAXS and GIXD experiments, the incident beam impinges under a very shallow angle around 0.1° onto the sample surface. Therefore, precise collimation of the incident X-ray beam in the direction parallel to the sample surface is required. For a precise and quick sample setting, a new soller slit and the PIN-photodiode system are installed in the vacuum path (Figure 1 (a)). In the GISWAXS measurement, this system can avert from the direct beam and the X-ray scattering from the sample as shown in Figure 1 (b). Furthermore, by using this system, a quick method of specular reflectivity becomes possible with the GISAXS measurement. Figure 1 (c) also shows the schematic view of a quick XR measurement with this soller slit system.

In addition to the GISWAXS/GIXD/XR compatible system, a linkage arrangement of the vacuum path in the first hutch and the second hutch achieved the extremely long camera length about 11.7 m as a smart grazing-incidence ultra small-angle X-ray scattering (GIUSAXS) measurement system using the detecting system installed in the second hutch. Figure 2 (a) show the scattering patterns from the dewetted polymer blend thin films. The in-plane profile at the Yoneda line indicated that the small angle resolution could reach to $6.0\ \mu\text{m}$ in the real space, which is corresponding to the correlation length of the dewetted structures (Figure2 (b)).

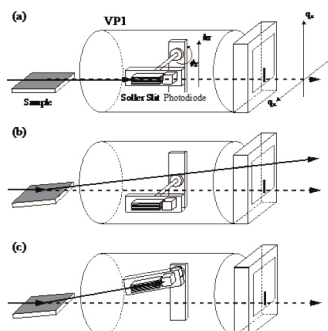


Fig. 1. Sketch for the position of the soller slit and PIN-photodiode system in the VPI for (a) the sample alignment, (b) the GISAXS measurement and (c) the quick XR measurement.

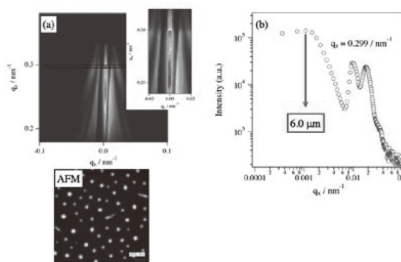


Fig. 2. 2D GIUSAXS pattern (a) and in-plane profile (b) of dewetted polystyrene/poly vinyl ether blend film at the wavelength of $0.1\ \text{nm}^{-1}$.

Dynamics of Relaxor Materials of $(1-x)\text{Pb}(\text{Mg}_{1/3}\text{Nb}_{2/3})\text{O}_3$ - $x\text{PbTiO}_3$ Studied by X-ray Scattering

Daisuke Shimizu^A, Kenji Ohwada^A, Jun'ya Sakamoto, Mitsuyoshi Matsushita^A, Shinya Tsukada^C, Satoshi Tsutsui^D, Alfred Q. R. Baron^{D,E}, Jun'ichiro Mizuki

^AKwansei Gakuin University, Sanda, Hyogo, 669-1337, Japan

^AJapan Atomic Energy Agency, Sayo, Hyogo 679-5148, Japan

^BJFE MINERAL Co., Ltd., Chiba 206-0826, Japan

^CFaculty of Education, Shimane University, Matsue, Shimane, 609-8504, Japan

^DJASRI, SPring-8, Sayo, Hyogo 679-5198, Japan

^ERIKEN, SPring-8, Sayo, Hyogo 679-5148, Japan

One of the most important topics of condensed matter physics is the effect of heterogeneous structure on physical properties. The relaxor ferroelectrics offer a playground for studying this issue, because it is believed that their physical properties are related to inhomogeneous domain structures from nanometer-to-micrometer spatial and THz-to-Hz time scales. Since () (/ /) () of relaxor ferroelectrics consists of normal ferroelectrics () and relaxor (/ /), the solid solution made of these two materials results in an interesting phase diagram. This system has a morphotropic phase boundary (MPB) () between rhombohedral phase of low PT concentration and tetragonal phase of high PT concentration. The material shows anomalous physical properties, e.g. extremely high dielectric constants in the wide temperature range near MPB.

However, the domain structures and physical properties near MPB strongly depend on the sample conditions and histories (thermal or electrical etc.). Such features make it great obstacle to elucidate the properties near MPB in relaxor system. Therefore, we prepared a single crystal sample of () with PT concentration gradient extending from 27.0% to 38.0% ($0.27 < x < 0.38$)[1] along the rectangular axis of the crystal. By using this sample, we can perform systematic study near MPB by changing the position of incident beam spot on the sample without changing the experimental set up.

We measured X-ray diffuse scattering (XDS) at BL22XU of SPring-8. XDS is related to a polarization fluctuation in the domain of the () system. The anisotropic correlation of polarization fluctuation could give the anisotropic pattern of XDS at reciprocal space. We observed the anisotropic pattern to change with PT concentrations at only small- q ([]) region. We also performed an inelastic X-ray scattering measurement at BL35XU of SPring-8 with the same sample to investigate the dynamic component of XDS at small- q region. As shown in Fig.1, the line width (life time) of transverse acoustic mode (open circle) shows clear anomaly near MPB, while the energy (solid circle) shows no clear change. We speculate that the results should be related to the fluctuation of local polarization, and could explain the characteristic dielectric properties near MPB.

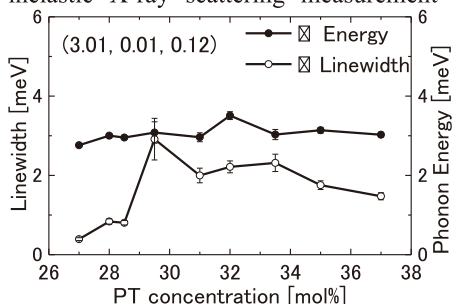


Fig.1 Line width and energy of TA mode



Designing new $n = 2$ Sillen-Aurivillius phases by lattice-matched substitutions in the halide and $[\text{Bi}_2\text{O}_2]^{2+}$ layer

Samuel Liu, Peter E R Blanchard, Maxim Avdeev, Brendan J Kennedy, Chris D Ling

*School of Chemistry, University of Sydney, Sydney 2006, Australia
The Bragg Institute, ANSTO, PMB 1, Menai 2234, Australia*

The chemical and structural flexibility of the perovskite structure, which makes it so ubiquitous in nature and useful in a range of technological applications, extends to layered variants such as Ruddlesden-Popper, Dion- Jacobson and Aurivillius phases. Ferroelectric and ferromagnetic properties have been particularly important drivers of research into layered perovskite phases. Sillen-Aurivillius phases are related to Aurivillius phases by the insertion of an additional halide layer between every second $[\text{Bi}_2\text{O}_2]^{2+}$ layers [1].

Sillen-Aurivillius phases exist in various A_nX_m combinations, where n is the number of perovskite layers A and m the number of halide layers X . We have synthesised a new $n = 2$ Sillen-Aurivillius compound $\text{Bi}_3\text{Sr}_2\text{Nb}_2\text{O}_{11}\text{Br}$ [2] based on $\text{Bi}_3\text{Pb}_2\text{Nb}_2\text{O}_{11}\text{Cl}$ [3] by simultaneously replacing Pb^{2+} with Sr^{2+} and Cl^- with Br^- . Rietveld refinements against X-ray and neutron powder diffraction data revealed a significant relative compression in the stacking axis (c axis) of the new compound. We could not stabilise other combinations such as $\text{Bi}_3\text{Sr}_2\text{Nb}_2\text{O}_{11}\text{Cl}$ and $\text{Bi}_3\text{Pb}_2\text{Nb}_2\text{O}_{11}\text{Br}$ due to inter-layer mismatch.

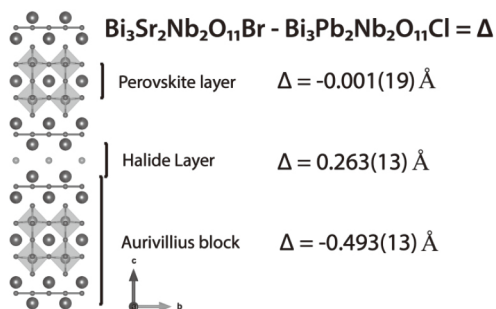


Fig. 1. The structure of the A_2X_1 Sillen-Aurivillius phase where Δ denotes differences between key distances in $\text{Bi}_3\text{Sr}_2\text{Nb}_2\text{O}_{11}\text{Br}$ and $\text{Bi}_3\text{Pb}_2\text{Nb}_2\text{O}_{11}\text{Cl}$.

In our new compound, Sr^{2+} doping reduces the impact of the stereochemically active $6s^2$ lone pair found on Pb^{2+} and Bi^{3+} , resulting in a contraction of the c axis by 1.22 % and an expansion of the a - b plane by

0.25 %. This improves the inter-layer compatibility with the larger halide Br^- . The NbO_6 octahedra themselves in the $n = 2$ perovskite layer are less distorted the parent compound and other $n = 2$ Aurivillius phases ($\text{Bi}_2\text{PbNb}_2\text{O}_9$ and $\text{Bi}_2\text{SrNb}_2\text{O}_9$).

Analysis of X-ray absorption near-edge spectroscopy data show that the ferroelectric distortion of the B -site cation is less apparent in $\text{Bi}_3\text{Sr}_2\text{Nb}_2\text{O}_{11}\text{Br}$ compared to $\text{Bi}_3\text{Pb}_2\text{Nb}_2\text{O}_{11}\text{Cl}$. Variable-temperature neutron diffraction data show no evidence for a ferroelectric distortion.

[1] B. Aurivillius, *Chemica Scripta* 23 (1984) 143-156.

[2] S. Liu, P. E. R. Blanchard, M. Avdeev, B. J. Kennedy, C. D. Ling, *Journal of Solid State Chemistry* (Accepted July 8, 2013)

[3] A. M. Kusunova, P. Lightfoot, W. Z. Zhou, S. Y. Stefanovich, A. V. Mosunov, V. A. Dolgikh, *Chemistry of Materials* 13 (2001) 4731-4737.



Materials Science Research at RIKEN SPring-8 via the Northeastern University-RIKEN co-op program

Ahmed Sajjad^{1,2}, Jungeun Kim^{1,3}, Akihiko Fujiwara³ & Masaki Takata^{1,3,4}

¹*RIKEN SPring-8 Center, Hyogo 679-5148, Japan*

²*Dept. of Chem. Eng., Northeastern University, Boston, MA 02115, U.S.A*

³*Jpn Synchrotron Radiation Res. Inst. JASRI/SPring-8, Hyogo 679-5198, Japan*

⁴*Dept. of Advanced Materials, The University of Tokyo, Chiba 277-8561, Japan*

The Cooperative Education program at Northeastern University provides undergraduate students with an excellent opportunity to experience life in the real work environment and gain valuable experience prior to graduating as well-rounded professionals.

RIKEN, as an affiliate of the co-op program, opens doors for two students from Northeastern University to travel to Japan and work at the Synchrotron Radiation facility at its SPring-8 campus, for a period of 6 months. This collaboration was made possible by the efforts of Dr. Masaki Takata of RIKEN and Dr. J. Murray Gibson of Northeastern. Students get the opportunity to work alongside and learn from well-qualified specialists, which contributes towards their experiential learning. From analyzing diffraction data to physically working on the beam-line, participating in a co-op at RIKEN SPring-8 campus provides students with a wealth of experience that they likely would not be able to obtain elsewhere.

For a student, such as myself, working towards a B.sc degree in Chemical Engineering, this co-op offers a platform to develop his practical skills and teaches how to employ book-knowledge in real-world applications. This not only contributes to better comprehension of concepts but also helps with developing a professional demeanor, a valuable and desired quality amongst fresh graduates.

Currently at the RIKEN SPring-8 campus, I am expanding on my knowledge of Synchrotron X-ray Powder Diffraction and the MEM/Rietveld analysis[1] to understand the relationship between the structure and properties of various materials. This is indispensable knowledge for developmental research and for the design of novel functional materials in the

field of Chemical Engineering. Once I absorb these concepts, under the supervision of the Dr. Jungeun Kim and Dr. Akihiko Fujiwara, I will work on Powder Diffraction at one of the Synchrotron beamlines (BL02B2) at RIKEN SPring-8. I plan to apply my knowledge of the MEM/Rietveld method for precise structure analysis using X-ray Powder Diffraction data. Examples include the structural studies of positive electrodes with spinel structures and materials with nano-sized spaces, along with their applications.

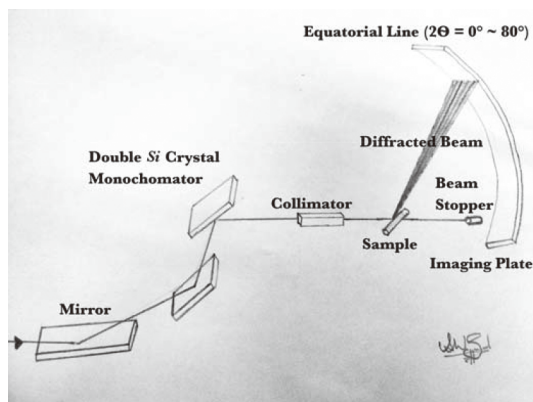


Fig. 1. Schematic diagram of beamline BL02B2, SPring-8.

[1] M. Takata, "The MEM/Rietveld method with nano-applications-accurate charge-density studies of nano-structured materials by synchrotron-radiation powder diffraction", *Acta Cryst. A* **64**, 232-245 (2008.)



Surface and interfacial morphology and crystallization in polymer light emitting devices

Seck Ngor Mbaye¹, Ajeong Kim¹, Jinback Kang¹, Gukil Ahn¹, Jerome Carnis¹,
Wonsuk Cha¹, Taejoo Shin², Jinwoo Kim³, Hyunjung Kim¹

¹*Department of Physics, Sogang University, Seoul 121-742, Korea*

²*Pohang Light Source, Pohang Accelerator Laboratory, Pohang 790-834, Korea*

³*National Core Research Center for Extreme Light Applications, Gwangju Institute of Science and Technology, Gwangju 500-712, Korea*

Recent advances in the development of polymer light emitting devices have led to the realization of devices with high operational stability, reflected in the device half-life time amounting to many thousands of hours [1,2]. Polymers light emitting devices enable full spectrum color displays and are relatively inexpensive compared to OLEDs and require little power to emit a substantial amount of light. Organic materials are more susceptible to chemical degradation from e.g. oxygen, nitrogen and water than inorganic materials. There is a rough division between chemical and physical degradation studies. Organic materials and metal electrode materials such as aluminum are susceptible to reactions with oxygen and water. There are subsections on the photo-degradation of polymers, on polymers with oxides composites and on degradation at the ITO and metal electrodes. A number of studies have been carried out and they showed that the stability and degradation issues are rather complicated and certainly not yet fully understood through the progress has been made.

In this work, we investigate the thermal degradation effect of surface and interfaces in PLEDs as a function of annealing temperature by X-ray reflectivity and transverse diffuse scattering. The techniques measure the thicknesses, roughnesses and electron densities of the layers in devices. Temperature dependence of crystallization of polymers was studied by grazing incidence wide angle x-ray scattering measurement. The results will be discussed further in detail.

This research was supported by the Basic Science Research Program through the National Research Foundation of Korea (NRF) funded by the Ministry of Education and the Ministry of Science, ICT & Future Planning of Korea (Nos. 2011-0012251 and 2008-0062606, CELA-NCRC), Sogang University Research Grant of 2012.

-
- [1] J.H. Burroughes, Asia Display/IMID'2004', Deagu Korea, 24-27 August 2004(unpublished), Session 11.3; N.Conway, C.Foden, M.Roberts, and I. Grizzi, Euro display 2005, Edingburgh Scotland, 19-22 September 2005, Session 18.4, p.492.
[2] J. S. Kim, R. H. Friend, I. Gizzi, and J. H. Burroughes, Appl. Phys. Lett. 87, 023506 (2005)



Responsive polymer brushes grafted from conducting PEDOT

Alissa Hackett^{1,2}, Jenny Malmström^{1,2}, Lisa Strover^{1,2}, Yiwen Pei³, Duncan McGillivray^{1,2}, Jadranka Travas-Sejdic^{1,2}

¹*School of Chemical Sciences, University of Auckland, Private Bag 92019, Auckland 1142, New Zealand*

²*MacDiarmid Institute for Advanced Materials and Nanotechnology, PO Box 600, Wellington 6140, New Zealand*

³*School of Chemical Sciences and Engineering, University of New South Wales, Sydney, NSW 2052, Australia*

Surfaces with readily-modulated properties show great promise in a range of applications, including microfluidic devices, self-cleaning surfaces, and biomedical devices. Recently, switching behaviour has been demonstrated in polymer brushes grafted from conducting polymer (CP) backbones [1-3]. The CP can be electrochemically switched between the oxidised (conducting) and reduced (insulating) states, causing changes in brush morphology. In this way, an applied potential may be used to modulate the physical properties of the material.

We report on the synthesis and characterisation of a novel surface based on insulating polymer brushes grafted from a conducting poly(3,4-ethylenedioxythiophene) (PEDOT) backbone that has been modified to include ATRP-initiating sites. A range of poly(oligo(ethylene glycol) methyl ether methacrylate) (POEGMA) brushes were grafted from the backbone by AGET ATRP. These brushes are known to exhibit thermoresponsive behaviour, which is sensitive to salt concentration. We aim to induce brush collapse by controlling the ion concentration at the CP-brush interface through the application of an electric potential. These brushes have potential in cell culture applications, as substrates that can reversibly control cell adhesion.

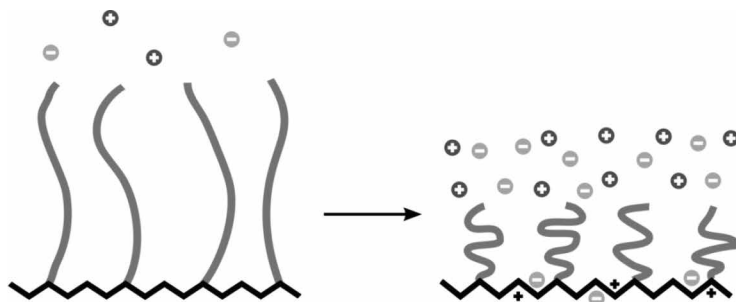


Fig. 1. Proposed salt-induced collapse of polymer brushes, caused by electrochemical oxidation of the conducting polymer backbone.

[1] J. Malmström *et al.*, *Macromolecules* **46**, 4955 (2013).

[2] L. Strover *et al.*, *Synth. Met.* **162**, 381 (2012).

[3] Y. Pei, J. Travas-Sejdic and D. E. Williams, *Langmuir* **28**, 13241 (2012).

Temperature dependent formation of ion tracks in apatite and quartz studied using SAXS

D. Schauries¹, M. Lang², O.H. Pakarinen³, B. Afra¹, M.D. Rodriguez¹, S. Botis², K. Nordlund³, R. Ewing², M. Bender⁴, D. Severin⁴, C. Trautmann^{4,5}, N. Kirby⁶, and P. Kluth¹

¹*The Australian National University, Canberra, Australia;* ²*University of Michigan, Ann Arbor, USA;* ³*University of Helsinki, Finland;* ⁴*GSI Helmholtzzentrum, Darmstadt, Germany,* ⁵*Technische Universität Darmstadt, Germany,* ⁶*Australian Synchrotron, Clayton, Australia.*

Ion tracks are narrow, cylindrical defects a few nanometres in diameter and up to tens of micrometres in length that result from the interaction of high-energy heavy ions with a target material. In nature, these tracks are produced by fission fragments from the decay of uranium in various minerals [1]. Quantitative and length analysis of these fission tracks provide information on the age and thermal history of geological material. Ion tracks also play an important role in high radiation reactor environments where they are formed at elevated temperatures.

We have previously shown that synchrotron-based small angle x-ray scattering (SAXS) is a powerful and non-destructive technique well suited for studying ion tracks with unprecedented precision [2]. SAXS can resolve small changes in the track radii that are challenging to resolve with conventional analytical techniques such as transmission electron microscopy. Thus SAXS is also an important tool in studying high temperature effects on ion track formation.

This work focuses on the effect of temperature on the size and morphology of ion tracks in apatite and natural quartz using SAXS at the SAXS/WAXS beamline at the Australian Synchrotron. The tracks were produced by irradiation with 2.2 GeV Au ions (GSI Helmholtz Centre) at temperatures between room temperature and 640°C. A linear increase in the track radius with temperature was observed [3]. In contrast, irradiation with low energy ions at elevated temperatures generally leads to lower defect concentrations due to increased thermally induced dynamic defect recovery. We were able to confirm the increase quantitatively by performing Molecular Dynamics (MD) simulations for quartz. The notion of increased track radii is particularly relevant for fission track dating in apatite, as natural occurring tracks can be formed at elevated temperatures in the earth crust. In addition, these findings are relevant when assessing the radiation resistance of nuclear materials that are often subjected to extreme conditions such as high temperatures and high-energy particles.

Work supported by the Australian Research Council and by Office of Basic Energy Sciences of the USDOE.

[1] G. A. Wagner and P. Van den Haute, *Fission-track Dating* (Kluwer Academic, Dordrecht, 1992).

[2] P. Kluth *et al.*, *Phys. Rev. Lett.* **101** (2008) 175503.

[3] D. Schauries *et al.*, *J. Appl. Cryst.* (2013) (under review)



Polymer materials studied by SAXS/WAXS at SSRF

Feng Tian, Jie Wang

Shanghai Institute of Applied Physics, Chinese Academy of Sciences,

Shanghai, 201800, China

It is hard to study the dynamic structure changes of polymer materials due to its high molecular weight and complex inner structure. now, we will take polytetrafluoroethylene (PTFE) and fibers for example.

(1) PTFE will be cracked when it was irradiated by γ -ray directly. It could be prepared ultrafine powder which is used as lubricant and easier, etc. While, PTFE will be cross-linked by electron beam irradiation in the molten state in an oxygen-free atmosphere. Compared with PTFE, the mechanical properties of cross-linked PTFE improved significantly, and extended its industrial application fields. The analysis of the change of the inner structure of irradiated polymer play an important role in irradiation technology[1].

(2) The characterization technique of fibers has been a research emphasis for its complex inner structure. We must choose statistical method to study a large number of fibers and different part of fibers[2].

Small angle X-ray scattering (SAXS) is a non-destructive technique which could test the inner scale between several nanometers and several hundred nanometers. It is mainly used to analysis the scale, morphology, crystalline and amorphous of the scatterer. So, SAXS is an ideal method to study the change of irradiated polymer and the inner structure of fibers. Now the third generation synchrotron radiation light source with its high flux density, providing a strong instrument for SAXS study of polymer.

[1] Tian Feng, Tang Zhongfeng, Xu Hongjie, Wang Jie, Wu Guozhong, Li Xiuhong. SAXS Studies on the Structure Behaviors of Crosslinked PTFE Irradiated by Gamma Ray, *Polymers & Polymer Composites*, 2011,19(4-5).

[2] Jinyou Lin, Feng Tian, Yanwei Shang, Fujun Wang, Bin Ding, Jianyong Yu, and Zhi Guo, "Co-axial electrospun polystyrene/polyurethane fibers for oil collection from water surface", *Nanoscale*, 2013,5.

Development of X-ray speckle visibility spectroscopy for breaking the limit of time resolution in X-ray Photon Correlation Spectroscopy

Ichiro Inoue^{1,2}, Yuya Shinohara^{1,3}, Akira Watanabe¹, Yoshiyuki Amemiya^{1,3}

¹*Graduate School of Frontier Sciences, The University of Tokyo,
5-1-5 Kashiwanoha, Kashiwa, Chiba 277-8561, Japan*

²*RIKEN SPring-8 Center, 1-1-1 Kouto, Sayo-cho, Sayo-gun, Hyogo
679-5148, Japan*

³*JST-CREST, 4-1-8 Honcho, Kawaguchi, Saitama 332-0012, Japan*

When coherent X-rays impinge upon a disordered system, a grainy scattering pattern called speckle pattern is observed [1]. When the system evolves with time, the corresponding speckle pattern also changes. Temporal changes in the speckle patterns therefore provide information on the system dynamics. This technique, which is called X-ray photon correlation spectroscopy (XPCS) [2], is a rather new technique, but has shown the potential to access dynamic properties of various materials, such as colloidal suspensions, block copolymer, supercooled liquids, alloys, and antiferromagnetic materials.

Although XPCS is a powerful technique for material science as recent studies show, it has a limitation of time resolution: dynamics faster than the frame rate of detector cannot be measured. When a two-dimensional (2D) detector is used in XPCS, the time resolution is limited to the order of milliseconds.

For improving the time resolution of XPCS, we have extended speckle visibility spectroscopy (SVS) in the region of visible light [3] to the region of X-rays (X-ray SVS; XSVS) [4]. Since the minimum exposure time of the scattering patterns determines the time resolutions of XSVS and SVS, micro- or nano- second dynamics can be measured even with a 2D detector. Thus, XSVS has potential to bridge the time gap between XPCS and inelastic neutron/X-ray scattering techniques, and will be one of the promising tools for material science in the next generation synchrotron X-ray facilities, such as diffraction limited storage rings and energy recovery linac X-ray sources.

In this presentation, we will describe the principle of XSVS and show the result of the application of XSVS to Brownian colloidal suspensions.

This study was performed under the approval of JASRI (2011A1112, 2011B1131). We acknowledge Drs. N. Yagi and N. Ohta for their kind support in performing experiments.

[1] M. Sutton *et al.*, *Nature* **352**, 608 (1991)

[2] G. Grübel and F. Zontone, *J. Alloy Comp.* **362**, 3 (2004), M. Sutton, *C. R. Phys.* **9**, 657 (2008), R. L. Leheny, *Curr. Opin. Colloid Interface Sci.* **17**, 3 (2012)

[3] P. K. Dixon and D. J. Durian, *Phys. Rev. Lett.* **90**, 184302 (2003), R. Bandyopadhyay *et al.*, *Rev. Sci. Instrum.* **76**, 093110 (2005)

[4] I. Inoue, Y. Shinohara, A. Watanabe, Y. Amemiya, *Opt. Express* **20**, 26878 (2012)



The Activation of E-H Bonds (E = H or C) by an Amido-Digermine with a Ge-Ge Single Bond

Jiaye Li,¹ Cameron Jones,¹ Gernot Frenking,² Christian Schenk¹

¹ School of Chemistry, Monash University, PO Box 23, Clayton, Melbourne, VIC, 3800, Australia.

² Fachbereich Chemie, Philipps-Universität Marburg, 35032, Marburg, Germany.

The activation of hydrogen (H₂) (either homolytically or heterolytically) has been extensively examined by both experimentalists and theoreticians, as this process has versatile applications to synthesis, catalysis and energy storage [1]. Previously, transition metal based complexes were widely applied as catalysts to activate H₂. However, since 2005, main group element based complexes have emerged which can activate H₂ and other small molecules under mild conditions [2]. Such advances highlight the potential for main group systems to replace expensive, toxic transition metal compounds in many processes reliant on H-H bond activations. We present recent results concerning the synthesis of the first singly-bonded amido-digermine, LGeGeL ($d_{\text{Ge-Ge}} = 2.7 \text{ \AA}$) [3]. The subsequent reactivity investigations

indicate that LGeGeL is quite reactive towards gas molecules. For example, H₂ can be activated unprecedentedly by LGeGeL in either solution or the solid state at low temperature (-10°C). Moreover, LGeGeL is the first example of low oxidation state germanium compound that can reduce CO₂ to CO quantitatively at -40°C [4].

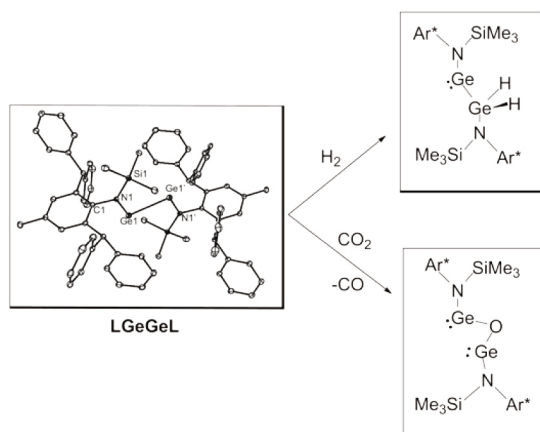


Fig. 1. Reactions of LGeGeL and H₂ or CO₂ (Ar* = C₆H₂{C(H)Ph₂}₂Me-2,6,4).

- [1] K. Gregory J, *Journal of Organometallic Chemistry* **2009**, 694, 2648-2653.
- [2] (a) A. L. Kenward, W. E. Piers, *Angewandte Chemie International Edition* **2008**, 47, 38-41; (b) D. Bourissou, O. Guerret, F. P. Gabbaï, G. Bertrand, *Chemical Reviews* **1999**, 100, 39-92; (c) G. H. Spikes, J. C. Fetting, P. P. Power, *Journal of the American Chemical Society* **2005**, 127, 12232-12233; (d) Y. Peng, M. Brynda, B. D. Ellis, J. C. Fetting, E. Rivard, P. P. Power, *Chemical Communications* **2008**, 6042-6044; (e) D. W. Stephan, G. Erker, *Angewandte Chemie International Edition* **2010**, 49, 46-76; (f) G. C. Welch, R. R. S. Juan, J. D. Masuda, D. W. Stephan, *Science* **2006**, 314, 1124-1126.
- [3] J. Li, C. Schenk, C. Goedecke, G. Frenking, C. Jones, *Journal of the American Chemical Society* **2011**, 133, 18622-18625.
- [4] J. Li, M. Hermann, G. Frenking, C. Jones, *Angewandte Chemie International Edition* **2012**, 51, 8611-8614.



Internal Deformation Field Distribution of Gold Nanoparticles and Zeolite Microcrystals by Coherent X-ray Diffraction Imaging

Jinback Kang¹, Wonsuk Cha¹, Carnis Jerome¹, Seck Ngor Mbaye¹, Gukil Ahn¹,
Ajeong Kim¹, Tung Cao Thanh Pham², Kyung Byung Yoon², Hae Chul Lee³,
Chung-Jong Yu³, Hyunjung Kim¹

¹*Department of Physics, Sogang University, Seoul, Korea*

²*Department of Chemistry, Sogang University, Seoul, Korea*

³*Pohang Light Source, Pohang Accelerator Laboratory, Pohang, Korea*

Coherent x-ray diffraction imaging (CXDI) technique restores the oversampled CXD patterns to the real 3-dimensional image of the sample and internal deformation field distribution by phase-retrieval algorithm [1]. In the recent study, we observed an unusual "triangular" deformation field structure of ZSM-5 zeolite microcrystals arising from the heterogeneous core-shell structure due to residual organic templates [2]. The experiments were performed at the 34ID-C beamline in Advanced Photon Source, USA and employed monochromatic radiation with X-ray energy of 9 keV. The CXD patterns were obtained at (200) and (020) Bragg condition with unfocused beam. We have made progress in similar setup at the beamline 9C in Pohang Light Source, Korea. The CXD patterns were measured on gold nanoparticles with size of ~100 nm and ZSM-5 zeolite microcrystals with size of ~2 um attached on Si (100) substrate were obtained. The development of CXDI setup will be reviewed and the results in terms of coherent volume of scattering will be discussed.

This research was supported by the Basic Science Research Program through the National Research Foundation of Korea (NRF) funded by the Ministry of Education and the Ministry of Science, ICT & Future Planning of Korea (Nos. 2011-0012251 and 2008-0062606, CELA-NCRC), Sogang University Research Grant of 2012.

[1] Ian K. Robinson and Ross Harder, *Nature Materials*, **8**, 291-298(2009)

[2] Wonsuk Cha, Nak Cheon Jeong, Sanghoon Song, Hyun-jun Park, Tung Cao Thanh Pham, Ross Harder, Bobae Lim, Gang Xiong, Docheon Ahn, Ian McNulty, Jungho Kim, Kyung Byung Yoon, Ian K. Robinson & Hyunjung Kim, *Nature Materials* doi:10.1038/nmat3698



Efficiency improvement of electrodeposited p - n homojunction cuprous oxide solar cells by surface passivation and annealing

KMDC Jayathilaka^{a,b}, LSR Kumara^c V. Kapaklis^d, W Siripala^b, JKDS Jayanetti^a

^aDepartment of Physics, University of Colombo, Colombo. Colombo 3, Sri Lanka

^bDepartment of Physics, University of Kelaniya, Kelaniya. Sri Lanka

^cSynchrotron X-ray Station at SPring-8, National Institute for Materials Science (NIMS), 1-1-1 Kouto, Sayo-cho, Sayogun, Hyogo 679-5148, Japan

^dDepartment of Physics and Astronomy, Uppsala University, Uppsala, Sweden

There is considerable interest on the efficiency improvement on Cu_2O based solar cells. However, the highest reported efficiencies on such structures have not exceeded 2% even though the theoretical efficiency is reported to be around 20%. It is generally accepted that a p - n homojunction of Cu_2O has the potential to become a structure with high conversion efficiency [1]. Mainly, the high resistivity and defects at the junctions are reported to have hindered the reliability and performance of resulting Cu_2O based devices. In this study two different electrodeposition media were used to produce n - Cu_2O layers [2] and p - Cu_2O layers [3]. Cuprous oxide homojunction thin films on Ti substrates were fabricated by two-step electrochemical deposition process depositing a p - Cu_2O layer on an n - Cu_2O layer. The p - Cu_2O surface layer was passivated by sulfur. Photocurrent spectral response and capacitance-voltage measurements were used to determine the conduction type of each layer. These measurements demonstrated the

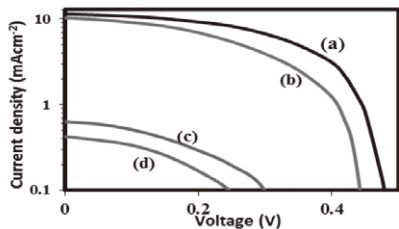


Figure 1. Current- voltage characteristics of (a) annealed and sulfur treated (b) unannealed and sulfur treated (c) annealed and untreated (d) unannealed and untreated Ti/ n - Cu_2O / p - Cu_2O /Ni solar cells.

successful formation of a p - n homojunction of cuprous oxide. XRD and SEM analysis revealed that the n and p type films were single phase and the substrates were well covered by the films. p -type Cu_2O layers which had undergone the sulfur treatment showed reduced resistivity and enhanced current-voltage (I - V) characteristics. Results revealed that, upon sulfur treatment, Cu_2O p - n homojunction solar cell had improved characteristics compared to those of untreated Cu_2O p - n homojunction solar cell due to the passivation of defects and reduced resistivity in the sulfur treated p - Cu_2O layer [3]. Annealing of the sulfur treated solar cell structures improved efficiency further yielding an optimum annealing temperature and annealing time of 150 °C and 20 min. respectively with

an energy conversion efficiency of 2.14 %, $V_{oc} = 485$ mV and $J_{sc} = 11.4$ mAcm^{-2} under AM 1.5 illumination. This was a significant improvement compared to the efficiency of unpassivated unannealed solar cell structures.

[1] A. Mittiga, E. Salza, F. Sarto, M. Tucci, and R. Vasanthi: Appl. Phys. Lett. 88 (2006) 163502.

[2] W Siripala, J.R.P Jayakody.: Solar Energy Materials 14, 23 (1986).

[3] K.M.D.C. Jayathilaka, V. Kapaklis, W. Siripala and J.K.D.S. Jayanetti; Electron. Mater. Lett. (submitted)



Resonant photoemission study of multiferroic YMnO_3 thin film

Manish Kumar, R. J. Choudhary and D. M. Phase

UGC-DAE Consortium for Scientific Research, Indore, M.P, India-452001

We have studied the electronic structure of pulsed laser deposited hexagonal- YMnO_3 film on Al_2O_3 (0001) substrate by photoemission spectroscopy using variable energy photon sources. The constant initial state (CIS) plots (obtained from resonance photoemission results) divulge the charge transfer nature of h- YMnO_3 and variation in strength of hybridization between oxygen 2p and Mn 3d states across the valence band region. The valence states sensitive to lattice distortion (inversion asymmetry) demonstrate the evolution of spin orbit interaction (SO). This SO along with its anisotropic behavior is well identified by the constant initial state plots. Since the effect of SO has its implications on the valence band spectra, it may affect the multiferroic properties in h- YMnO_3 .

[1] Manish Kumar, R. J. Choudhary, and D. M. Phase, Appl. Phys. Lett. **102**, 182902 (2013)



Formation of Silicon Nanocrystallites on Amorphous Hydrogenated Silicon Thin Film Using Dense Plasma Focus Device

^ANgoi Siew Kien, ^ALim Lian Kuang, ^BGoh Boon Tong, ^AYap Seong Ling,
^AWong Chiow San, ^BSaadah Abdul Rahman

^A*Plasma Technology Research Center, Department of Physics,
University of Malaya, 50603, Kuala Lumpur, Malaysia*

^B*Low Dimensional Material Research Center, Department of Physics,
University of Malaya, 50603, Kuala Lumpur, Malaysia*

Dense Plasma Focus (DPF) is a device that can generate a short-lived hot and dense plasma column. The pinching of the plasma column can give rise to radiation such as X-ray. The disruption of the plasma column will generate a strong electric field that accelerates the ions in the end on direction of the coaxial electrodes forming an ion beam. The beam with average energy of about hundreds of keV can be used to irradiate material surface and induce phase changes. In this work we demonstrate the effect of ion beam irradiation on hydrogenated amorphous silicon (a-Si:H) thin film leading to the formation of nanosilicon crystallite embedded in the amorphous matrix. The film is studied with FESEM and Raman Spectroscopy to confirm the presence of the nano crystallite.



Synthesis, Characterization, and Dielectric Properties of Y_2NiMnO_6 Ceramics Prepared by A Simple Thermal Decomposition Route

Theeranun Siritanon^a, Naphat Chathirat^b, Chivalrat Masingboon^c,
Teeraporn Yamwong^d, and Santi Maensiri^b

^a*School of Chemistry, Institute of Science, Suranaree University of Technology, Nakhon Ratchasima, 30000, Thailand*

^b*Advanced Materials Physics Laboratory (Amp.), School of Physics, Institute of Science, Suranaree University of Technology, Nakhon Ratchasima, 30000, Thailand*

^c*Faculty of Science and Engineering, Kasetsart University, Chalermphrakiat Sakon Nakhon Province Campus, Sakon Nakhon, 47000, Thailand*

^d*National Metals and Materials Technology Center (MTEC), Thailand Science Park, Pathumthani, 12120, Thailand*

In attempt to search for an improved material preparation technique, Y_2NiMnO_6 dielectric material is prepared by a one-step thermal decomposition route where a solution of stoichiometric mixtures of metal acetates is directly heated. Structural characterization by X-ray diffraction and electron diffraction shows that the samples are successfully prepared at relatively low temperature comparing to a standard solid state synthesis. Results from several techniques including thermal analysis, electron microscopy, and X-ray absorption are used to investigate compound formation. It is revealed that metal acetates decompose at 300-350°C resulting in mixture of several metal oxide intermediates which continue to react to form the desired product. Y_2NiMnO_6 nanoparticles are first obtained at 800°C. Later, these nanoparticles agglomerate and grow at higher temperature and/or longer heating time to give larger particle size and more crystallinity. Although the starting reagent contains Mn in 2+ oxidation state, X-ray absorption (XANES) analysis indicates that the obtained Y_2NiMnO_6 contain Mn and Ni in 4+ and 2+ oxidation states, respectively. Ceramic sample shows large dielectric constant of about 6000-7000 at 30-120°C at 1kHz. Dielectric constant and dielectric response of the sample are consistent with those reported in other works where different synthetic techniques were used [1]. The activation energy of dielectric relaxation is similar to the energy required to transfer electrons between Ni^{2+} to Mn^{4+} , thus the observed large dielectric constant is intrinsically related to electronic ferroelectricity due to charge ordering of Ni^{2+} and Mn^{4+} .

[1] M. H. Tang, Y. G. Xiao, B. Jiang, J. W. Hou, J. C. Li, and J. He, Appl. Phys. A. **105**, 679 (2011).



Hybrid polymer/quantum dot materials for optoelectronic applications

Thitikorn Boonkoom¹, Saif Haque², John de Mello³

¹*National Nanotechnology Center, National Science and Technology Development Agency, 130 Thailand Science Park, Paholyothin Rd., Klong Luang Pathumthani 12120, Thailand Email: thitikorn@nanotec.or.th*

²*Department of Chemistry, Imperial College London, South Kensington Campus, London, SW7 2AZ, UK Email: s.a.haque@imperial.ac.uk*

³*Department of Chemistry, Imperial College London, South Kensington Campus, London, SW7 2AZ, UK Email: j.demello@imperial.ac.uk*

Indium phosphide (InP) is a III-V semiconductor whose electronic properties are suitable for optoelectronic applications. Moreover, the less toxicity of InP compared to Cd-based materials make it an alternative material for optoelectronic devices. In this work InP quantum dots (InP QDs) were synthesised and surface-modified to enhance compatibility with polymers. For photovoltaic applications, a light harvesting layer was obtained by blending InP QDs (as electron acceptors) with a well-known electron donor polymer, poly-3-hexylthiophene (P3HT). Charge transfer between the polymer and the QDs was investigated by photoluminescence spectroscopy (PL) and Transient absorption spectroscopy (TAS). The TAS decay (Figure 1, left) indicates increasing charge carrier generation with increasing the QD concentration. This emphasises the potential of using InP QDs as electron acceptors in hybrid photovoltaic devices. In addition to the photovoltaic applications, InP QDs were investigated as a light emitter in hybrid light emitting devices with poly(9,9-dioctylfluorenyl-2,7-diyl) (PFO) as a host polymer. The improvement of InP emission with increasing InP loading in the electroluminescence spectra (Figure 1, right) suggests the possibility of using InP QDs as emitters in light emitting applications. Better understanding on relative band offsets of these materials will help designing efficient hybrid systems. Therefore, further studies will focus on photoemission spectroscopy (PES) measurement for energy band determination.

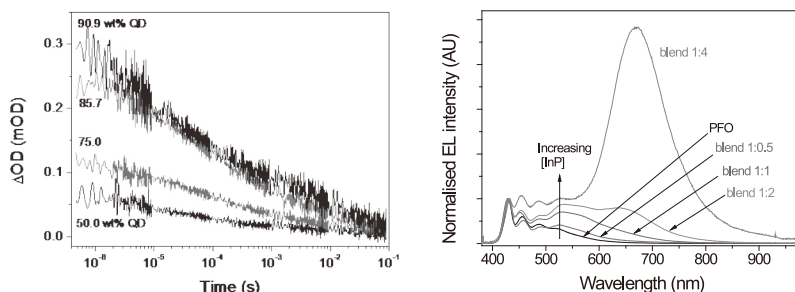


Figure 1. Left: transient absorption decays of P3HT⁺ polaron in the P3HT:InP blends. Right: electroluminescence spectra showing the InP QD emission in the PFO:InP QD blends. [1]

[1] T. Boonkoom, InP Quantum Dots for Hybrid Photovoltaic Devices, Ph.D. thesis, Department of Chemistry, Imperial College London, London, 2013

Development of Convenient Experimental and Analytical Methods for Diffraction Anomalous Fine Structure

Tomoya Kawaguchi,¹ Katsutoshi Fukuda,² Tetsu Ichitsubo,¹
Koki Shimada,¹ Kazuya Tokuda,¹ Masatsugu Oishi,³
Jun'ichiro Mizuki,⁴ and Eiichiro Matsubara¹

¹*Department of Materials Science and Engineering,
Kyoto University, Kyoto 606-8501, Japan*

²*Office of Society-Academia Collaboration for Innovation,
Kyoto University, Kyoto 611-0011, Japan*

³*Graduate School of Engineering, Kyoto University,
Kyoto 606-8501, Japan*

⁴*Department of Physics, Kwansei Gakuin University, Hyogo 669-1337, Japan*

Diffraction anomalous fine structure (DAFS) is a spectroscopic analysis established by coupling XRD and XAFS [1]. DAFS has some remarkable aspects such as a site-selectivity and a spatial-selectivity, with which XAFS-like spectra can be obtained at a certain site and a certain phase by selecting diffraction peaks. Though it is a power-full tool for the materials science, DAFS previously took a relatively long measurement time. (e.g. 0.5 day for 1 spectrum), because of optical alignment at every incident energy. In addition, the data analysis of the DAFS spectrum is complicated due to the phase problem to extract resonant terms from the spectrum. In the present study, we have developed the measurement techniques of DAFS at BL28XU in SPring-8 by using a channel cut monochromator with a small gap, a one-dimensional detector and a polycrystalline sample. Furthermore, we also have developed a direct solution method of DAFS without any iteration process.

Figure 1 shows a DAFS spectrum from 111 diffraction of metallic Ni polycrystalline foil (left) and a resultant imaginary part of the resonant term, f''_{Ni} , and μE of XAFS measured simultaneously (right). The total DAFS spectrum of 430 eV energy width around Ni K-edge was acquired for 326 s, which is extremely fast compared with the conventional measurement (e.g. 0.5 day). The measured spectrum was analyzed by the method mentioned above. μE should be equivalent to f''_{Ni} since Ni atoms occupy only one site in a Ni fcc metal unit cell. The shape of f''_{Ni} at the absorption edge and the energy of the oscillation above the edge show a good agreement with that of μE except for some difference of the two spectra above the edge due to the truncation error in the Kramers-Kronig relation. These

results verified the measurement technique and analysis method in this study.

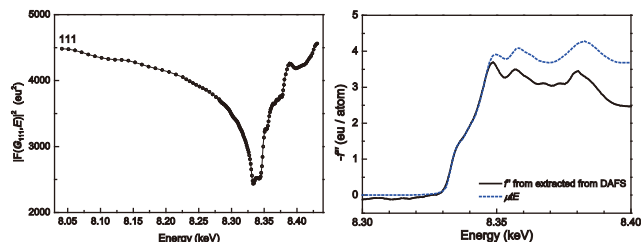


Fig. 1. DAFS spectrum from 111 diffraction of Ni metal foil (left), f'' and μE (XAFS) near the Ni K-edge (right).

[1] H. Stragier, J. Cross, J. Rehr, L. Sorensen, C. E. Bouldin, and J. C. Woicik, Phys. Rev. Lett. **69**, 3064 (1992).



Resonant Multiple-Beam Diffraction Results of $\text{La}_{0.5}\text{Sr}_{1.5}\text{MnO}_4$

Wen-Chung Liu¹, Yi-Hua Chiu¹, Po-Yu Liao¹, Chih-Hao Cheng¹, Yi-Wei Tsai¹,
Chia-Hung Chu², and Shih-Lin Chang^{1,2}

¹*Department of Physics, National Tsing Hua University,
101 Shin-Ann Road, Hsinchu, Taiwan 30076*

²*National Synchrotron Radiation Research Center,
No. 101, Section 2, Kuang-Fu Road, Hsinchu, Taiwan 30013*

We have used resonant multi-beam diffraction to investigate electronic configuration of strongly correlated material: $\text{La}_{0.5}\text{Sr}_{1.5}\text{MnO}_4$. The manganese forms charge ordering and orbital ordering once the temperature is below the phase transition temperature 217K [1]. We used $(3/2\ 3/2\ 0)$ as the primary reflection and found several Aulfhelung-type four-beam diffraction. A more detailed research was carried out on $(0\ 0\ 0)/(3/2\ 3/2\ 0)/(1\ -1\ 0)/(5/2\ 1/2\ 0)$ OUT diffraction, which exhibits strong asymmetry whenever the incident x-ray energy is tuned away from manganese K-edge. We also used the dynamical theory of x-ray diffraction accompanied with the FDMNES software [2] to simulate the four-beam diffraction profiles. It clearly shows that the intensity of the primary reflection plays an important role on affecting the intensity distribution asymmetry which reflects the phase change due to charge ordering in the four-beam diffraction process.

[1] Y. Murakami, H. Kawada, H. Kawata, M. Tanaka, T. Arima, Y. Moritomo, and Y. Tokura, Phys. Rev. Lett. **80**, 1932 (1998)

[2] O. Bunau and Y. Joly, J. Phys.: Condens. Matter **21**, 345501 (2009).



Octahedral Tilting in SrRuO₃ Films Studied by Half-Order Reflexions

Wenlai Lu¹, Ping Yang², Gan Moog Chow¹
Jingsheng Chen¹

1. Department of Materials Science and Engineering, National University of Singapore, Singapore 117576, Singapore
2. Singapore Synchrotron Light Source (SSLS), National University of Singapore, 5 Research Link, Singapore 117603, Singapore

Octahedral tilting has been of great interest since it is intimately linked to the electronic structure and thus the physical properties of ABO₃ perovskite oxides. Recently, there are reports on the modification of octahedral tilting in SrRuO₃ films either by strain engineering [1] or by varying film thickness [2]. Despite the extensive studies on the crystal structures of SrRuO₃ films, direct evidence for the accurate octahedral tilt system is missing.

In our study, half-order reflexions have been employed to investigate the octahedral tilting in SrRuO₃ films. According to Glazer [3], there are basically two types of tilt: tilts where octahedra rotate in-phase along one axis, denoted by the superscript +, and tilts where the octahedra are rotated out-of-phase,

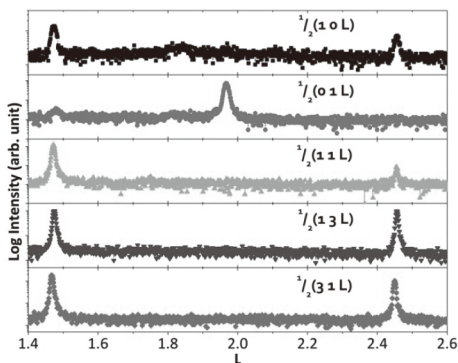


Fig. 1. L scans of $\frac{1}{2}(1\ 0\ L)$, $\frac{1}{2}(0\ 1\ L)$, $\frac{1}{2}(1\ 1\ L)$, $\frac{1}{2}(1\ 3\ L)$ and $\frac{1}{2}(3\ 1\ L)$ around half-order peaks in the SrRuO₃ films deposited on SrTiO₃ substrates. The tilt system is determined to be $a^+a^+c^-$ from the half-order peaks.

denoted with the superscript -. The in-phase and out-of-phase tilt about a particular axis can be easily distinguished by the presence of odd-odd-even type and odd-odd-odd type peaks. As shown in Figure 1, the presence of $\frac{1}{2}103$ and $\frac{1}{2}105$ peaks implies that there are in-phase tilts about [010] axis, denoted by b^+ . The absence of $\frac{1}{2}013$,

$\frac{1}{2}015$ peaks and existence of $\frac{1}{2}113$, $\frac{1}{2}115$ peaks indicates that the rotations about a axis are out-of-phase, denoted by a^- . Similarly, there are purely - tilts about c axis, indicated by the absence of $\frac{1}{2}132$, $\frac{1}{2}312$ and the presence of $\frac{1}{2}133$ peak. Considering the equality of lattice parameters a_c and b_c based on the pseudocubic cell, the tilt system is immediately determined to be $a^+a^+c^-$, which is consistent with the tilt system inferred from the lattice parameter measurements as reported previously [1].

These results show that the measurement of half-order peaks is a straightforward approach for determining the octahedral tilt system and can be applied to other perovskites.

Acknowledgment The author would like to thank Shanghai Synchrotron Radiation Facility (SSRF) for the support.

[1] A. Vailionis, H. Boschker, W. Siemons, E. P. Houwman, D. H. A. Blank, G. Rijnders and G. Koster, Phys. Rev. B **83**, 064101 (2011).

[2] Seo Hyung Chang, Young Jun Chang, S. Y. Jang, D. W. Jeong, C. U. Jung, Y.-J. Kim, J.-S. Chung and T. W. Noh, Phys. Rev. B **84**, 104101 (2011)

[3] A. M. Glazer, Acta Cryst. A **31**, 756 (1975)

Coronary Microangiography System for Rat Heart Functional Imaging at SPring-8

Keiji Umetani¹, James T. Pearson², Daryl O. Schwenke³, and Mikiyasu Shirai⁴

¹ Japan Synchrotron Radiation Research Institute, 1-1-1 Kouto, Sayo-cho, Sayo-gun, Hyogo 679-5198, Japan, ² Monash University, PO Box 13F, Clayton, Victoria 3800, Australia, ³ The University of Otago, PO Box 913, Dunedin, New Zealand, ⁴ National Cerebral and Cardiovascular Center Research Institute, 5-7-1 Fujishiro-dai, Suita-shi, Osaka 565-8565, Japan

A rat microangiography system in Fig. 1 was developed for *in vivo* visualization of the coronary, cerebral, and pulmonary arteries without exposure of organs and with spatial resolution in the micrometer range and temporal resolution in the millisecond range [1]. We refined the system continuously in terms of spatial resolution and exposure time using synchrotron radiation in the SPring-8 BL28B2 beamline [2]. The spatial resolution has improved to 6 μm , yielding sharp images of small arteries. Exposure time has been shortened to around 2 ms using a new rotating-disk X-ray shutter, enabling imaging of beating hearts.

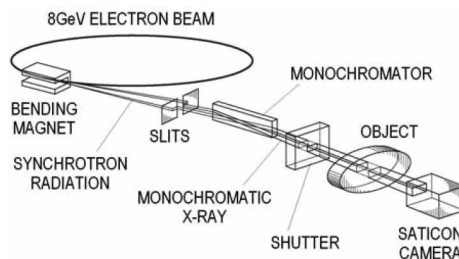


Fig. 1 Experimental arrangement for synchrotron radiation microangiography system

Quantitative evaluations of the rat coronary microangiography system were extracted from measurements of the smallest-detectable vessel size and detection of vessel function. The smallest-diameter vessel viewed for measurements is determined primarily by the concentration of iodinated contrast material. The iodine concentration depends on the injection technique. It is extremely difficult to inject contrast agent directly into small rat coronary arteries. Instead, the contrast agent was injected into the aorta close to the origin of the coronary arteries in the rat coronary angiography.

The vascular internal diameter response of coronary arterial circulation was analyzed to evaluate the vessel function. Small blood vessels of around 50- μm diameter or above were visualized clearly at heart rates of 300–360 per minute. Vasodilation compared to the control was observed quantitatively using drug manipulation. The technique can enable direct investigation of the mechanisms of vascular dysfunction. It is expected to be useful to evaluate the severity of damage to arterial inner walls resulting from diseases.

[1] M. Shirai, D. O. Schwenke, H. Tsuchimochi, K. Umetani, N. Yagi, J. T. Pearson, *Circ Res.* **112**, 209–221 (2013).
 [2] K. Umetani, K. Fukushima, *Rev Sci Instrum.* **84**, 034302-1–10 (2013).

Structural Basis of the γ -Lactone-ring formation in ascorbic acid biosynthesis by the the Senescence Marker Protein-30/Gluconolactonase

Ayaka Harada¹, Shingo Aizawa², Miki Senda¹, Naoki Maruyama²,
Akihito Ishigami², Toshiya Senda¹

¹*Photon Factory, Tsukuba 305-0801, Japan*

²*TMIG, 35-2 Sakaemachi, Itabashi-ku, Tokyo 173-0015, Japan*

1 Introduction

The senescence marker protein-30 (SMP30) exhibits gluconolactonase (GNL) activity. Biochemical and biological analyses revealed that SMP30/GNL catalyzes formation of the γ -lactone-ring of L-gulonate in the ascorbic acid biosynthesis pathway. The molecular basis of the γ -lactone formation, however, remains elusive due to the lack of structural information on SMP30/GNL in complex with its substrate. Here, we report the crystal structures of mouse SMP30/GNL and its complex with xylitol, a substrate analogue, and those with 1,5-anhydro-D-glucitol and D-glucose, product analogues.

2 Method

Diffraction data of mouse and human SMP30/GNL crystals were collected at 95K with an ADSC CCD detector using synchrotron radiation at BL-5A, BL-17A, and PF-AR NE-3A of Photon Factory (PF) in KEK (Tsukuba Japan). The diffraction data were processed and scaled using the programs XDS and XSCALE, respectively. The crystal structure of human SMP30/GNL was determined by the molecular replacement (MR) method with the program MOLREP in the CCP4 program suite using the earlier determined crystal structure of human SMP30/GNL (PDB ID: 3G4E) as a search model. Then, the structure of mouse SMP30/GNL was determined by the MR method using the structure of human SMP30/GNL. The crystal structures of mouse and human SMP30/GNL were refined using the program phenix.refine. Molecular models were built using the program COOT.

3 Results and Discussion

The overall structure of mouse SMP30/GNL was essentially the same as that of human SMP30/GNL. SMP30/GNL adopts a β -propeller structure, which is composed of six β -sheets each of which is formed with four β -strands. The superposition of mouse and human SMP30/GNL revealed that residues 120–129, which are located in a loop region connecting two β -strands, have different conformations between them. These residues are located at the top of the SMP30/GNL molecule, serving as a lid over the substrate-binding cavity of the SMP30/GNL molecule.

Crystal structure of SMP30/GNL in complex with substrate/product homologues suggested that L-gulonate coordinates to the divalent metal ion. Then, Arg101, Asn103, and Glu121 seem to interact with the L-gulonate in the substrate-binding cavity, and the L-gulonate seems to bind to the substrate-binding cavity in a folded conformation. A manual modeling study suggested that L-gulonate in a folded conformation could be accommodated by the substrate-binding cavity of mouse SMP30/GNL. Then, nucleophilic attack of the hydroxyl group at C4 to the C1 atom may lead to the formation of the γ -lactone ring. In this step, Asp204 may serve as a catalytic base, which deprotonates OH(4) of the substrate, to facilitate the nucleophilic attack. In this catalytic reaction, hydroxyl groups of the substrate seem to be recognized by Arg101, Asn103, and Glu121, which are located at the one side of the inner surface of the substrate-binding cavity. These interactions seem to properly place the substrate in the active site and induce the substrate binding in a folded conformation.

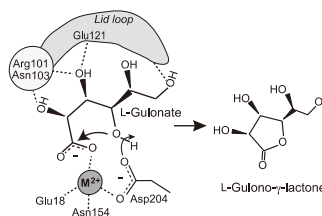


Fig. 1. Proposed catalytic reaction mechanism of mouse SMP30/GNL



Design and installation of Protein Complex Crystallography beamline at SSRF

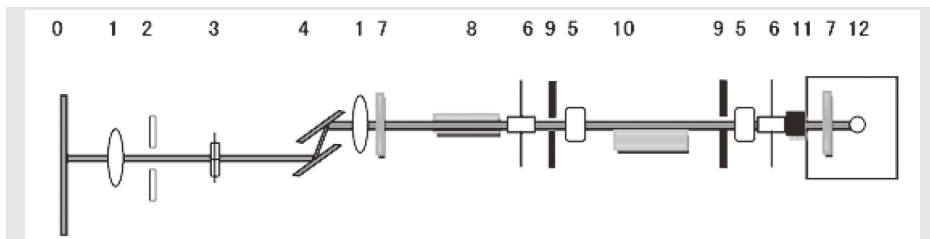
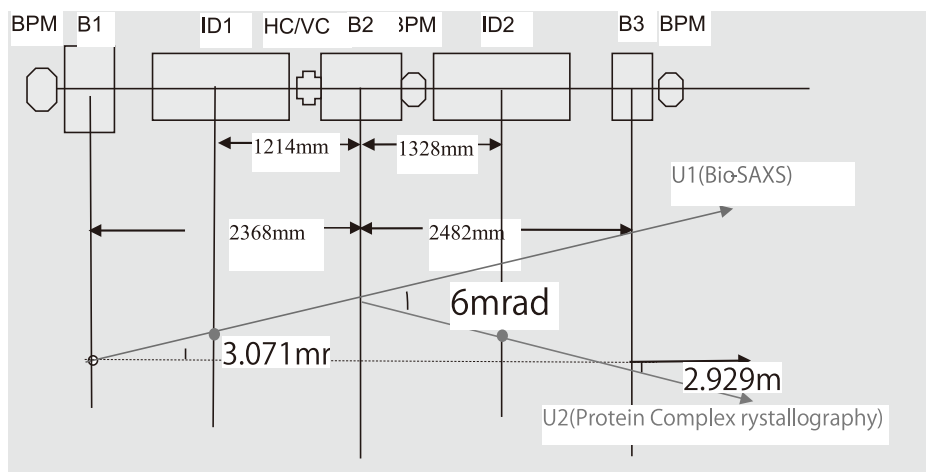
Kunhao Zhang¹, Sisheng Wang¹, Lin Tang² and Jianhua He¹

¹ Shanghai Institute of Applied Physics, CAS,
NO.2019 JiaLuo Road, Jiading District, Shanghai, 201800, China

² Shanghai Institutes for Biological Sciences, CAS,
NO. 320 Yueyang Road, Shanghai, 200031, China

Structure determination of protein complex is now one of the most important of structural biology development. This beamline is design mainly for solving the crystal structures of protein complex, especially those of large protein complexes and membrane proteins with huge molecular weight and large unit-cell parameters.

The protein complex crystallography beamline is composed of the canted undulator source, the front end, the beamline and the experimental station. The following figures show the layout of the canted undulator in the straight section and the optical set-up of protein complex beamline.



Crystal structure of pyridoxine 4-oxidase from *Mesorhizobium loti*

Andrew Njagi Mugo^a, Jun Kobayashi^b, Taiji Yamasaki^a, Bunzo Mikami^b, Yu Yoshikane^a, Toshiharu Yagi^a and Kouhei Ohnishi^c.

^a*Faculty of Agriculture and Agricultural Science Program, Graduate School of Integral Arts and Science, Kochi University, Nankoku, Kochi 783-8502, Japan,*

^b*Division of Applied Life Sciences, Graduate School of Agriculture, Kyoto University, Gokasho, Uji, Kyoto 611-0011, Japan, and* ^c*Research Institute of Molecular Genetics, Kochi University, Nankoku, Kochi 783-8502, Japan.*

[Aims] To elucidate the complex structure of pyridoxine 4-oxidase (PNOX) with its substrate analogue, pyridoxamine (PM). PNOX, an FAD-dependent enzyme from *Mesorhizobium loti* MAFF303099, is the first enzyme in the degradation pathway 1 for pyridoxine and belongs to Glucose-methanol-choline (GMC) oxidoreductases family [1].

[Methods] PNOX with a His₆ tag was overexpressed in *E.coli* JM109 cells and purified with a Ni-NTA agarose column and a QA52 column [2]. Crystallization was done by the sitting-drop vapour-diffusion method at 277 K. The structure was solved by molecular replacement method.



[Results] The crystal structures of PNOX and PNOX-PM were determined at 2.2 Å and 2.1 Å resolutions respectively. The overall structure consisted of FAD-binding and substrate-binding domains. The FAD interacts with the PNOX protein through a network of hydrogen bonds which are mainly found in the ribose and pyrophosphate moieties of the FAD molecule. The surface structure of PNOX molecule showed that it had an opening socket for access of substrates. The opening was followed by a bottleneck, formed from mainly hydrophobic residues, and a tunnel. The tunnel was linked to the active site cavity. In the cavity, active site residues were located on the re-face of the isoalloxazine ring of the FAD. A Proline residue, instead of His or Asn in other GMC oxidoreductases family members, was found in the active site [3].

Fig. 1. The Cartoon view of PNOX-PM tertiary structure. The substrate binding-domain is colored red; the FAD-binding domain green; FAD orange and PM blue.

-
- [1] B.Yuan, Y. Yoshikane, N. Yokochi, K. Ohnishi and T. Yagi, *FEMS Microbiol. Lett.* **234**, 225-230 (2004).
[2] A.N. Mugo, J. Kobayashi, B. Mikami, K. Ohnishi, T. Yagi, *Acta Cryst. Sec. F Struct. Biol. Cryst. Commun.* **68**, 66-68 (2012).
[3] A.N. Mugo, J. Kobayashi, T. Yamasaki, B. Mikami, K. Ohnishi and T. Yagi, *Biochim Biophys Acta*, **1834**, 953-963 (2013).

Operation Status of SACLA, the Japanese Compact XFEL facility

XFEL Research and Development Division, RIKEN SPring-8 Center^{*1}
 XFEL Utilization Division, JASRI^{*2}

^{*1} 1-1-1, Kouto, Sayo-cho, Sayo-gun, Hyogo 679-5148, Japan

^{*2} 1-1-1, Kouto, Sayo-cho, Sayo-gun, Hyogo 679-5198, Japan

Commissioning of the world's first compact X-ray FEL (XFEL) facility named SPring-8 Angstrom Compact free electron LAser (SACLA) started in the spring of 2011 and soon demonstrated lasing at a wavelength of 1 Angstrom. Owing to elaborate beam tuning efforts, a shortest laser wavelength of 0.63 Angstrom and the laser power saturation was achieved in a wide wavelength range from 1 to 3 Angstrom in the autumn of 2011 [1]. Via the short preparation period SACLA has been open for user experiments since March 2012. The first year (FY2012) operation was successfully done and the scheduled operation time of 7000 hr including user time of 3000 hr was achieved without any serious machine trouble. Averaged laser availability was beyond 92%. The laser performances, i.e., laser intensity, stability, tunability, shot-by-shot characterization, manipulation and reliability seem to be good enough for applying XFEL to various innovative experiments. This presentation will report the present laser performances and future upgrade plan at SACLA.

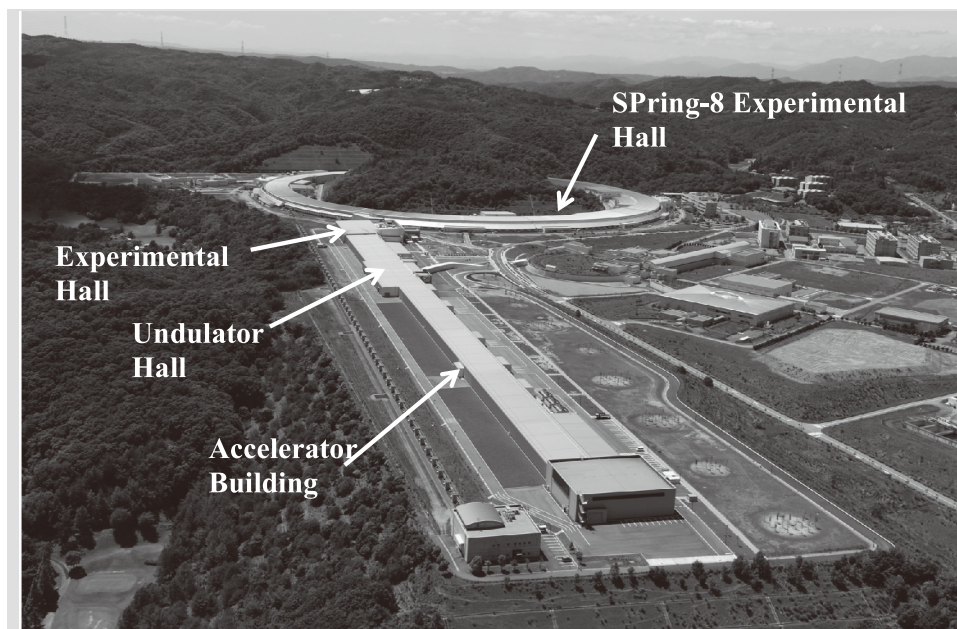


Fig. 1. Aerial photo of SACLA taken from the upstream side.

[1] T. Ishikawa et al., *Nature Photonics*. **6**, 540-544 (2012).



Image reconstruction from diffraction patterns in coherent X-ray diffraction imaging using the dark-field phase-retrieval method

Amane Kobayashi^{1,2}, Yuki Takayama^{1,2}, Tomotaka Oroguchi^{1,2},
Masayoshi Nakasako^{1,2}

¹*Department of Physics, Faculty of Science and Technology, Keio University,
3-14-1 Hiyoshi, Kohoku-ku, Yokohama 223-8522, Japan.*

²*RIKEN SPring-8 Center, RIKEN Harima Institute, 1-1-1 Kouto, Sayo, Hyogo
679-5148, Japan.*

In coherent X-ray diffraction imaging (CXDI) experiment, we reconstruct the electron density map of specimen particle, which is projected along the direction of incident X-ray, using the iterative phase-retrieval (iPR) method. We have developed a program suite [1,2], in which the iPR algorithm is implemented together with miscellaneous subroutines, and applied to simulation studies on the possibility of molecular imaging using X-ray free electron laser [1,2] and structure analysis for experimentally obtained diffraction patterns of chloroplasts [3]. One of problems in CXDI experiment is the difficulty to collect diffraction patterns of very small-angle region, where the information regarding particle shape is included.

Recently, the dark-field phase-retrieval (DFPR) method [4] is applied to diffraction patterns lacking the diffraction patterns of small-angle region, and demonstrated the possibility to give shape information. In the method, a monotonously decreasing mask function is multiplied to high angle diffraction pattern prior to conduct ordinary iPR calculation. After that, the ordinal iPR method is applied.

In the present study, we implemented the DFPR algorithm to our iPR program suite and examined carefully the effectiveness of the methods through a series of phase-retrieval simulations regarding a protein molecule. Even when lacking a large area around the incident beam up to the 5-th speckle patterns counted from the incident beam, the shape of the protein molecule is correctly reconstructed. Subsequent iPR calculation using the density map obtained by the DFPR method successfully retrieved the projection molecular image. In this poster session, we report the details of the DFPR method and future application.

[1] W. Kodama and M. Nakasako (2011) *Phys. Rev. E* **84**, 021902.

[2] T. Oroguchi, and M. Nakasako, *Phys. Rev. E* **87**, 022712 (2013).

[3] Y. Takayama and M. Nakasako (2012) *Rev. Sci. Instrum.* **83**, 054301.

[4] A. V. Martin *et al.* (2012) *Opt. Express* **20**, 13501.



Software suite “SHITENNO” for automatically processing diffraction patterns in coherent X-ray diffraction imaging experiments at SACLA

Yuki Sekiguchi^{1,2}, Tomotaka Oroguchi^{1,2}, Yuki Takayama^{1,2},
and Masayoshi Nakasako^{1,2}

¹*Department of Physics, Faculty of Science and Technology, Keio University,
3-14-1 Hiyoshi, Kohoku-ku, Yokohama, 223-8522 Japan*

²*RIKEN SPring-8 Center, RIKEN Harima Institute, 1-1-1 Kohto, Sayo,
Sayo-gun, Hyogo 679-5148 Japan*

Using a diffraction apparatus named KOTOBUKI-1[1], we have been conducting cryogenic coherent X-ray diffraction imaging (cCXDI) experiments at X-ray free electron laser facility SACLA. In the experiments, we aim to visualize the internal structures of metal nano-particles and non-crystalline biological specimens such as cells and organelle at a resolution of a few tens nm. Sample particles scattered randomly on carbon or silicon nitride membrane are prepared under humidity controlled atmosphere and flash-cooled to the frozen-hydrated state [2]. The specimen membrane loaded into the vacuum chamber of KOTOBUKI-1 is raster-scanned against X-ray pulses at 1 Hz. Because of the wide range of diffraction intensity, we collect data using tandem detectors. One is an Octal multi-port CCD detector for high-angle diffraction patterns, and the other is a Dual multi-port CCD detector with attenuator for small-angle diffraction patterns. This experimental setup enables X-ray pulses to hit specimen particles at a rate of 30-100%. As a result, we obtain several terabyte of diffraction patterns during a few days. Now, we have been developing a software suite named SHITENNO for processing huge amount of diffraction patterns automatically and efficiently.

The SHITENNO suite treats diffraction patterns of HDF5 format, which are numbered according to X-ray shots in each measurement run. After subtracting dark current background of CCD detectors, we select diffraction patterns with significant level of intensity as expected from the scattering cross-section of particles by monitoring the sum of diffraction intensities in a specified small-angle area. Next, beam center positions in detectors for every diffraction pattern are determined. Based on the Friedel's symmetry, we search beam center positions in detectors, which maximize the similarity in the diffraction patterns between a specified small-angle region and its centrosymmetry mate. Then, diffraction patterns from Octal and Dual detector are merged to a single file using geometrical parameters. The parameters are determined by approximating a diffraction pattern from a cube-shaped copper particle with an approximate dimension of 200 nm with sinc function. Merged diffraction data are submitted to the subsequent phase-retrieval calculation using the hybrid-input-output algorithm in combination with the shrink-wrap algorithm [3]. Immediately after a few hundreds of diffraction patterns per sample are recorded, the SHITENNO suite provides low resolution images of specimen particles within ten minutes.

In the presentation, we introduce the SHITENNO suite and demonstrate its performance in the cCXDI experiments at SACLA.

[1] M. Nakasako *et al. Rev. Sci. Instrum.* (submitted)

[2] Y. Takayama & M. Nakasako, *Rev. Sci. Instrum.* **83**, 054301 (2012)

[3] T. Oroguchi & M. Nakasako, *Phys. Rev. E* **87**, 022712 (2013)

Feasibility study on explosives using synchrotron radiation: Chemical fertilizers

Pisutti Dararutana^{1,*}, Jiraphan Dutchaneephet², Krit Won-in³

¹ *The Royal Thai Army Chemical School of the Royal Thai Army Chemical Department, Bangkok 10900 Thailand*

² *Faculty of Science, Chiang Mai University, Chiang Mai 50200 Thailand*

³ *Faculty of Science, Kasetsart University, Bangkok 10900 Thailand*

**Corresponding author, email: pisutti@hotmail.com*

Abstract:

In this work, chemical fertilizers that used as explosive stimulants were analyzed based on synchrotron radiation by using X-ray Photoelectron Spectroscopy (XPS) and Wide Angle X-ray Scattering (WAXS). It was known that an explosive was defined as a material which contained a large amount of energy stored in chemical bonds. The energetic stability of gaseous products, and hence, their generation came from the formation of strongly bonded like carbon (mono/di)oxide and (di)nitrogen. Consequently, most commercial explosives were contained with -NO₂, -ONO₂ and -NHNO₂ groups which when detonated release gases like the aforementioned ones, e.g., nitroglycerin, TNT, HMX, PETN, nitrocellulose, etc. It was revealed that the elemental compositions, especially N was found in most of the explosive and fertilizer. Scanning electron microscope coupled with energy-dispersive X-ray fluorescence spectroscopy (SEM-EDS) and Proton induced X-ray emission spectroscopy (PIXE) were also carried out to characterize them. XPS and WAXS spectra showed the characterized peaks in the various samples. The elemental analysis showed the presence of trace elements. Explosives and fertilizers have differences in specific compositions. It can be concluded that these methods seem to be used as fingerprint to identify the various explosives and fertilizers.



Fabrication of Metallic Microstructures using X-ray Lithography Process

Rungrueang Phatthanakun, Chanwut Sriphung, Watcharapon Pummara

*Synchrotron Light Research Institute (Public Organization)
111 University Avenue, Nakhon Ratchasima 30000, Thailand*

X-ray lithography is one of micro-fabrication techniques which has been applied to generate microstructures based on batch fabrication process [1-2]. Soft X-ray from synchrotron radiation is exposed through X-ray mask to define irradiated areas in photoresist, resulting in vertical sidewall structures used for micromolds. Metallic microstructures such as nickel, copper, silver, and gold can be formed in these micromolds by electroforming method. Figure 1 shows the developed photoresist which was applied as micromolds for metal electroforming, and figure 2 displays metallic microgears made of nickel released from substrate after electroforming process.

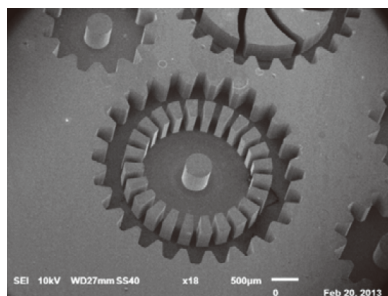


Fig. 1. SEM image of micromolds for metal electroforming.

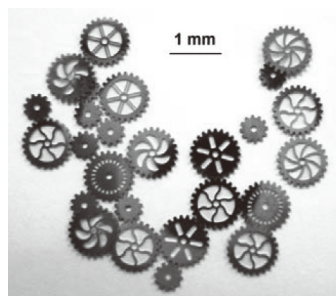


Fig. 2. Microgears made of nickel released from substrate.

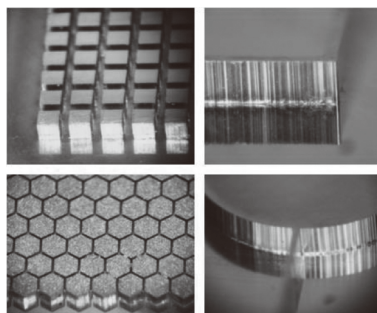


Fig. 3. Metallic micromolds for PDMS replication in microfluidic applications.

Deep X-ray lithography based on synchrotron radiation can provide thick microstructures layer from several micrometers to millimeters with high aspect ratio up to 40. The structures with sidewall roughness in the range 20 to 30 nm have been used in optical, micro-fluidic and mold insert applications. Figure 3 shows metallic micromolds for PDMS replication applied in microfluidic applications. As X-ray lithography is a unique tool for batch fabrication, it can be used to generate certain structures which could not be manufactured with any other tool. Industrial process can apply this technique in micromolds fabrication and used the micromolds in plastic injection machine.

[1] K. Kim, et al., *Microsystem technologies*, **9**, (2002).

[2] M. Wissmann, et al., *Proc. Of SPIE*, 6992 (699208) (2008).

Synchrotron-Based Data-Constrained Modeling Analysis of Microscopic Mineral Distributions in Limestone

Yudan Wang, Tiqiao Xiao

*Shanghai Institute of Applied Physics, Chinese Academy of Sciences, Shanghai,
201800, China*

Three dimensional (3D) microscopic distributions of dolomite and calcite in a limestone sample have been analyzed with a data-constrained modeling (DCM) technique using synchrotron radiation (SR) based multi-energy X-ray CT data as constraints. Multi-energy X-ray CT scans were performed at the Shanghai Synchrotron Radiation Facility (SSRF) at beam energies of 25 and 35keV. The high resolution distributions of mineral phases of a natural limestone have been obtained using CT slices via the DCM approach [1], as shown in **Fig. 1**. It is found that a fraction of calcite formed clusters inside dolomite, and pores was concentrated in some parts of the sample. The figures also indicate that there was a significant proportion of pores and dolomite which were smaller than the CT resolution ($3.7\mu\text{m}$), which is shown as unsaturated pixel intensity for images. The volume fractions of calcite, dolomite and pores were calculated as average voxel values in **Fig. 1** (c, d), which were 15%, 81% and 4% respectively. The results are useful for quantitative understanding of

mineral, porosity, and physical property distributions in relation to oil and gas reservoirs hosted in carbonate rocks, which account for more than half of the world's conventional hydrocarbon resources [2].

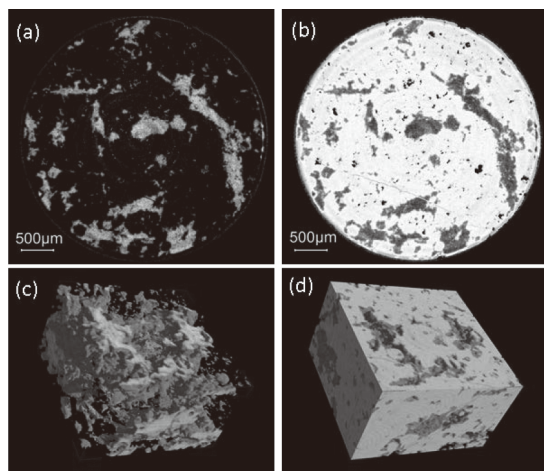


Fig. 1. Distribution of mineral phases on the X-Y plan and its 3D structures of part of sample with the size of $500\times500\times300$ pixels. (a) and (c) are calcite, (b) and (d) are dolomite.

[1] Y. Wang, Y. Yang, I. Cole, A. Trinchì, T. Xiao, *Materials and Corrosion*, **63**, 180 (2013).

[2] Y.D. Wang, Y.S. Yang, T.Q. Xiao, K.Y. Liu, B. Clennell, G.Q. Zhang, H.P. Wang, *International Journal of Geosciences*, **4**, 344 (2013).



Suitability of Hydrated Magnesium Carbonates as Hosts for Atmospheric Carbon Dioxide: An *In-Situ* Powder Diffraction Study

Bree Morgan¹, Ian C. Madsen¹ and Siobhan A. Wilson²

¹CSIRO Process Science and Engineering, Clayton Sth, VIC, 3169, AUSTRALIA

²School of Geosciences, Monash University, Clayton, VIC 3800, AUSTRALIA

With growing concerns over the likely contribution of carbon dioxide (CO₂) to rising global temperatures, the need to reduce atmospheric concentrations of this greenhouse gas is becoming increasingly urgent. One proposed strategy for lowering CO₂ concentrations is by sequestration during industrially controlled precipitation of magnesite (MgCO₃); an environmentally benign mineral which is stable over geological time periods. The strategy is hindered by MgCO₃ precipitation being kinetically inhibited under ambient conditions. While enhancing MgCO₃ formation with increased temperatures and pressures is technologically feasible, it is not currently financially viable owing to low carbon taxes and CO₂ prices.

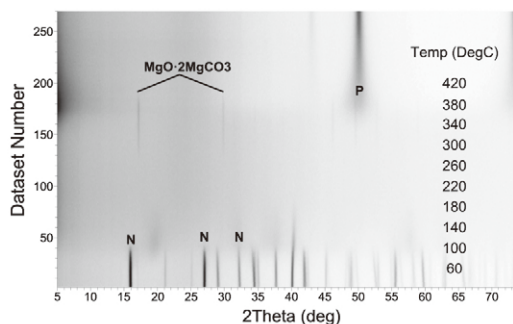


Fig.1. Raw laboratory powder diffraction data showing the thermal decomposition (30-550 °C) of nesquehonite viewed down the intensity axis. N= Nesquehonite, P = Periclase

Hydrated magnesium carbonate minerals, such as nesquehonite (MgCO₃·H₂O), represent promising alternatives to *ex-situ* CO₂ sequestration in magnesite. They readily precipitate at the low temperatures (<100 °C) that dominate the Earth's surface and can sequester significant quantities of atmospheric CO₂ [1]. While the breakdown of nesquehonite at ~100 °C (Figure 1) infers its stability over a majority of global surface temperatures, the decomposition kinetics of hydrated magnesium carbonates exposed to non-thermal environmental stressors are poorly understood. This information is crucial

to understanding the stability of these minerals on the millennial timescales needed to mitigate atmospheric CO₂ pollution.

Utilising *in-situ* powder diffraction, our study will provide novel kinetic and mechanistic insights into decomposition of hydrated magnesium carbonates at varied pH, humidity, salinity and concentrations of organic/inorganic ligands. This represents the wide range of environmental conditions that may exist at surface disposal sites for the minerals. Understanding the mechanisms and kinetics of hydrated magnesium carbon decomposition is critical to ensuring their suitability as long-term mineral stores for CO₂. The outcomes of our research will facilitate effective monitoring and predictions for long-term stability of CO₂ storage in geological hosts.

[1] S.A.Wilson, G.M. Dipple, I.M. Power, S.L.L. Barker, S.J. Fallon and G. Southam, Environ. Sci. Technol. 45, 7727 (2011).

Discriminative Separation of CO₂ and CH₄ Using a Novel “Molecular Trapdoor” Zeolite: Materials and Process Study

J. Shang^{1,2}, G. Li^{1,2}, R. Singh^{1,2}, P. Xiao^{1,2}, J.Z. Liu^{3*}, and P.A. Webley^{1,2*}

¹Cooperative Research Centre for Greenhouse Gas Technologies (CO2CRC), Melbourne, Australia

²Department of Chemical and Biomolecular Engineering, The University of Melbourne, Victoria 3010, Australia

³Department of Mechanical and Aerospace Engineering, Monash University, Clayton, Victoria 3800, Australia

The efficient separation of CO₂ from natural gas streams is becoming increasingly important as wells containing higher CO₂ content are targeted for LNG production. Conventional techniques for CO₂ removal such as acid gas scrubbing, while effective for low level CO₂ removal, are energy intensive for removal of high CO₂ levels, and can lead to additional environmental problems associated with the solvent. While adsorbents are effective for low level removal of CO₂ at low pressures, an appropriate adsorbent for use at high well head pressure (~ 100 bar) and low to medium CO₂ content has not been identified to date. Existing adsorbents show poor CO₂/CH₄ selectivity at high pressure and high CO₂ level and their use would lead to substantial methane loss.

By conducting a combined experimental (including material synthesis, adsorption characterization, binary breakthrough, Pressure Swing Adsorption process, PALS, NMR, and *in situ* synchrotron powder X-ray diffraction experiment of gas adsorption) and computational (using *ab initio* Density Functional Theory) study, we report on a novel zeolite which is capable of exclusive CO₂ adsorption at high pressure. The zeolite is in the CHA family with Si:Al ratio of 1-3 and contains large cations such as K⁺ or Cs⁺. We show that these materials are capable of guest-induced cation motion providing access of CO₂ to the internal pore space while preventing access of CH₄. The access is based not on molecular size but rather on the ability of the guest to induce temporary and reversible cation movement. This reversible movement is also temperature dependent. We term it “molecular trapdoor” mechanism (see Figure 1) and provide strong evidence to support this hypothesis through spectroscopic and modeling approaches [1].

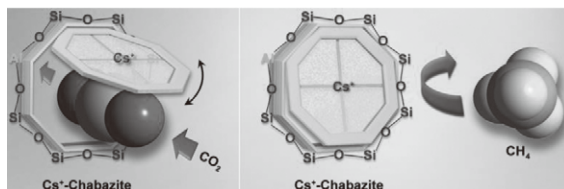


Fig. 1. Schematic representation of the molecular trapdoor for gas discrimination.

Using a 2-bed high pressure PSA apparatus, we demonstrate high methane purity and recovery is attainable provided the temperature of operation is below the temperature at which methane is able to penetrate the zeolite “windows”. A methane purity of close to 100% at a recovery of great than 95% is achievable.

[1] J. Shang, G. Li, R. Singh, Q. Gu, K. Nairn, T. Bastow, N. Medhekar, C. Doherty, A. Hill, J. Liu, and P.A. Webley, *J. Am. Chem. Soc.* **134**, 19246 (2012).



***In situ* X-ray and neutron studies to investigate proton conduction in proton exchange membranes for direct alcohol fuel cells**

Krystina Lamb^a, Roland De Marco^a, John Bartlett^a, Vanessa Peterson^b,
Dominique Appadoo^c, and San Ping Jiang^d

^a *University of the Sunshine Coast, Locked Bag 4
Maroochydore DC, Queensland, 4558, Australia*

^b *Australian Nuclear Science and Technology Organisation, Locked Bag
2001, Kirrawee DC, New South Wales, 2232*

^c *Australian Synchrotron, 800 Blackburn Road, Clayton, Victoria, 3168,
Australia*

^d *Fuel and Energy Technology Institute, 1 Turner Ave, Technology Park, Bentley,
Perth Western Australia, 6102, Australia*

Medium temperature proton exchange membrane fuel cells (MT-PEMFCs) are solid-state energy conversion devices that electrochemically convert chemical energy (e.g., from alcohols) into electricity. MT-PEMFCs have advantages such as elimination of carbon monoxide poisoning of the electrocatalyst, enhanced oxidation kinetics of alcohol fuels such as methanol, and the use of liquid fuels. Heteropoly acids (HPA) such as phosphotungstic acid (HPW) can be used to functionalize ordered mesoporous silica (MSN) to make nanocomposite proton exchange membranes (PEMs).

While these HPW MSN composites have been studied extensively as catalysts, HPW functionalized MSNs have only recently been studied for use in MT-PEMFCs using methanol as a fuel. Previous studies have investigated the relationship between physical stability, temperature and fuel cell performance. However, the exact mechanism of proton conduction in these materials, and how this is altered by changes in the physical and chemical environment of the materials has not been investigated *in situ*.

In this project, MT-PEMFCs with HPW MSN will be operated under a variety of physical and chemical conditions, and the mechanism of proton conduction will be studied *in situ* using small angle neutron scattering (SANS), far- and mid-infrared spectroscopy (far- and mid-IR) and quasi-elastic neutron scattering (QENS). These techniques will be compared to molecular dynamics models, both from literature and developed by the research team. To conduct these studies, a specialized fuel cell testing station will be designed and constructed. Work at the Australian Synchrotron's (AS's) High Resolution Infrared beamline will be conducted in July 2013 using a custom-designed fuel cell tailored for the beamline at the AS.

Synchrotron Light Brightening Research in Volcanology

¹Marco Brenna, ¹Natalia Pardo, ¹Shane J. Cronin, ²Felix W. von Aulock & ²Ben M. Kennedy

¹*Volcanic Risk Solutions, Massey University, Private Bag 11222,
Palmerston North 4442, New Zealand*

²*Department of Geological Sciences, University of Canterbury,
Private Bag 4800, Christchurch, New Zealand*

Volcanology research combines physical, chemical and geological research methods into understanding the processes by which magmas are formed deep in the Earth and how they are erupted at the surface. One research topic of great relevance for hazard assessment is the search for factors modulating the degree of explosivity of volcanic eruptions. This quest takes us deep into the root zones of volcanoes to examine the conditions of magma formation and evolution of volatile solubility. It is the content and behavior of these volatiles (H₂O, CO₂, S, halogens and light metals) that influences transitions magmas undergo in volume and rheology during the final stage of rise through a conduit to the surface. Analyses of increasingly higher spatial resolution are required to pinpoint the fundamental phase and chemical transformations occurring. For these studies, the application of synchrotron techniques offers great potential, but is yet in its infancy.

X-ray Fluorescence Microscopy (XFM) is a powerful tool for investigating the fine-scale distribution of chemical elements within portions of a rock or single mineral/interface. The unparalleled speed of data acquisition associated with the Maia detector at the Australian Synchrotron enables a hitherto impossible ability to map and generate chemical profiles throughout multiple interfaces within a rock sample. This technique was applied to understand rocks at Ulleung volcano, Republic of Korea, where the inter-diffusion of trace elements (e.g. Zr, Rb, Rare Earth Elements) between volcanic glass and crystals, and zonation patterns within crystals is being used to determine magma affinity, residence time and ascent rates.

The degree of magma explosivity during volcanic eruptions is controlled to a large degree by the pre-eruptive dissolved volatile (mainly water) content. The growth of water bubbles in magma initiates catastrophic volcanic eruptions by building up pressure, followed by collapse of the residual foam of bubbles and magma which leaves a degassed magmatic plug behind. Our recent studies at the Australian Synchrotron have shown that water can be both enriched as well as depleted in a very thin margin around the bubbles. The fast processes during volcanic eruptions and the high viscosities of magma limit diffusion of volatiles. Therefore, the high spatial resolution and signal-to-noise ratios of synchrotron sourced Fourier transform infrared spectroscopy (FTIR) are needed to measure the distribution of volatiles and to model the diffusion that drives the growth and collapse of bubbles in magma.

If the process of bubble growth in magma is rapid, a sudden volume expansion drives explosive eruptions. Vesicles remaining in cooled eruption products therefore provide insights into the last stages of eruptions. Synchrotron sourced X-ray micro computed tomography (micro CT) enables non-destructive 3D visualization of these. The heterogeneity in vesicle and crystal content within pumice from Mount Ruapehu, New Zealand could be quantified by synchrotron sourced microCT to infer complex flow and degassing processes within the volcanic conduit that related to both stable and collapsing eruption columns. A greatly improved quantification of magma decompression rates from such studies helps define the types of volcanic hazards expected at volcanoes around the world.



Nucleation and crystallization kinetics of a complex lithium disilicate glass: *in situ* and time-resolved synchrotron powder diffraction study

Saifang Huang, Peng Cao, Wei Gao

Department of Chemical & Materials Engineering, The University of Auckland, Auckland 1142, New Zealand

Introduction: Lithium disilicate glass-ceramic has been documented since 1950s [1] and now it has applications such as dental restorations and magnetic disks. P_2O_5 is one of the most widely used nucleating agents.[2] Even though many techniques have been employed, such as laboratory XRD, electron microscopy, thermal analysis and NMR, the fundamental understanding of the nucleation and crystallization process is incomplete, and the role of P_2O_5 as a nucleating agent is still unclear.[3]

Objectives: The aims of this study were to investigate the effects of temperature and holding time on phase transformation and crystallite size; to estimate its nucleation kinetics by using a KM-JMA equation;[4] and to investigate the crystallization kinetics and mechanism of this glass. Moreover, we revisited the role of P_2O_5 on the nucleation of this glass.

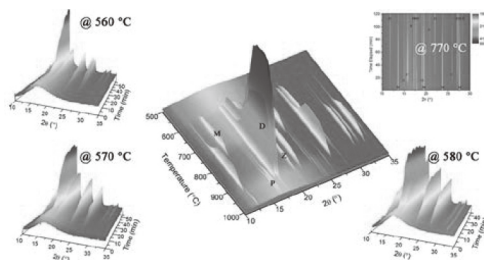


Fig. 1. XRD patterns of a lithium disilicate glass at isothermal and non-isothermal annealing processes.

Methods: To investigate nucleation and crystallization kinetics, we conducted isothermal annealing at 560, 570, 580 and 770 °C and non-isothermal annealing from 500 to 1010 °C on a multi-component lithium disilicate glass in the SiO_2 – Li_2O – P_2O_5 – Al_2O_3 – ZrO_2 glass system, and the high-temperature XRD patterns of this glass (Fig. 1) were monitored *in situ* and *real time* with synchrotron radiation during annealing processes. The high-resolution synchrotron XRD data were used for the quantitative phase analysis via Rietveld method. [3]

Results: The nucleation kinetics is temperature dependent, and the induction period of nucleation is longer at a lower temperature. The volume fraction data of the isothermal nucleation experiments were modelled using a modified KM-JMA equation to incorporate the initial induction period. The Avrami exponent (n) for $Li_2Si_2O_5$ (LS_2) phase (1.74–1.84) is higher than that of Li_2SiO_3 (LS) phase (1.24–1.49). The activation energy E_a of LS_2 and LS are calculated to be 275 and 213 kJ/mol, respectively. The LS_2 crystals grow at the expense of the LS , cristobalite and quartz phases in the glass during the isothermal crystallization process at 770°C. Besides, it is found that the nucleation of LS and LS_2 in this complex glass is triggered by the steep compositional gradients associated with the disordered lithium phosphate precursors in the glass matrix. [3]

[1] S. D. Stookey, *Ind. Eng. Chem.* **51**, 805-808 (1959).

[2] E. Apel, C. van't Hoen, V. Rheinberger, W. Höland, *J. Eur. Ceram. Soc.* **27**, 1571-1577 (2007).

[3] S. F. Huang, P. Cao, Y. Li, Z. H. Huang and W. Gao, *Cryst. Growth Des.* (2013) Revision under review.

[4] M. Hillert, *Metall. Mater. Trans. A* **42**, 3241-3241 (2011).

The infrared beamline BL43IR at SPring-8: present status and recent studies

Yuka Ikemoto, Taro Moriwaki and Toyohiko Kinoshita

JASRI/SPring-8, 1-1-1 Koto, Sayo, Hyogo 679-5198 Japan

The infrared beamline BL43IR at SPring-8 has been in operation since 2000. The high brilliance property of infrared synchrotron radiation is utilized by a microspectroscopy measurement at BL43IR [1]. In this study, we present the current status and recent studies.

BL43IR has three microspectroscopy stations, i.e., a high spatial resolution microscope, a long working distance microscope and a magneto-optical microscope. In addition, in order to overcome the diffraction limit, we are developing a near-field spectroscopy apparatus. Fig. 1 shows end stations at BL43IR.

At BL43IR, various fields of studies have been conducted. Physics researches have been the most productive. The representative activities are, for example, high pressure experiments of strongly correlated electron system [2], microspectroscopy studies of molecular organic conductors [3] and microspectroscopy experiments under multi-extreme conditions [4]. Recently, studies in other fields than physics are increasing. A research to verify the effect of a hair treatment agent was done as an industrial use. In the study, a mapping image of a sliced hair was measured to identify the penetration of the functional components of the treatment agent into the hair [5]. One of the archaeological studies related to the identification of a kind of excavated textile fibers. New procedure was suggested to identify the bast fibers by analyzing the polarization angle dependence of spectral pattern [6]. One of a polymer science

studies was conducted to investigate a wetting behaviour of a polyelectrolyte brush surface. By infrared microspectroscopy, the presence of the water was confirmed even outside the water droplet, and the wetting mechanism was discussed [7].

SPring-8 covers wide energy range and various fields of researches have been conducted at the many beamlines. We are currently trying to promote utilizations of the multiple synchrotron beamlines, in order to encourage more use of BL43IR.

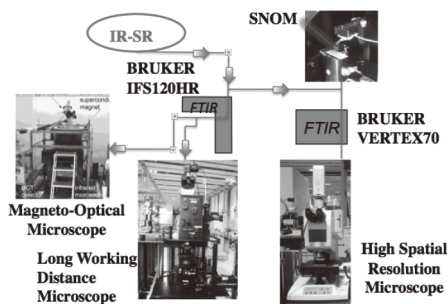


Fig.1 End stations at BL43IR.

- [1] T. Moriwaki and Y. Ikemoto, *Infrared Phys. and Tech.* **51** (2008) 400.
- [2] H. Okamura, K. Shoji, M. Miyata, H. Sugawara, T. Moriwaki and Y. Ikemoto, *J. Phys. Soc. Jpn.* **82** (2013) 074720, and others.
- [3] K. Kubo, T. Shiga, T. Ymamoamoto, A. Tajima, T. Moriwaki, Y. Ikemoto, M. Yamashita, E. Sessini, M. L. Mercuri, P. Deplano, Y. Nakazawa and R. Kato, *Inorganic Cehmistry* **50** (2011) 9337.
- [4] T. Nishi, S. Kimura, T. Takahashi, Y. Mori, Y. S. Kwon, H. J. Im and H. Kitazawa, *Phys. Rev. B* **71** (2005) 220401(R).
- [5] S. Inamasu, *Fragrance Journal* **40** (2012) 39.
- [6] M. Okuyama, M. Sato and M. Akada, *Sen'i Gakkaishi* **68** (2012) 55; M. Okmuraya, M. Sato and M. Akada, *Sen'i Gakkaishi* (in Japanese) **68** (2012) 59.
- [7] D. Murakami, M. Kobayashi, T. Moriwaki, Y. Ikemoto, H. Jinna i and A. Takahara, *Langmuir* **29** (2013) 1148.



Powder X-ray Diffraction Studies of the Betaine-ester Imidazolium-based Amphotropic Ionic Liquid Crystals: As Nano-ion Channel Networks and Organogelators.

Jing C. W. Tseng and Ivan J. B. Lin

Department of Chemistry, National Dong-Hwa University, Shoufeng, Hualien, 974, Taiwan

Imidazolium ionic liquid crystals (ImILCs), which have become a major class of materials with wide spread of applications in scientific and technological fields have been reported in the literature ^[1]. Ester functionalized Im salts are cleavable and biodegradable, and have been utilized for drug delivery as soft drugs ^[2]. Here, we present a series of betaine- ester analogues of imidazolium salts exhibiting both thermotropic and lyotropic liquid crystal behaviors are reported as amphotropic ionic liquid crystals. Doping lithium salt to these salts lowers the melting temperatures and raises the clearing temperatures substantially to form room temperature ILCs. Effective interactions between Li^+ ions and $\text{C}=\text{O}$ group through well-ordered pathways lead to the enhancement of the ionic conductivities. These compounds are gelators, which form gels in a variety of organic solvents such as chloroform, methanol, ethanol, tetrahydrofuran, while exhibiting lamellar mesophase. Powder X-ray diffraction (PXRD) study was employed to characterize the mesophase and gel state structures of these salts.

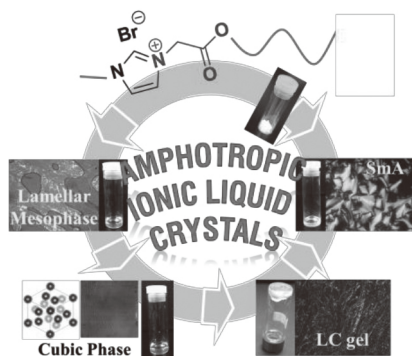


Fig. 1. Schematic diagram of Amphotropic Ionic Liquid Crystals and LC gels.

[1] (a) K. Binnemans, Chem. Rev. 105, 4148 (2005); (b) K. V. Axenov, S. Laschat, Materials, 4, 206 (2011).

[2] (a) S. T. Elder, A. Preuss, K.U. Schoning, K. Muhlbauer; Pub. No.: US 2008/0070966 A1; (b) Nicholas Gathergood, Peter J. Scammells*, and M. Teresa Garcia*, Green Chem., 8, 156 (2006).

Multivariate evaluation, feature extraction, classification and clustering of images and spectral data sets by using R environment

Krzysztof Banas¹, Agnieszka Banas¹ and Mark B. H. Breese^{1,2}

¹*Singapore Synchrotron Light Source, National University of Singapore, 5 Research Link, Singapore 117603*

²*Physics Department, National University of Singapore, 2 Science Drive 3, Singapore 117551*

Analysing the large number of variables in data sets (images and spectra) collected in contemporary laboratories is unquestionably a major challenge. In order to be able to extract essential information from a plethora of recorded bytes one must turn to statistical methods. Multivariate evaluation of the experimental results enable for significant dimension reduction (principal component analysis [1], partial least squares [2]), segmentation or clustering (hierarchical clustering analysis, k-means [3], density-based clustering, self-organizing maps [4]) and finally classification (linear discriminant analysis [5], decision trees and random forest [6], support vector machine [7]). These chemometric approaches adapt to spectral data and images can provide new insights on the spatial and spectroscopic information. In this contribution various examples of multivariate statistical analysis of spectral data and images by using R open source [7] environment will be presented.

[1] J. E. Jackson, A user guide to principal components. Wiley: New York (1991).

[2] D. Haaland, E. Thomas, *Analytical Chemistry* **60**(11) 1193 (1988)

[3] C. Fraley, A. Raftery, *Journal of the American Statistical Association* **97**(458), 611 (2002).

[4] T. Kohonen, *Biological Cybernetics* **43**(1), 59 (1982).

[5] A. Martinez, A. Kak *IEEE Transactions on Pattern Analysis and Machine Intelligence* **23**(2) 228 (2001)

[6] L. Breiman, *Machine Learning* **45**(1) 5 (2001)

[7] C. Cortes, V. Vapnik, *Machine Learning*, **20**(3) 273 (1995).

[8] R Core Team, R: A Language and Environment for Statistical Computing, <http://www.R-project.org/> (2013)



Identification of a cassava bacterial blight pathogen, *Xanthomonas axonopodis* pv. *manihotis* using FT-IR spectroscopy

Natthiya Buensanteai^{1*}, Kanjana Thumanu², Mathukorn Sompong¹, Dusit Athinuwat⁴, Khanistha Kooboran¹ and Sutruedee Prathuangwong⁵

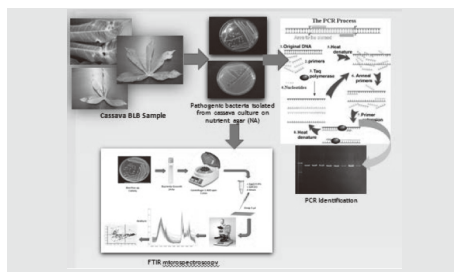
¹School of Crop Production Technology, Institute of Agriculture Technology, Suranaree University of Technology, Nakhon Ratchasima, 30000 Thailand

²Siam Photo Laboratory, Suranaree University of Technology, Nakhon Ratchasima, 30000 Thailand

⁴Major of Organic Farming Management, Faculty of Science and Technology, Thammasat University, Pathumthani, 12121 Thailand

⁵Department of Plant Pathology, Faculty of Agriculture, Kasetsart University, Bangkok, 10900 Thailand

Xanthomonas axonopodis pv. *manihotis* is the causal agent of cassava bacterial blight disease, reduced yield of cassava economic crops around the world, especially Thailand [1]. In this study, we developed a novel strategy for the rapid identification of *X. axonopodis* pv. *manihotis* based on Fourier transform infrared microspectroscopy (FTIR microspectroscopy). Two reference strains and 5 isolates of gram-negative bacteria isolated from cassava field were used in this study. The isolates were identified according to the guidelines of bacteriology. Cassava bacterial blight pathogen were further identified by 16S rDNA and sequencing. A standardized experimental protocol was established, and FTIR spectral database containing more than 200 infrared spectra was investigated. FTIR microspectroscopy identification system consisted of two hierarchical levels. The top-level FTIR network allowed the identification of *X. axonopodis* pv. *manihotis* and an identification success rate more than 95%. The second-level network was developed to differentiate the two most relevant species of *X. axonopodis* pv. *manihotis* and *X. axonopodis* pv. *cassavae*, with a correct identification rate more than 95%. Our results demonstrate the high degree of reliability and strong potential of FTIR spectrum analysis for the rapid identification of plant pathogenic bacteria suitable for use in routine *X. axonopodis* pv. *manihotis* diagnosis.



Schematic of cassava bacterial leaf blight (BLB) identification using polymerase chain reaction with *Xanthomonas* specific primers and Fourier-transform infrared (FTIR) microspectroscopy.

[1] N. Buensanteai et.al. SLRI PR. (2013).



Infrared Spectroscopy and Imaging Beamline at the Siam Photon Laboratory

Sirinart Srichan¹, Pongjakr Tarawarakarn¹, Apirak Suthummapiwat¹, Supawan Srichan¹, Surapong Kokkratok¹, Kanjana Thumanu¹, Wanwisa Limpirat¹, Saroj Rujirawat², Prayoon Songsiriritthigul², Supagorn Rugmai¹, Thierry Moreno³, Paul Dumas³

¹*Synchrotron Light Research Institute (Public Organization), 111 University Avenue, Suranaree, Muang, Nakhon Ratchasima, 30000 Thailand*

²*Suranaree University of Technology, 111 University Avenue, Suranaree, Muang, Nakhon Ratchasima, 3000 Thailand*

³*Synchrotron-SOLEIL Synchrotron-SOLEIL, L'orme des Merisiers, BP48, 91192 Gif sur Yvette Cedex, France*

An infrared (IR) beamline has been designed, constructed and installed at the Siam Photon Laboratory, Thailand. The modified bending magnet chamber allowing large opening angles (both vertically and horizontally) has been designed in order to collect the infrared synchrotron radiation emitted from an edge and constant field radiation in the infrared wavelengths(1). All chambers, mirror holders and mechanical components have been in-house designed, fabricated and conditioned. A slotted mirror (M1) with water cooling system, located at 2.2 m from the source, is used to collect the near, mid- and far- IR in the wavelength between 1.5-100 μm .

The first four mirrors, located inside the tunnel, are used to collect, propagate and focus the extracted beam through a CVD diamond window (diameter 20 mm) located just outside the shielding wall. We have recently observed the IR beam after the diamond window.

A deviation chamber has been installed after the diamond window in order to split the IR beam into three quasi-collimated beams to allow them to propagate over a long distance. The three quasi-collimated beams may be recombined in any combination, allowing us to install IR experimental stations up to three stations. The current status of beamline installation and alignment will be demonstrated.

[1] W. Pattanasiriwisawa, P. Songsiriritthigul, P. Dumas, in: Proceedings of the IP Conference, SRI 2009, 10th International Conference On Radiation Instrumentation, 1234, 371–374 (2010)



Long- and short-ranged structure of multiferroic $\text{Pb}(\text{Fe}_{0.5}\text{Nb}_{0.5})\text{O}_3$

Hasung Sim^{1,2,3,4}, Sanghyun Lee¹, Kun-Pyo Hong¹, Seongsu Lee⁵, Takashi Kamiyama⁶, Toshiya Otomo⁶, Sang-Wook Cheong⁷, and Je-Geun Park^{1,2,3,4}

¹ IBS Research Center for Functional Interfaces and Correlated Electron Systems, Seoul National University, Seoul 151-747, Korea

² FPRD Department of Physics & Astronomy, Seoul National University, Seoul 151-747, Korea

³ Center for Strongly Correlated Materials Research, Seoul National University, Seoul 151-747, Korea

⁴ Center for Korean J-PARC Users, Seoul National University, Seoul 151-747, Korea

⁵ Neutron Science Division, Korea Atomic Energy Research Institute, Daejeon 305-353, Korea

⁶ Institute of Materials Structure Science & J-PARC Center, KEK, Tsukuba 305-0801, Japan

⁷ Rutgers Center for Emergent Materials and Department of Physics and Astronomy, Rutgers University, Piscataway New Jersey 08854, USA

Lead iron niobate $\text{Pb}(\text{Fe}_{0.5}\text{Nb}_{0.5})\text{O}_3$ (PFN) is a multiferroic disordered system. It has a G-type antiferromagnetic transition at $T_N = 143$ K and a ferroelectric transition at $T_C = 385$ K. Its reported high dielectric constant makes it a suitable candidate material for multilayer ceramic capacitors as well as other electronic devices. Despite the interesting properties, however there is still controversy over the room temperature structure: for example, two competing space groups of R3m and Cm structure have been so far proposed. More importantly, it is not clear whether this material has Pb-disorder. More recently, it was reported to have interesting negative thermal expansion behavior below the antiferromagnetic transition.

In order to understand the properties better and resolve some of the controversies, we carried out both high resolution neutron powder diffraction and total scattering experiments using S-HRPD and NOVA beamlines of J-PARC, respectively. By taking advantage of the data, we could analyze both long-ranged and short-ranged structures systematically.

For example, we found that there is no negative thermal expansion behavior below the antiferromagnetic transition by carefully examining the S-HRPD data. Our high resolution S-HRPD data also showed that the thermal parameter of Pb ion is unusually large, indicative of the existence of static disorder at the Pb site. This observation is corroborated by our total scattering analysis using the NOVA data.



Release of encapsulated dye from monolayer of gold nanoparticles by using UV light and Glutathione

Apiwat Chompoosor,^{1,2} Kaniknan Sreejivangsa¹

*¹Materials Science and Nanotechnology Program, Faculty of Science,
Khon Kaen University, Khon Kaen, 40002, Thailand*

²Department of Physics, Khon Kaen University, Khon Kaen, 40002, Thailand

We prepared a drug carrier which can be simultaneously controlled release of drug using both internal and external stimuli. Gold nanoparticles (AuNPs) were functionalized by di-nitrobenzyl photo-cleavable group that was dissociated upon light irradiation. Monolayers of AuNPs composed of hydrophobic interior and hydrophilic exterior. A hydrophobic drug was intercalated into an interior of AuNPs by non-covalent strategy which avoided chemical bonding between drug and carrier. So, the release of drug can be controlled by UV light irradiation. In addition, release efficiency was increased by Glutathione. Photo-cleavable ligands of AuNPs were replaced by Glutathione while the drug was released. AuNPs were characterized by UV-VIS absorption spectroscopy and Transmission electron microscopy (TEM) and Dynamic light scattering (DLS). Release study was characterized by fluorescence spectroscopy. It was found that the release of hydrophobic drug was pronounced in the presence of UV light and glutathione.



Fate of Zinc Oxide Nanoparticles during Anaerobic Digestion of Wastewater and Post-Treatment Processing of Sewage Sludge

Enzo Lomb¹, Erica Donner^{1,3}, Ehsan Tavakkoli², Terence W. Turney⁴, Ravi Naidu^{1,3}, Bradley Miler⁵, Kirk Scheckel⁵

¹ *Centre for Environmental Risk Assessment and Remediation, University of South Australia, Building X, Mawson Lakes Campus, South Australia 5095, Australia*

² *School of Agriculture, Food and Wine, The University of Adelaide, 5064, Glen Osmond, SA, Australia*

³ *CRC CARE, PO Box 486, Salisbury, South Australia 5106, Australia*

⁴ *Centre for Green Chemistry and Department of Materials Engineering, Monash University, Clayton, Victoria 3800, Australia*

⁵ *National Risk Management Research Laboratory, U.S. Environmental Protection Agency, 5995 Centre Hill Avenue, Cincinnati, Ohio, 45224, United States*

The rapid development and commercialization of nanomaterials will inevitably result in the release of nanoparticles (NPs) to the environment. As NPs often exhibit physical and chemical properties significantly different from those of their molecular or macrosized analogs, concern has been growing regarding their fate and toxicity in environmental compartments. The wastewater–sewage sludge pathway has been identified as a key release pathway leading to environmental exposure to NPs. In this study, we investigated the chemical transformation of two ZnO-NPs and one hydrophobic ZnO-NP commercial formulation (used in personal care products), during anaerobic digestion of wastewater. Changes in Zn speciation as a result of postprocessing of the sewage sludge, mimicking composting/stockpiling, were also assessed. The results indicated that “native” Zn and Zn added either as a soluble salt or as NPs was rapidly converted to sulfides in all treatments. The hydrophobicity of the commercial formulation retarded the conversion of ZnO-NP. However, at the end of the anaerobic digestion process and after postprocessing of the sewage sludge (which caused a significant change in Zn speciation), the speciation of Zn was similar across all treatments. This indicates that, at least for the material tested, the risk assessment of ZnO-NP through this exposure pathway can rely on the significant knowledge already available in regard to other “conventional” forms of Zn present in sewage sludge.



Enhanced Photoassisted Field Emission of AuNPs Ligated by Alkanethiols

Fei Wang
Xingyu Gao

Shanghai Institute of Applied Physics
NO.2019 JiaLuo Road, Jiading District, Shanghai, China
Zip code: 201800

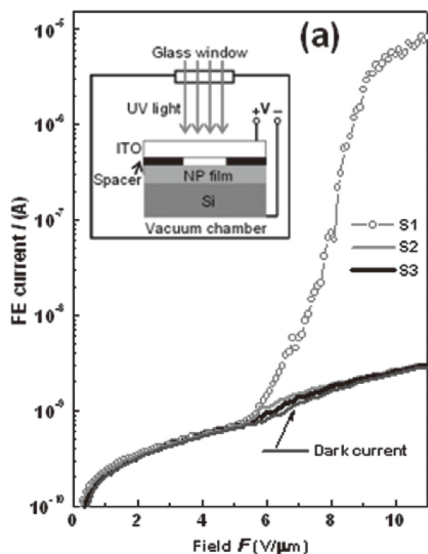


Fig. 1. Comparison of FE current of samples S1-3 under 405 nm light (40 mW/cm²) illumination. The typical IV (or dark current) of the samples obtained without light illumination is also shown. The inset shows the FE experimental setup.

Photoenhanced field emission by AuNP interband and surface plasmon excitations is demonstrated, and enhancement factor up to 300 is observed. The photoenhancement effect allows for large scale and stable field emission from a flat 2D NP film, in contrast to the usual field emission based on high-aspectratio 1D nanostructures.[1]

Thus, we prepared several kinds of AuNPs films with different sizes and different ligands. To find out the optimum conditions of large enhancement in field emission, further work is ongoing.

[1] Xian Ning Xie, Xingyu Gao, Dongchen Qi, Yilin Xie, Lei Shen, Shuo-Wang Yang, Chong Haur Sow, and Andrew Thye Shen Wee †, *ACS Nano*, 2009, 3 (9), p 2722–2730.

The origin of the intraband plasmons on Au/Si(5512) surface

J. G. Kim, S. J. Sung, P. R. Lee, M. T. Ryu, H. M. Park, S. Y. Shin
and J. W. Chung

*Department of Physics, Pohang University of Science and Technology, Pohang,
790-784, Kyungbuk, KOREA*

We have investigated the electronic excitations for several Au-induced facet structures formed on the Si(5512) surface using high-resolution electron-energy-loss spectroscopy (HREELS). We find a characteristic loss peak from each of the three metallic surfaces, the (337)x2, the (5511), and the Au/Si(557). These loss peaks are identified as one-dimensional (1D) intraband plasmons and their energy-momentum dispersions appear to be quite similar, and are well described by the RPA theory when the Rashba spin-orbit interaction is included. This strongly suggests that they stem from the same origin of the Au-Si band split by the spin-orbit interaction rather than from the band associated with step-edge atomic chains. In addition, we find a weakly dispersing loss peak from the semiconducting (225) facets, which is attributed to an interband transition.

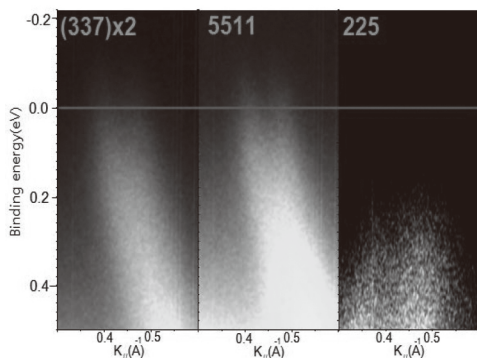


Fig. 1. Au-Si band split of the (337)x2, (5511) facets and non-metallic nature of the (225) facets.

-
- [1] J. W. Dickinson, J. C. Moore and A. A. Baski, Surf. Sci. 561, 193 (2004).
 - [2] J. R. Ahn, H. W. Yeom, E. S. Cho and C. Y. Park, Phys. Rev. B 69, 233311 (2004).
 - [3] P. C. Snijders and H. H. Weitering, Rev. Mod. Phys. 82, 307 (2010).



Topotactic synthesis of mesoporous ZnS and ZnO nanoplates and their Photocatalytic Activity

Jum Suk Jang and Sun Hee Choi

Beamline Research Division, Pohang Accelerator Laboratory, POSTECH, San 31, Hyojadong, Namgu, Pohang 790-784, Korea

The solvothermal method using ethylenediamine as a liquid medium has been regarded as an economic and convenient route to obtain nanostructured materials [1,2]. Zinc sulfide (ZnS) is a wide-bandgap semiconductor of 3.80 eV for hexagonal wurtzite phase and of 3.66 eV for cubic zinc-blend phase. Similarly ZnO is one of the most important functional oxides for optoelectronics and photocatalysis due to its bandgap energy of 3.20 eV. Its potential applications were demonstrated as nanosized sensors and field-effect transistors based on ZnO nanobelts, and for photocatalytic degradation of organic dyes [3]. A few studies have recently been done to fabricate nanostructured ZnS and ZnO with high surface-to-volume ratios for improved performance. It is interesting to note the result of Hue et al. that nanoporous ZnS nanoparticles prepared via a low-cost and self-assembly route, can have high ratio of surface to volume and aggregation of nanoparticles during photocatalytic reaction of dyes [4]. Nevertheless the fabrication of porous ZnS and ZnO platelets has not been reported yet.

In this contribution we prepared the $\text{ZnS(en)}_{0.5}$ complex precursor by solvothermal routes using ethylenediamine as a single solvent and obtained porous ZnS and ZnO nanoplates through thermal treatment of the complex. In particular, the local structures confined in the platelets were elucidated with synchrotron radiation techniques of powder XRD and XAFS. Photocatalytic water splitting and photocatalytic degradation of organic dye were performed in order to measure the catalytic performance of the synthesized $\text{ZnS(en)}_{0.5}$ complex and its derivatives.

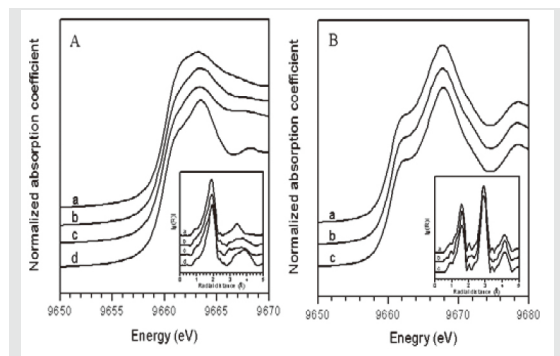


Fig. 1. Zn K-edge XANES spectra of the $\text{ZnS(en)}_{0.5}$, its calcined derivatives, and reference materials: (A) (a) $\text{ZnS(en)}_{0.5}$, (b) Zn400, (c) Zn500, and (d) bulk ZnS, and (B) (a) Zn550, (b) Zn600, and (c) bulk ZnO. Inset plots are their respective Fourier-transformed RSF spectra.

Fig. 1A displays Zn K-edge XANES of $\text{ZnS(en)}_{0.5}$ (a), Zn400 (b), Zn500 (c), and bulk ZnS (d). We found that the XANES features of Zn400 and Zn500 are closer to those of $\text{ZnS(en)}_{0.5}$, rather than those of bulk ZnS. On the other hand, Fig. 1B shows that the Zn K-edge XANES spectra of grains produced by calcinations at 550 and 600 °C are almost the same as that of bulk ZnO.

[1] J. S. Hu, L. L. Ren, Y. G. Guo, H. P. Liang, A. M. Cao, L. J. Wan and C. L. Bai, *Angew. Chem. Int. Ed.* **44**, 1269 (2005).

[2] S.H. Yu and M. Yoshimura, *Adv. Mater.* **14**, 296 (2002).



RGO-TiO₂ nanocomposite with highly exposed {001} facets for photoelectrochemical performance and electrochemical determination of dopamine

Gregory Thien Soon How, Huang Nay Ming

Low Dimensional Materials Research Center, Department of Physics, Faculty of Science, University of Malaya, 50603 Kuala Lumpur, Malaysia

Crystal facet engineering has attracted worldwide attention in the facet manipulation of TiO₂ surface properties. An improved synthesis solvothermal route has been employed for the formation of TiO₂ nanosheets with highly exposed {001} facets decorated on reduced graphene oxide (RGO) sheets. The RGO-TiO₂ nanocomposite could be materialized with high yield by following a stringently methodical yet simple approach. Photocurrent response of RGO-TiO₂ nanocomposite was discovered to outperform that of pure TiO₂ as a tenfold increase in photocurrent density was observed for the RGO-TiO₂ electrodes. This may be contributed by faster electron transport and delayed recombination of electron-hole pairs due to improved ionic interaction between titanium and carbon. In contrast to bare GCE, the RGO-TiO₂ nanocomposite modified glassy carbon electrode (GCE) displays reversible redox event and reduced peak-to-peak separation which indicates decreased overpotential, signifying the minimal use of energy to drive a reaction. The electrode manifests its use as a sensor for dopamine (DA) as it possesses a detection limit of 4 μM over a satisfactory linear range of 2-200 μM.



SSRF XIL beamline BL08U1-B introduction

Wu Yanqing, Zhao Jun
Zhao Jun

239 Zhang Heng Road, Pudong New District, Shanghai 201203, P. R. China

The Soft X-ray interference lithography beamline (XIL) BL08U1-B is one of the Shanghai Synchrotron Radiation Facility (SSRF) beam lines, it started preliminary design at the beginning of 2004, the project starts from April 2009 to December 2011, and it is open to the customer since January 2013.

Soft-X ray interference lithography (XIL) is a newly developed technique for production of periodic nano-structures with resolution below 100 nm. The technique is based on coherent radiation obtained from undulators at synchrotron radiation (85-150 eV). Because of its small wavelength (typical value: 13.4 nm) and practical absence of the proximity effect, high density resolution lines/dots with high density can be afforded. The throughput of this parallel exposing method is much higher than that of the serial electron-beam lithography. Interference schemes based on diffraction (gratings) optics have been constructed at BL08U1-B beamline in SSRF. Both one-dimensional and two-dimensional patterns such as arrays of dots have been achieved.

XIL technology finds use in a variety of fields. Below are just some examples of common uses: photonic Crystals for Light Extraction from LEDs; high sensitivity gas detector; the template for self-assembly, nanoimprint and cell growth; novel EUV photo resist test; calibration samples for SEM, SFM, STM, TEM microscopes.

Up to now, XIL beam line can provide user with at least 100nm period 1D or 2D periodic photo resist nanostructures. According to the request of the user, we can also transfer these photo resist pattern to other films such as dielectric and metal.

Evidence of ultraviolet transparency of graphene on SrTiO₃ induced by excitonic Fano anti-resonance

Pranjal Kumar Gogoi^{1,2,3}, Paolo E. Trevisanutto^{1,8}, Chan La-O-Vorakiat⁷, Ming Yang², Iman Santoso^{1,3,4}, Teguh Citra Asmara^{1,2,3}, Yuan Ping Feng^{1,2}, Kian Ping Loh^{1,4,5}, T. Venkatesan^{1,2,6}, Elbert E. M. Chia⁷, Antonio H. Castro Neto^{2,4}, Andrivo Rusydi^{1,2,3}

¹NUSNNI-NanoCore, NUS, Singapore 117576

²Department of Physics, NUS, Singapore 117542

³SSLs, NUS, 5 Research Link, Singapore 117603, Singapore

⁴Graphene Research Centre, Faculty of Science, NUS, Singapore 117546

⁵Department of Chemistry, NUS, Singapore 117543

⁶Department of Electrical and Computer Engineering, NUS, Singapore 117576

⁷Division of Physics and Applied Physics, School of Physical and Mathematical Sciences, NTU, Singapore 637371

⁸National Nanotechnology Laboratory (NNL), Istituto di Nanoscienze-CNR, Via per Arnesano 16, I-73100 Lecce, Italy

Graphene manifests prominent signatures of many-body effects of electron-electron and electron-hole interactions. This is distinctly revealed in the optical conductivity as red-shift and asymmetry of the van Hove peak observed at ~ 4.6 eV. Interestingly, due to its two-dimensional

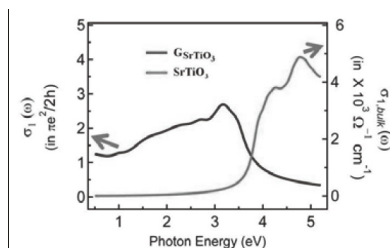


Fig.1. Real part of the optical conductivity ($\sigma_1(\omega)$) and Fano line-shape analysis.

nature, one may expect to tailor its many-body effects by substrate properties. Here we present a intriguing phenomenon of the electronic bands of substrate interacting strongly with graphene bands. Using spectroscopy ellipsometry, for graphene on

SrTiO₃ we observe a drastic renormalization of the optical conductivity with almost full transparency in the ultraviolet region. Through phenomenological analysis this can be explained with Fano anti-resonance due to excitonic states residing between graphene conduction bands and new hybridized valence bands originating from carbon p_z -orbital of graphene and oxygen p_z -orbital of SrTiO₃. Ultrafast optical pump-optical probe measurements and density functional theory calculations further support existence of hybridization and also explain important features of the optical conductivity.



Structural properties of mixed magnetic oxide determined from synchrotron powder diffraction

To Thanh Loan¹, Nguyen Phuc Duong¹, Luong Ngoc Anh¹, Tran Quoc Tien²

¹ International Training Institute for Materials Science (ITIMS), Hanoi University of Science and Technology, 1 Dai Co Viet Road, Hanoi, Vietnam

² Institute of Materials Science (IMS), Vietnam Academy of Science and Technology (VAST), 18 Hoang Quoc Viet, Cau Giay, Hanoi, Vietnam

Atomic structure and microstructure of two series of spinel ferrite $\text{NiFe}_{2-x}\text{Cr}_x\text{O}_4$ (with $x = 0.7$ and 0.9) and perovskite $\text{La}_{2/3}\text{Pb}_{1/3}\text{Mn}_{1-x}\text{Co}_x\text{O}_3$ (with $x = 0, 0.20, 0.25$ and 0.30) have been investigated by synchrotron powder diffraction method. On applying the full pattern fitting of Rietveld method using FullProf program, unit cell dimensions, atomic positional parameters, ion occupancy and microstructure (coherent scattering region and microstrain) of the samples have been determined.

For the ferrite spinel $\text{NiFe}_{2-x}\text{Cr}_x\text{O}_4$, the result showed that all investigated compounds were phase pure. The crystal structure symmetry of the compounds was confirmed to be cubic (space group $\text{Fd}\bar{3}\text{m}$). The change of Cr content in the samples leads to the variation of their atomic structure, microstructure and cation distribution.

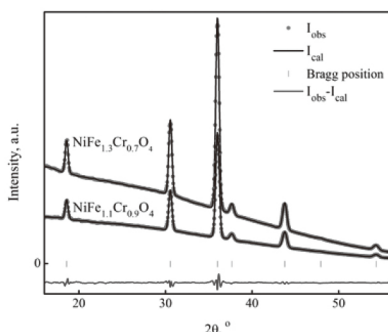


Fig. 1. Diffraction pattern for $\text{NiFe}_{1-x}\text{Cr}_x\text{O}_4$ measured in SLRI at $T=300$ K ($\lambda = 1.5499$ Å) and processed by the Rietveld method.

For the samples $\text{La}_{2/3}\text{Pb}_{1/3}\text{Mn}_{1-x}\text{Co}_x\text{O}_3$, our result shows that all the compounds are described by slightly distorted perovskite like structure with rhombohedral symmetry (sp. gr. $\text{R}\bar{3}\text{c}$). The lattice parameters and bond distances $\text{Mn/Co} - \text{O}$ are typical of rhombohedral manganites.

Only negligible changes of samples microstructure with composition were observed. The correlation of structural character of these compounds with their fundamental properties was confirmed.

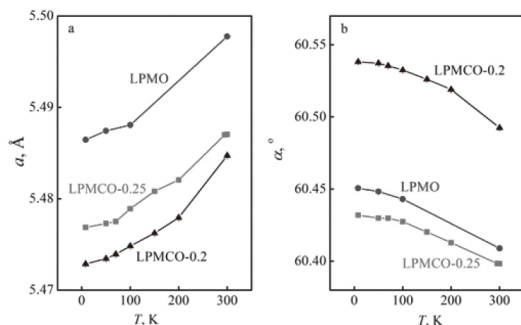


Fig. 2. Temperature dependence of unit cell parameters a (fig. 2.a) and α (fig. 2.b) of the samples $\text{La}_{2/3}\text{Pb}_{1/3}\text{Mn}_{1-x}\text{Co}_x\text{O}_3$

CuO/TiO₂ - Low cost semiconductor photocatalysts for solar hydrogen production

Wan-Ting Chen, Geoffrey I.N. Waterhouse*

*School of Chemical Sciences, The University of Auckland, New Zealand
g.waterhouse@auckland.ac.nz*

CuO/TiO₂ photocatalysts (CuO loadings 0-15 wt.%) were prepared, characterized and evaluated for H₂ production from ethanol-water mixtures (80 vol.% ethanol, 20 vol.% H₂O) under UV excitation. Degussa P25 TiO₂ (85 wt.% Anatase, 15 wt.% Rutile) was used as the support phase. XRF, EDAX, EPR, Raman and TGA measurements showed that the CuO content in the samples increased linearly with nominal CuO loading. XPS and Cu L-edge NEXAFS analyses verified that Cu(II) was the dominant copper species in the near surface region of the photocatalysts. At CuO loadings < 5 wt.%, no CuO crystallites were seen by TEM, indicating that the CuO was highly dispersed over the TiO₂ support, possibly as a monolayer dispersion. At CuO loadings > 5 wt.%, CuO crystallites of diameter 1-2 nm were identified. Photoluminescence studies established that CuO deposition strongly suppresses electron-hole pair recombination in TiO₂. The photocatalytic activity of CuO/TiO₂ photocatalysts was highly dependent on the CuO loading, with 1.25 wt.% CuO being optimal (H₂ production rate = 21 mmol g⁻¹ h⁻¹). Above 1.25 wt.% CuO, the H₂ production activity of the CuO/TiO₂ photocatalysts decreased sharply with increasing CuO loading. The decrease in activity at higher CuO loadings coincided with the onset of CuO nanoparticle formation, which is postulated to alter electronic properties the CuO/TiO₂ interface in a manner detrimental to H₂ production. CuO itself was inactive as a photocatalyst under the applied testing conditions. Results suggest that sub-monolayer coverages of CuO on TiO₂ are highly beneficial for H₂ generation, and support the development of a sustainable H₂ economy.

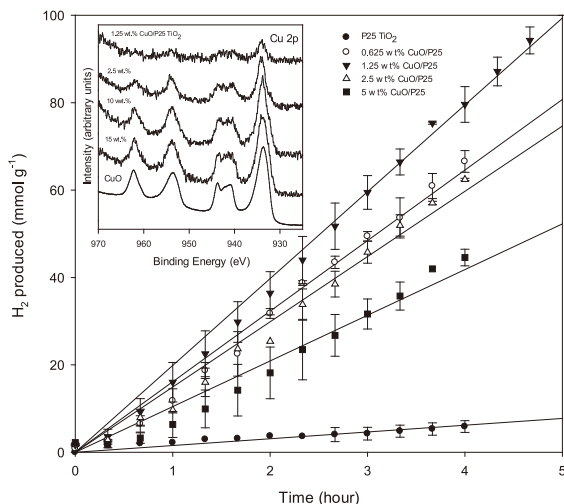


Fig. 1. Plots of H₂ production versus time for various CuO/TiO₂ photocatalysts. The inset shows Cu 2p XPS spectra for selected CuO/TiO₂ photocatalysts and bulk CuO.

The Cu 2p XPS spectra for the CuO/TiO₂ photocatalysts were similar to data collected for a CuO reference powder, with Cu 2p_{3/2} = 933.7 eV and Cu 2p_{1/2} = 953.6 eV (2:1 area ratio). The presence of characteristic “shake up” satellites ~7 eV above the Cu 2p peaks, provide further evidence for the presence of paramagnetic Cu²⁺ species (formally 3d⁹). No CuO reduction occurred under UV excitation.

Small Angle X-ray Scattering and Fluorescence Spectroscopy of Lanthanide Binding Peptide Complexes

Jessica Veliscek-Carolan^a, Tracey L. Hanley^a, Katrina A. Jolliffe^b

^a*Australian Nuclear Science and Technology Organisation, New Illawarra Rd, Lucas Heights, NSW 2232, Australia*

^b*School of Chemistry (F11), The University of Sydney, NSW 2006, Australia*

Lanthanide binding peptides are of great interest as structural probes in biological systems as they combine the luminescent properties of lanthanide ions with the biological selectivity of peptide scaffolds [1]. Peptides that demonstrate selective binding of lanthanides may also be of interest for separations [2]. However, in order to design peptides that effectively and selectively bind lanthanides it is necessary to better understand the complexation process. Therefore a simple model system of three diastereomers of tetraglutamic acid was chosen for investigation. In order to harness the luminescent properties of the lanthanide ions for investigation of the peptide-lanthanide complexation process, 1,8-naphthalimide was attached to these peptides as a sensitizing antenna [3].

Luminescence titrations with europium (Eu) in HEPES buffer and water were performed and showed that the three diastereotopic tetrapeptides demonstrated different binding behaviours. Also, in some cases, complex formation was dependent on the media in which the reaction was performed. Small-angle x-ray scattering (SAXS) of these peptide:Eu complexes at the Australian Synchrotron showed that the kinetics of complex formation was very fast and that at ~0.1mg/mL concentrations large aggregates were formed that were subject to radiation damage. Decreasing the concentration tenfold allowed SAXS data to be collected for the 1:1 peptide:Eu complex for all three tetrapeptides. This result shows the importance of synchrotron radiation for measurement of dilute samples as this data could not have been collected without the high flux of the synchrotron SAXS instrument.

[1] A. Niedzwiecka, F. Cisnetti, C. Lebrun and P. Delangle, *Inorg. Chem.* **51**, 5458 (2012).

[2] S. Ozcubukcu, K. Mandal, S. Wegner, M.P. Jensen and C. He, *Inorg. Chem.* **50**, 7937 (2011).

[3] C.S. Bonnet, M. Devocelle and T. Gunnlaugsson, *Org. Biomol. Chem.* **10**, 126 (2012).

Gap state tuning at the organic/metal interface by quantum-size effects

Meng-Kai Lin¹, Yasuo Nakayama², Chin-Hung Chen³, Chin-Yung Wang¹,
Shin-ichi Machida², Hisao Ishii², and S.-J. Tang^{1,3}

¹ *Department of Physics and Astromony, National Tsing Hua University,
Hsinchu 30013, Taiwan*

² *Center for Frontier Science, Chiba University, and Graduate School of
Advanced Integration Science, Chiba University, 1-33 Yayoi-cho, Inage-ku,
Chiba 263-8522, Japan*

³ *National Synchrotron Radiation Research Center, 101 Hsin-Ann Road,
Hsinchu Science Park, Hsinchu, Taiwan*

We have studied the interfacial electronic structure between Phthalocyanine (Pc)-based molecules and the uniform Ag films by using angle-resolved photoemission spectroscopy (ARPES). Ag films at various thicknesses were deposited and grown uniformly on the Ge(111) surface. Then Pc-based molecules such as CuPc, H₂Pc, and TTB-H₂Pc were deposited on top of the Ag film step by step up to the coverage of 10 Å, respectively. We found the emergence of gap states at the organic molecules coverage about 3 Å, and it shift in energies with the increasing thickness of the Ag films. Furthermore, we found that the energy positions of the gap states are pinned at the energy position where the quantum well state (QWS) band cross the Ge heavy hole (HH) band edge. In this energy region, the QWS band becomes very flat, and it corresponds to the abrupt change of the 2-dimensional (2D) density of state (DOS). The abrupt change of the DOS will induce and pin the gap state after the adsorption of the organic molecules. In this study, we take CuPc as a modeling system, and introduce the Newn-Anderson model [1,2] which considers the interaction between a single molecular state and the substrate band to explain the origin of the gap state and the pinning effect.

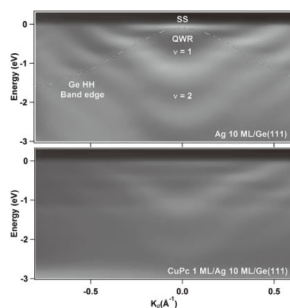


Fig. 1. The upper graph shows the 2-dimensional (2D) angle-resolved photoemission spectra for 10 monolayer (ML) Ag thin film on Ge(111). The lower graph shows the 2D spectra for CuPc 1 ML on top of 10 ML Ag thin film [3].

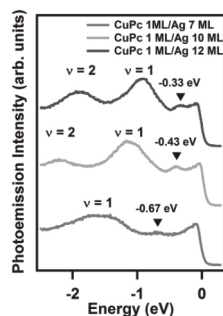


Fig. 2. Normal emission spectra for CuPc 1 ML on top of the 7, 10, and 12 ML Ag thin films. The black wedges indicate the energy positions of the gap state [3].

[1] P. W. Anderson, Phys. Rev. **124**, 41 (1961)

[2] D. M. Newns, Phys. Rev. **178**, 3 (1969)

[3] M. K. Lin, Y. Nakayama, C. H. Chen, C. Y. Wang, S. Machida, T. W. Pi, H. Ishii, S. -J. Tang, in preparation.



Introduction to X-Ray Diffraction at RIKEN SPring-8

Jordan DeWitt^{1, 2}, Eiji Nishibori¹, Kenichi Kato¹ and Masaki Takata^{1, 3, 4}

¹*RIKEN SPring-8 Center, Hyogo 679-5148, Japan*

²*Dept. of Physics, Northeastern University, Boston, MA 02115, U.S.A.*

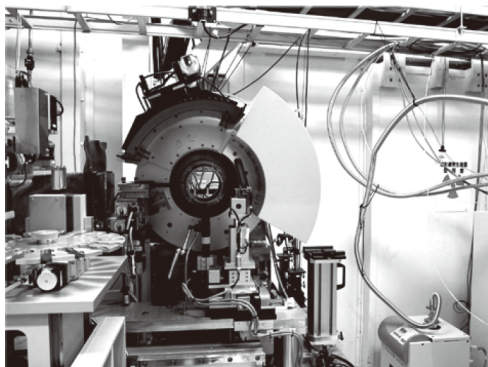
³*Jpn Synchrotron Radiation Res. Inst. JASRI/SPring-8, Hyogo 679-5198, Japan*

⁴*Dept. of Advanced Materials, University of Tokyo, Chiba 277-8561, Japan*

The Northeastern University Cooperative Education Program (Co-op Program), in affiliation with RIKEN SPring-8, provides undergraduate students in science and engineering fields with the opportunity to experience first-hand what it's like to work in a fully-operational Synchrotron Radiation facility. Thanks to the efforts of Dr. Masaki Takata of RIKEN and Dr. J. Murray Gibson of Northeastern, students are offered the chance to travel from the U.S. to Japan to work at SPring-8 for 6 months. From analyzing diffraction data to physically working on the beamline, participating in a co-op at RIKEN SPring-8 provides Northeastern students with a wealth of experience that they likely would not be able to obtain elsewhere.

As a student at Northeastern studying for a BSc degree in Physics, having the chance to work hands-on with powerful electromagnetic waves for the purpose of scientific research is a great opportunity. For all the mathematical theories and formulae we study as students, if we never learn how these methods are applied, or how the acquired data from experiments is analyzed, we will be lost when we truly enter the field of scientific research. Currently, in my work at SPring-8, I am bolstering my knowledge of X-ray diffraction and analysis techniques. In the near future, I will be assigned to a beamline under the supervision of Dr. Eiji Nishibori, using powder and single crystal diffraction to analyze the properties of metallofullerenes, or thermoelectric materials, and potentially assisting in the correction of a newly installed detector.

Fig. 1. Photograph of newly installed X-ray detector Imaging Plate (IP) at RIKEN Materials Science Beamline number BL44B2 at SPring-8.



BL5S1: A new hard X-ray XAFS Beamline at the Aichi Synchrotron Radiation Center

H. Asakura¹, M. Tabuchi¹, H. Morimoto¹, A. Mano¹,
N. Takao², N. Watanabe¹, Y. Takeda², Y. Baba¹

1. *Synchrotron Radiation Research Center, Nagoya University, Furo-cho, Chikusa, Nagoya, 464-8603 Japan*
2. *Aichi Synchrotron Radiation Center, ASTF, Minami-Yamaguchi, Seto, 489-0965 Japan*

A new synchrotron radiation facility, “Aichi Synchrotron Radiation Center” (formerly called as Central Japan Synchrotron Radiation Facility) located at Aichi prefecture in the central region of Japan is open to the public since March 2013. At present, five beamlines for hard X-ray XAFS (BL5S1), X-ray powder diffraction (BL5S2), soft X-ray XAFS and XPS/PES (BL6N1), X-ray reflectivity and diffraction (BL8S1), and SAXS/WAXS (BL8S3) are in operation.

BL5S1 is designed for standard XAFS measurements using hard X-ray of 5 – 20 keV emitted from a super-conducting bending magnet (5T) installed into a storage ring operated at 1.2 GeV. The emitted X-ray reaches the experimental hatch through a Rh-coated collimating mirror, a Si(111) double-crystal X-ray monochromator, and a Rh-coated focusing mirror. The X-ray optics is presently operated in two different modes; a standard mode for the energy range of 7 – 20 keV and a lower energy mode for the energy range of 5 – 7 keV rejecting higher order reflections. The observed photon flux at the sample position is shown in Fig. 1.

BL5S1 has standard detectors such as ion chambers for the transmission mode, a 19-elements Ge detector (SSD) and a Lytle detector for the fluorescence yield mode. So-called quick XAFS mode is also developed and already dedicated to users. For example, a Cu K-edge XAFS spectrum of Cu foil can be recorded in 60 sec in good quality. Gas supply system for *in situ* experiments (O₂, H₂, and N₂), and sample changers are provided. It is also planned to provide a micro-XAFS system with a X-ray polycapillary glass (focused beam size is expected to be several tens of micrometer), a cryostat to cool samples, a conversion electron yield detector, and an *in situ* XAFS cell developed at the Photon Factory (<800 K). Beamline details and measurement examples of BL5S1 will be discussed at the presentation.

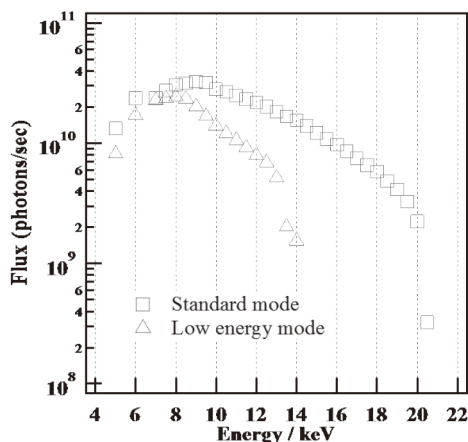


Fig. 1. Photon flux at BL5S1 (at sample position)

Current Status of Scanning Transmission X-ray Microscopy Beamline at UVSOR

Takuji Ohigashi^{1,2} and Nobuhiro Kosugi^{1,2}

¹ UVSOR Facility, Institute for Molecular Science, 38 Nishigo-naka, Myodaiji, Okazaki, Aichi 444-8585, Japan

² The Graduate University for Advanced Studies, 38 Nishigo-naka, Myodaiji, Okazaki, Aichi 444-8585, Japan

The UVSOR facility, a 750 MeV synchrotron radiation facility in the Institute for Molecular Science (IMS, Okazaki, Japan), has been in operation since 1983. From April 2012, we started the UVSOR-III project to improve the beam emittance by optimizing eight bending magnets [1]. Along with this project, a scanning transmission X-ray microscope (STXM) beamline, BL4U, was constructed to utilize the improved ability of the UVSOR-III. The STXM is a high spatial resolution microscope (~30 nm) based on near edge X-ray absorption fine structure (NEXAFS) spectroscopy measured in transmission mode. The STXM enables to analyze 2-dimensional chemical states around a target element with high spatial resolution. Moreover, the STXM has many unique features which cannot be achieved with any other microscopic method, such as 3-dimensional observation, observation of orientations of molecules, that of the sample in water and so on. Then, to bring out satisfactory performance of the STXM, an in-vacuum undulator and a variable included angle Monk-Gillieson mounting monochromator were installed to obtain both high photon density and high energy resolving power and an interface software to integrate these equipment has been developed. Since June 2013, the commissioning was finished and our beamline has been opened to general users from domestic, abroad and companies.

As a test measurement, thin specimen of printer toner particles were observed at the oxygen K edge. A stack of 78 X-ray transmission images was acquired with the x-ray energy range from 522 to 564 eV. Then, the dwell time was 3 msec for each pixel. A spectrum of each component of the specimen, matrix, resin, and wax, is shown in Fig. 1 (a). They were extracted from the each specific region of the image stack. By fitting these spectral data to the original image stack, chemical distributions of the components are obtained. They are clearly distinguished as shown in Fig. 1 (b), (c) and (d).

We are now developing several observation methods to explore new applications in molecular science. Current status, sciences and perspective of BL4U will be discussed.

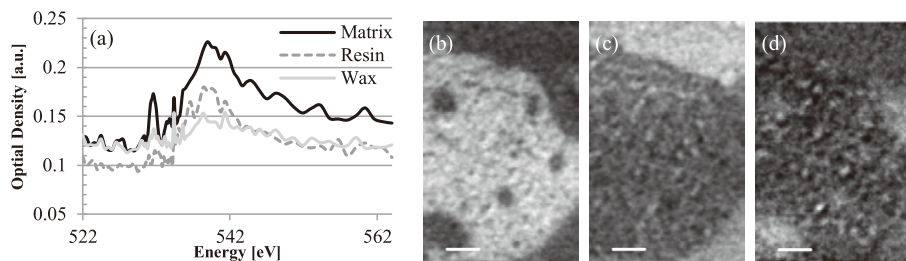


Figure 1: (a) Absorption spectrum of components of a printer toner sample and its chemical distributions of three components, (b) matrix, (c) resin and (d) wax. Higher concentrations of each component are brighter. Scale bars are 1 μm.

Performance of two Public Beamlines with insertion devices at SAGA Light Source

Kazushi Sumitani, Masahide Kawamoto, Daisuke Yoshimura,
Hiroyuki Setoyama,
Kotaro Ishiji, Moriya Kikuchi, Eiichi Kobayashi, and Toshihiro Okajima

*Kyushu Synchrotron Light Research Center,
8-7 Yayoigaoka, Tosu, Saga, 841-0005, Japan*

SAGA Light Source is a compact-size synchrotron radiation facility which has a 1.4 GeV electron storage ring with a circumference of 75.6 m and a 270 MeV linac [1, 2]. The facility opened in February 2006 with three public and a contracted beamlines. The public beamlines use bending magnets as a light source, one for hard X-rays (BL15) [3], one for soft X-rays (BL12), and one for white X-rays (BL09). A hard X-ray beamline (BL11) was also constructed in 2009.

In addition, two beamlines has been constructed in recent years which utilize insertion devices at the straight section on the storage ring as a light source. One is a soft X-ray beamline named BL10 with an APPLE-II type undulator which enables polarity control [4]. The light is monochromatized by a varied-line-spacing plane grating (VLSPG). Designed resolving power and photon flux are 3,000 - 10,000 and 1012 - 109 photons/second at 300 mA stored ring current. High-resolution angle-resolved photoemission spectroscopy (ARPES) and photoelectron emission microscopy (PEEM) have been performed in this beamline. Another one is a beamline named BL07 [5] for the use of high-energy X-rays from a newly developed 4-Tesla superconducting wiggler [6]. The critical energy of the X-rays becomes much higher as 5.2 keV than the one of the bending magnet as 1.9 keV. At the energy of 20 keV, the brilliance from the wiggler is 100 times as high as from the bending magnet. The experimental station was separated by two hutches. The front hutch is for X-ray protein crystallography, in which a diffractometer and a CCD camera have been installed. In the rear hutch, computed tomography by diffraction enhanced imaging (DEI) method and scanning microscopic analysis using X-ray microbeam generated by Fresnel zone plate have been performed. XAFS measurement is also performed in the rear hutch for analyses of electronic state and local structure of heavy atoms such as Zr, Mo, Ag and Sn, which are difficult for the bending magnet beamlines.

In the presentation, we will present the details of the two public beamlines with insertion devices. The typical examples of the measurements at these beamlines will be demonstrated

-
- [1] T. Tomimasu, S. Koda, Y. Iwasaki, H. Ohgaki, M. Yasumoto, K. Kitsuta, Y. Yamatsu, M. Mori, and Y. Oshiai, Proc. PAC2003, 902-905 (2003).
 - [2] Y. Iwasaki, S. Koda, T. Tomimasu, H. Ohgaki, M. Yasumoto, Y. Yamatsu, T. Kitsuka, Y. Hashiguchi, and Y. Ochiai, Proc. PAC2003, 3270-3272 (2003).
 - [3] T. Okajima, Y. Chikaura, Y. Suzuki, M. Tabata, Y. Soejima, K. Hara, R. Haruki, K. Nagata, N. Hiramatsu, A. Kohno, M. Takumi, H. Setoyama, and D. Yoshimura, AIP Conf. Proc. 879, 820-823 (2007).
 - [4] D. Yoshimura, H. Setoyama, and T. Okajima, AIP Conf. Proc. 1234, 423 (2009).
 - [5] M. Kawamoto, K. Sumitani, and T. Okajima, AIP Conf. Proc. 1234 355 (2009).
 - [6] S. Koda, Y. Iwasaki, Y. Takabayashi, T. Kaneyasu, T. Semba, T. Yamamoto, Y. Murata, and M. Abe, IEEE Trans. Appl. Supercond. 21, 32 (2011).

Development of X-ray imaging beamline at INDUS-2 synchrotron source, India

Yogesh S. Kashyap, Ashish Agrawal, Mayank Shukla, Balwant Singh, P. S. Sarkar, Tushar Roy and Amar Sinha

Neutron and X-ray Physics Division, Bhabha Atomic Research Centre, Mumbai, India-40085

Third generation x-ray sources viz. Synchrotron Radiation provide coherent x-ray source with added advantage of tunability of energy, high x-ray flux etc. With availability of Indus-2 synchrotron source, operating at 2.5Gev energy and current of 300mA, we are setting up an imaging beamline for carrying out both absorption and phase sensitive imaging applications. This facility will be used for material science research, medical science research, and non-destructive characterization of advanced materials. The experimental techniques available at the beamline include propagation and analyzer based phase imaging, laminography, tomography, dual energy imaging, real-time imaging etc.

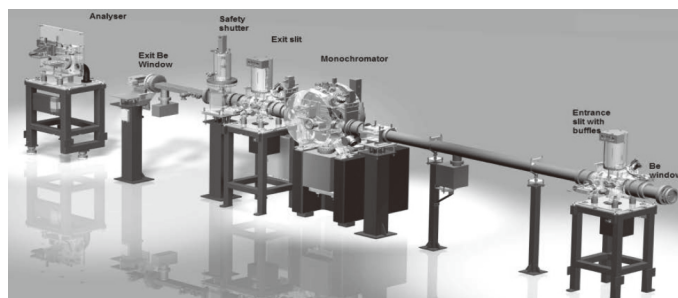


Figure 1 Schematic of Imaging beamline at INDUS-2, India

The beam-line has monochromatic as well as white beam mode of operation. In monochromatic mode the energy range covered is 6-35keV while in white beam mode energy upto 50keV is available. The maximum beam-dimension in the experimental station is 150mm X 10mm and photon flux is 10^8 ph/s in mono-chromatic mode while it is 10^{16} ph/s in white-beam mode. In this presentation, we will discuss about design, development, and current status of the beamline along with its future plans.

[1] Y.S. Kashyap, P.S. Yadav, P.S. Sarkar, A. Agrawal, T. Roy, Amar Sinha, K. Dasgupta, D. Sathiyamoorthy
NDT&E International 42 (2009) 384–388



Development of High- and Low-Energy Scanning Transmission X-ray Microscope (STXM) for Bacterial Samples

H. Suga,¹ Y. Takeichi,² N. Inami,² K. Ono,² and Y. Takahashi¹

¹*Dept. Earth and Planet. Systems Sci., Hiroshima University,
Higashi-Hiroshima, Hiroshima 739-8526, Japan*

²*IMSS, KEK, Tsukuba, Ibaraki 305-0801, Japan*

Scanning Transmission X-ray Microscope (STXM) enables XRF/XAFS imaging with high resolution down to several tens of nanometers using Fresnel Zone Plate (FZP). The functional group mapping can be obtained by tuning the photon energy at correspondening absorption structures. The sample chamber should be used under He-purged environment to permit the study of hydrated samples under near-natural condition with additional possibilities of sample tilting, heating, and cooling. STXM has a wide range of applications including material sciences, earth and environmental sciences, and biological and bio-medical sciences.

Aim of our study here is to obtain rare earth element (REE) distribution image on the bacterial cell surface by STXM. Previous study reported that phosphate group is main binding site of REE when REE is adsorbed on the bacterial cell wall [1]. However, REE distribution image on the cell wall has not been obtained yet, while development of STXM in Japan has been delayed. For example, STXM that is able to use K-edge absorption energy of phosphorus (2.1 keV) is not available in Japan.

Therefore, to obtain REE and phosphorous distribution image, High (0.05-2 keV) and Low (2-5 keV) energy versions of STXM (PF-STXMs) are being developed in Photon Factory (PF) at High Energy Accelerator Research Organization (KEK) in Japan. By combining the two types, it will be possible for us to measure K-edges of P (2.1 keV) and M-edge of REE (0.8-1.5 keV) for such bacterial samples. In this workshop, we will introduce the current status of PF-STXMs and their application to bacterial samples.

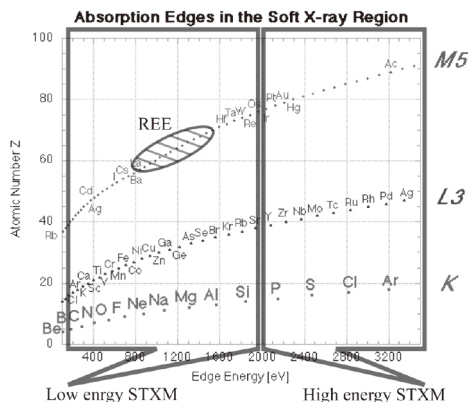


Fig. 1. Absorption edge of elements in soft X-ray region. High and low energy STXM measurement range is drawn. (<http://pfwww.kek.jp/sxspec/sx/sxme.html>)

[1] Y. Takahashi *et al.*, *Geochimica et Cosmochimica Acta*. **74**, 5443 (2010).

The status of hard x-ray microfocusing at Shanghai Synchrotron Radiation Facility (SSRF)

Shuai Yan

*Shanghai Synchrotron Radiation Facility, Shanghai Institute of Applied Physics, CAS
NO.239 Zhangheng Road, Pudong District, Shanghai, China
Zip code: 201204*

The hard x-ray microprobe upgrade project at beamline BL15U1 at SSRF has obtained initial results. The new focusing system (fig. 1) is based on the hard x-ray fresnel zone plates with 50nm outermost width. The achieved resolution $\sim 200\text{nm}$ (fig. 2) is dominated by the source size and the optical aberrations of transport optics rather than by diffraction.

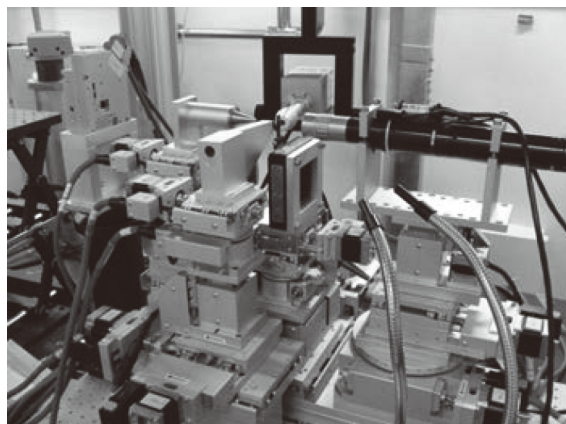


Fig. 1. The fresnel zone plates hard x-ray nano-focusing system.

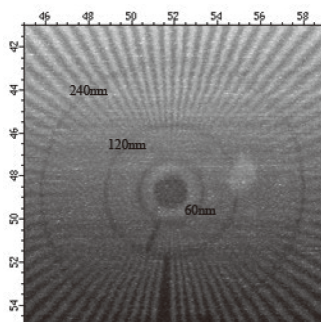


Fig. 2. Raster scanning XRF images of the Siemens star test pattern.

Status of UVSOR-III Light Source

Kenji Hayashi, Taro Konomi, Junichiro Yamazaki and Masahiro Katoh

*UVSOR Facility, Institute for Molecular Science
Myodaiji, Okazaki 444-8585, Japan*

UVSOR-III is a low energy and compact synchrotron light source. The electron energy is 750 MeV and its circumference is 53.2 m. Its relatively low electron energy is suitable to produce synchrotron radiation in longer wavelength region, from terahertz wave to soft X-rays. Fourteen beamlines are operational [1]. UVSOR-III is an inter-university research facility and about 800 visiting researchers carry out investigations related to molecular/material science every year.

The first light was generated in 1983. To meet the increasing demands for brighter light, we made major upgrade twice in 2003 and 2012 and renamed the accelerator UVSOR-II and UVSOR-III, respectively. Now UVSOR-III is routinely operated in the top-up injection mode with the beam current of 300 mA. It is equipped with six undulators. The emittance is about 17 nm-rad. The high beam current, the low emittance and many undulators make this machine one of the brightest among the low energy light sources below 1 GeV.

At UVSOR, resonator free electron laser has been intensively studied from 1980's. Other new light source technologies such as coherent harmonic radiation, coherent synchrotron radiation, laser Compton gamma-rays, are being developed.

In the conference, status of the accelerator and the coherent light source development are presented.

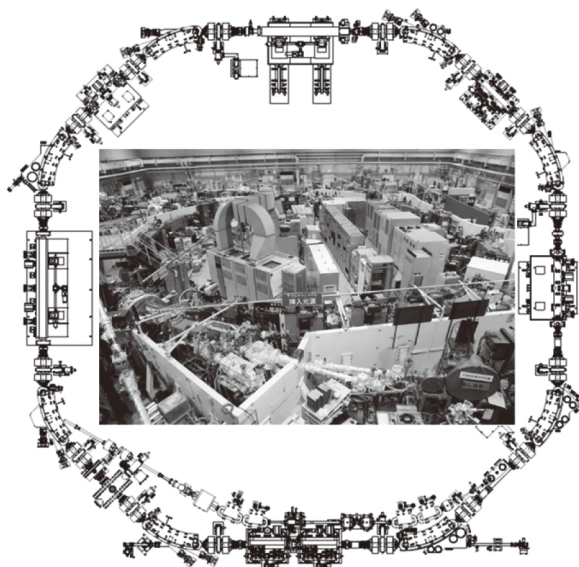


Figure 1. Storage ring of UVSOR-III.

<i>Storage Ring parameter</i>	
Operation Energy	750 MeV
Injection Energy	750 MeV
Beam Current	300 mA
Circumference	53.2 m
No. of Superperiods	4
Straight Sections for I.D.	4 m × 4
	1.5 m × 2
Emittance	16.9 nm-rad
Energy Spread	5.4×10^{-4}
Betatron Tunes	(3.60, 3.20)

Table 1. Parameters of UVSOR-III storage ring.

[1] F. Teshima, this conference.

Present Status of the SPring-8 Storage Ring and Performance Improvements

Accelerator Division

*Japan Synchrotron Radiation Research Institute (JASRI)
1-1-1 Kouto, Sayo-cho, Sayo-gun, Hyogo 679-5198 Japan*

The SPring-8 Storage Ring (SR) provides the high brilliant and stable synchrotron radiation of hard X-ray for the user experiments. The electron beam energy is 8 GeV, the stored current 100 mA, and the natural emittance 2.4 nm.rad. The top-up operation, where the electron beam is frequently injected to the SR during the user experiments, keeps the variation of the stored current within 0.03 %, which is extremely beneficial for the precise user experiments. It is one of the most remarkable characteristics of the SR operation that there are various bunch filling patterns. For the time resolved experiments the several bunch operation modes are arranged according to the user request, e.g. the 203-bunches mode, the mode of 1/7-partially filled multi-bunch with 5 isolated bunches (1/7-filling + 5 bunches), and so on. The impurity of the single bunch is kept in order of 10^{-10} by means of the bunch purifying system at the booster synchrotron.

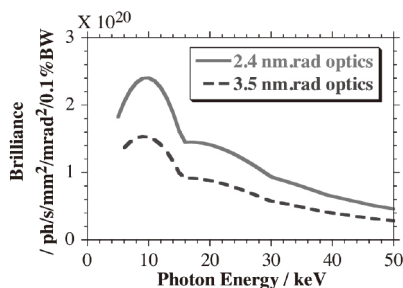


Fig. 1. Brilliance of the SPring-8 standard undulator with 3.2 cm period length and 4.5 m total length.

A new optics with 2.4 nm.rad emittance has been adopted in user operation from May of this year. Until April the emittance had been 3.5 nm.rad, and it is lowered to 2.4 nm.rad by modifying the lattice functions of the SR [1]. The emittance reduction brings the enhancement of the brilliance and the flux density of the synchrotron radiation from undulators by about 30 % as shown in Fig. 1. The operation performance, i.e. the injection efficiency, and the beam lifetime, etc., of the lower emittance optics was not degraded by means of the elaborate machine tuning.

Until November 2012 the maximum

single bunch current in user operation was 3.0 mA for the filling mode of 1/7-filling + 5 bunches. The higher the bunch current becomes, the stronger the beam instability is due to the influence of the electromagnetic field generated by the high current bunch itself. This instability can be suppressed by the bunch-by-bunch feedback system (BBF) [2], and in order to achieve the higher bunch current, the upgrade of the feedback system is essential. By developing the BBF for higher bunch current [3], the new hybrid filling mode of 11/29-partially filled multi-bunch with a 5 mA isolated single bunch is now open to user operation since December 2012. In order to increase the single bunch current up to 10 mA, further improvement of the BBF is in progress.

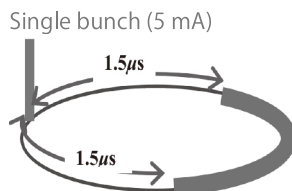


Fig. 2. 11/29-filling + single bunch.

[1] Y. Shimosaki, et al., Proc. of IPAC'13 (2013), 133.

[2] T. Nakamura and K. Kobayashi, Proc. of EPAC'04 (2004), 2649.

[3] K. Kobayashi and T. Nakamura, Proc. of ICALEPCS2009 (2009), 659.

Accelerators of Aichi Synchrotron Radiation Center

Naoto Yamamoto¹, Masahito Hosaka¹, Takumi Takano¹,
Atsushi Mano¹, Yoshifumi Takashima¹, Masahiro Katoh²

1. NUSR, Nagoya University, Chikusa-ku, Nagoya, Japan

2. UVSOR, IMS, Myodaiji-cho, Okazaki, Aichi, Japan

Construction of the Aichi Synchrotron Radiation Center, formerly called Central Japan Synchrotron Radiation Facility, has been completed in the Aichi prefecture of Japan and the user operation was successfully started in March, 2013. The user operation is performed with 300 mA top-up mode on four days in a week.

The key equipments of our accelerators are an 1.2 GeV compact electron storage ring that is able to supply hard X-rays and a full energy injector for top-up operation. The beam current and natural emittance of the storage ring are 300 mA and 53 nmrad. The circumference is 72 m. The magnetic lattice consists of four triple bend cells and four straight sections. The bending magnets at the centers of the cells are 5 T superconducting magnets and the critical energy of the SR is 4.8 keV. The injector consists of a 50 MeV linac and a booster synchrotron with the circumference of 48 m. To save construction expenses, the injector is built at inside of the storage ring. More than ten hard X-ray beam-lines can be constructed. One variable polarization undulator has been also installed.

In this paper, details and present statuses of accelerators of Aichi SR will be reported

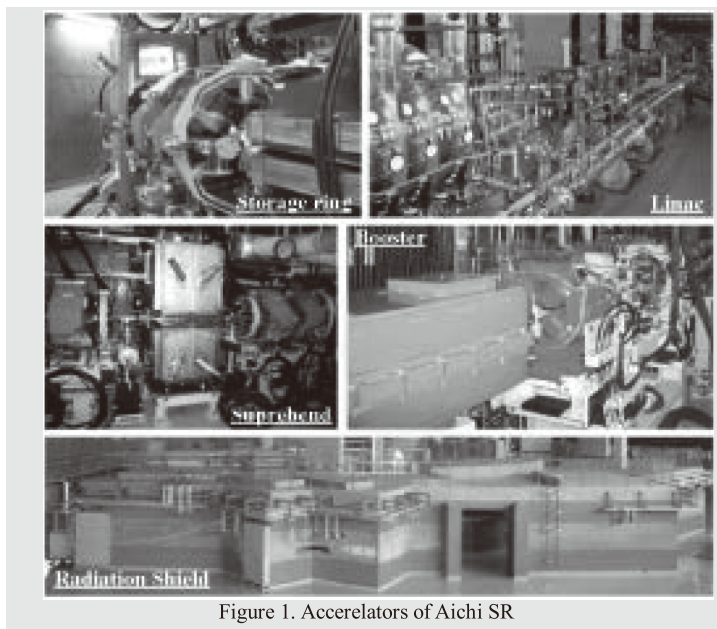


Figure 1. Accelerators of Aichi SR

Chronology of Carriers at Semiconductor Surfaces Studied by Time-Resolved Photoemission Spectroscopy

Susumu Yamamoto and Iwao Matsuda

*Laser and Synchrotron Research Center, the Institute for Solid State Physics,
the University of Tokyo, 5-1-5 Kashiwanoha, Chiba 277-8581, JAPAN*

Photoemission spectroscopy using synchrotron radiation has been the significant experimental method to *probe* electronic structure of semiconductor surfaces *directly*. Recently, we have developed time-resolved photoemission spectroscopy system at synchrotron radiation beamline to *trace* temporal variation of electronic state at semiconductor surface *in real time*[1,2].

Surfaces have been known to play crucial role in relaxation of the surface photovoltage effect (SPV) effect, the basic process in photovoltaics and photocatalysis. On the other hand, surfaces have been also known to change their electronic properties significantly even with submonolayer adsorption of foreign atoms. Thus, it is inferred that relaxation of the SPV effect is highly sensitive to surface characters that can be regulated by surface treatments. In the present research, we have systematically performed time-resolved photoemission experiments to trace the relaxation process *in real time* on various semiconductor surfaces with distinct surface electronic structure, surface disorder, and surface potential. The temporal variation was monitored by the one-pump and multi-probes method using pulses of laser and synchrotron radiation at SPring-8 BL07LSU.

On the metal-covered Si(111) surface system, the time evolution does depend on the surfaces and the relaxation essentially proceeds in two steps, a fast process at the initial stage and the following slow process. The former and the latter can be described in terms of the tunneling and the thermionic relaxation schemes, respectively. The transition between the two mechanisms was found at the certain amount of the surface potential, which likely corresponds to the critical width for the tunneling transport. The crossover can be understood by breakdown of the quantum tunneling regime by the increase in width of the space charge layer during the relaxation.

On the Si(111)7x7 clean surface[3], we discovered that when the power density of the pumping laser is greater than $1000 \mu\text{J cm}^{-2} \text{ pulse}^{-1}$, the relaxation exhibits damped oscillations with temporal periods of several tens of nanoseconds at delay times faster than 100 ns. Observation of the oscillation likely indicates the existence of the nonlinear effect during the surface recombination process that potentially leads to a new technique of ultrafast optical control of photovoltage at a surface.

[1] S. Yamamoto and I. Matsuda, J. Phys. Soc. Jpn. **82**, 021003 (2013).

[2] M. Ogawa, S. Yamamoto, Y. Kousa, F. Nakamura, R. Yukawa, A. Fukushima, A. Harasawa, H. Kondoh, Y. Tanaka, A. Kakizaki, and I. Matsuda, Rev. Sci. Instrum. **83**, 023109 (2012).

[3] M. Ogawa, S. Yamamoto, R. Yukawa, R. Hobara, C.-H. Lin, R.-Y. Liu, S.-J. Tang, and I. Matsuda, Phys. Rev. B **87**, 235308 (2013).



Development of Sub-picosecond Ultrafast X-ray Diffraction and Research of Ultrafast Photoinduced Strain

Bingbing Zhang

Ye Tao

*Beijing Synchrotron Radiation Facility, Institute of High Energy Physics,
19B yuquan Road, Shijingshan District, Beijing*

Ultrafast X-ray diffraction based on laser-driven plasma fs X-ray source[1] has allowed for sub-picosecond laser pump- X-ray probe experiment.(Fig1)

The poster includes salient features of the laser system and X-ray source, as well as some characterized pump-probe experiments based on this instrumentation, including the research of ultrafast lattice dynamics of GaAs single crystal[2] and perovskite superlattices (SRO/STO)[3], which can strongly demonstrate the feasibility to develop sub-picosecond experiments on this system.

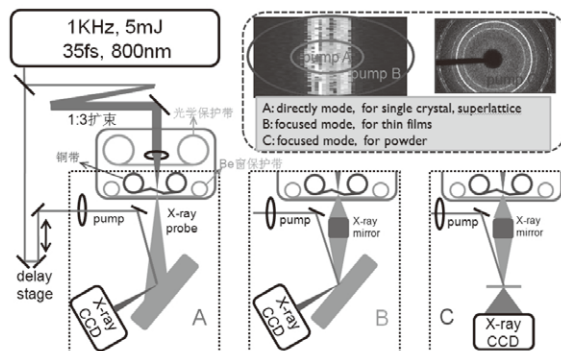


Fig1: The layout of ultrafast XRD system and three different experiment setups, the inset shows the diffraction signals of GaAs single crystal and (NH₄)₂SO₄ powder.

[1] F. Zamponi, Z. Ansari and C. v. Koroff Schmising, Appl. Phys. A 96:51-58(2009),

[2] C.Rose-Petruck, R. Jimenez and T. Guo, Nature, 398(6725), 310-312(1999),

[3] M. Woerner, C.v.Koroff Schmising and M.Bargheer, Appl. Phys. A 96:83-90(2009),



Gelation Mechanism and Hierarchical Structure of P3HT/PCBM in Xylene Solution

Kuei-Yu Kao¹, Shen-Chuan Lo², Hsin-Lung Chen^{1*}, Show-An Chen¹, and Jean-Hong Chen^{3*}

¹Department of Chemical Engineering, National Tsing Hua University, Hsin-Chu 30013, Taiwan

²Material and Chemical Research Laboratories, Industrial Technology Research Institute, Chutung, Hsin-Chu, Taiwan

³Department of Materials Engineering, Kun Shan University, Tainan 71003, Taiwan

Poly(3-hexylthiophene) (P3HT) is one of the most widely used electron donor materials in polymer solar cells. The structure of the polymer formed in the solution may have a drastic impact on the morphology of the subsequently cast film; therefore, investigating the solution structure of conjugated polymers is of great importance for optimizing the performance of the optoelectronic devices. It has been shown that the solutions of P3HT with relatively poor solvents undergo gelation upon prolonged aging at room temperature or under subambient condition. Here we investigate the mechanism of such a gelation process for P3HT/xylene solution and also for the solutions of xylene with P3HT and [6,6]-phenyl-C61-butyric acidmethyl ester (PCBM). A macrophase separation generating P3HT-enriched phase and solvent-rich phase of μm in length scale occurred during the aging. The phase separation took place via the nucleation and growth (NG) mechanism and was followed by the formation of nanowhiskers in the P3HT-enriched domain.¹ The jamming of the P3HT-enriched macrodomains which were mechanically stabilized by the networking of the nanowhiskers led to the gel property of the system. Here we investigate the mechanism of such a gelation process for P3HT/xylene solution and also for the solutions of xylene with P3HT and PCBM (a common acceptor material for polymer solar cell) by means of time-resolved SAXS conducted at beamline BL23A1 in NSRRC.

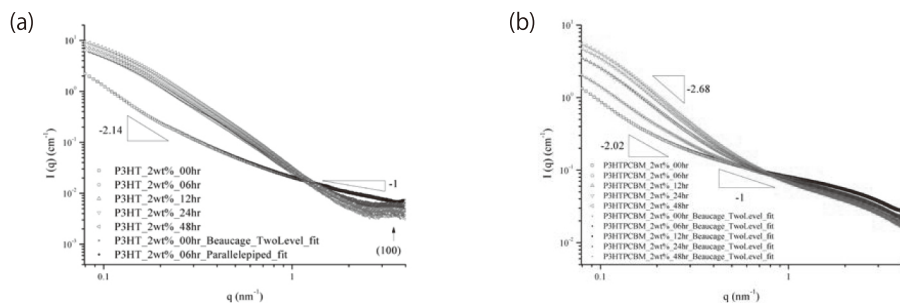


Figure 1 Time-resolved SAXS profile of the P3HT and P3HT/PCBM in xylene solution for monitoring the developments of nanowhiskers and crystallinity of P3HT during the room-temperature aging: (a) P3HT (b) P3HT/PCBM

[1] Chen, C. Y.; Chan, S. H.; Li, J. Y.; Wu, K. H.; Chen, H. L.; Chen, J. H.; Huang, W. Y.; Chen, S. A. *Macromolecules* 2010, 43, 7305–7311

Synchrotron based VUV spectroscopy in gas and matrix isolated phase

Param Jeet Singh, Anuvab Mandal, Vijay Kumar, A. Shastri, B.N. Raja Sekhar, B.N. Jagatap.

*Atomic and Molecular Physics Division, BARC,
Trombay, Mumbai 400 085 India.*

Using indigenously developed beamlines and experimental work stations at Indus-1 (450MeV) synchrotron radiation source, VUV photoabsorption spectroscopy of polyatomic molecules in gas and matrix isolated phases is performed. Issues pertaining to electronic structure, vibrational modes, vibronic interactions, geometries and symmetries of excited states of molecules are clarified using gas phase studies [1]. On the other hand, the matrix isolation spectroscopy technique under cryogenic temperatures in conjunction with a synchrotron source is used to develop understanding of valence or Rydberg character of excited states of isolated molecules in rare gas matrices and molecular processes in astrophysical ices [2]. *ab initio* quantum chemical calculations are used for interpretations of the observed spectra.

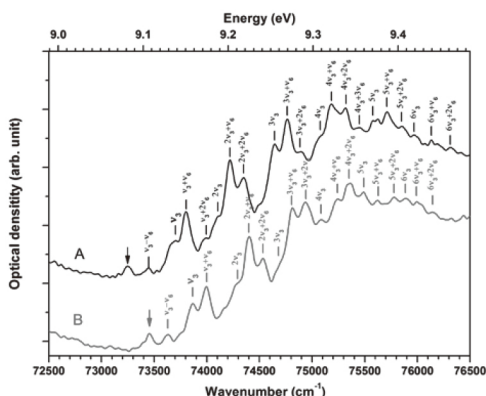


Fig. 1: $1a_2 \rightarrow 4p$ system of CHCl_3 (curve A) and CDCl_3 (curve B). For clarity of presentation, curve A is displaced vertically from curve B.

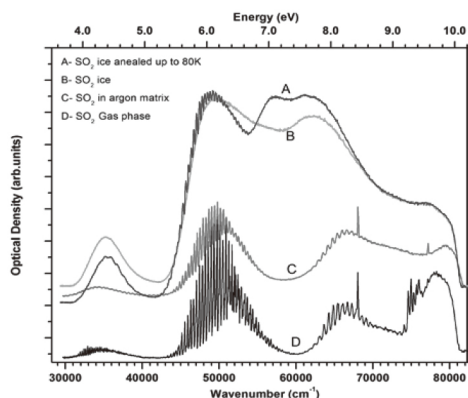


Fig. 2: VUV absorption spectrum of SO₂ in gas phase, isolated in argon matrix and ice phase. Curve D is displayed vertically down from others for clarity.

From analysis of SO₂ spectra, we observed that dominating excitations giving rise to $\tilde{E} - \tilde{\chi}$ system are $\tilde{\chi}^1A_1 \rightarrow 3^1A_1$, 2^1A_1 and 2^1B_1 and the vibrational features are mainly due to excitation of the modes ($\nu_1 + \nu_2$) and ($\nu_2 + \nu_3$) with some contributions from ν_1 and ν_3 . In case of chloroform (Fig.1), vibrational progressions observed in the region of 72,500 – 76,500 cm⁻¹ are reassigned to ν_3 and ($\nu_3 + \nu_6$) belonging to the $1a_2 \rightarrow 4p$ transition in contrast to earlier assignment of ν_3 progression of the $3e \rightarrow 4p$ Rydberg transition. Quantum defect values are found to be consistent with excitation from the chlorine lone pair orbitals. Matrix isolated spectra of SO₂ (Fig.2) in Argon show blue shift for most of observed band systems. Detailed investigations of VUV spectra of the chloroform, SO₂, and acetone will be presented.

- [1] Param Jeet Singh *et. al.* J Quant. Spectrosc. Radiat. Transf. - (a). In Press, Corrected Proof (2013) (b). **114**, 20 (2013); (c). **113**, 1553 (2012); (d) **113**, 267 (2012).
[2] N.J. Mason *et.al.* Faraday Discuss., 133, 311(2006).



Electron Injection Enhancement in OLEDs with Interfacial Chemical Reactions between 8-hydroxyquinolitolithium and Aluminum

Young Mi Lee¹, Yeonjin Yi², Jeong Won Kim³, and Youngsup Park⁴

¹*Soft X-ray Team, Beamline Research Division, Pohang Accelerator Laboratory, Pohang, 790-784, Republic of Korea*

²*Institute of Physics and Applied Physics, Yonsei University, 50 Yonsei-ro, Seodaemun-Gu, Seoul 120-749, Republic of Korea*

³*Korea Research Institute of Standards and Science, Daejeon, 305-340, Republic of Korea*

⁴*Department of Physics, Kyung Hee University, Seoul, 130-701, Republic of Korea*

One of organic electron injection layer materials, 8-hydroxyquinolitolithium (Liq) showed improved device performance and chemical stability as well as a mild preparation process.¹⁻³ Here the interface chemical reaction at the Liq/Al interfaces was investigated by using high resolution synchrotron radiation photoelectron spectroscopy. The different deposition sequence gives different reactions. While strong reactions are observed throughout the Liq film when Al is deposited on Liq layer, an interface localized reaction occurs just at the interface upon the Liq deposition onto Al surface. Either sequence of film stacks, Liq/Al and Al/Liq produce an interface gap state respectively at 2.1 eV and 2.8 eV below the Fermi level. Both of the highest occupied molecular orbital (HOMO) and N 1s core level peaks are shifted to the high binding energy side by 0.35 eV on Al/Liq whereas it is not the case on Al/Liq. Based on these observations, the differences in electron injection barrier and interface dipole between the two opposite deposition sequences could be drawn.

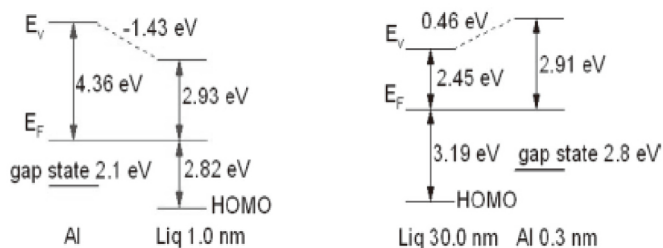


Fig. 1. Energy level alignment diagrams: Liq/Al (blue line) and Al/Liq (black line).

[1] C. Schmitz, H.-W. Schmidt and M. Thelakkat, Chem. Mater. **12**, 3012 (2000).

[2] S. H. Kim, J. Jang, J. Y. Lee, Appl. Phys. Lett. **91**, 103501 (2007).

[3] K. Cho, S. W. Cho, P. E. Jeon, H. Lee, C. Whang, K. Jeong, S. J. Kang, Y. Yi, Appl. Phys. Lett. **92**, 093304 (2008).

Current status of UVSOR beam-lines.

Fumitsuna Teshima

*UVSOR Facility, Institute for Molecular Science
Okazaki, Aichi 444-8585, Japan*

It has been widely recognized that the UVSOR facility is one of the highest brilliance light sources among synchrotron radiation facilities with electron energy less than 1 GeV. In 2012, we made the second major upgrade to the storage ring and started to call it UVSOR-III. It has small emittance around 17 nm-rad and six undulators. It is fully operated in the top-up mode with the beam current of 300mA

There is a total of 14 operational beam-lines, most of which are open to the public use. Six of them are undulator beam-lines and others are bending ones. We have one soft X-ray station equipped with a double-crystal monochromator, seven extreme ultraviolet and soft X-ray stations with a grazing incidence monochromator, three vacuum ultraviolet stations with a normal incidence monochromator, two infrared (IR) stations equipped with Fourier-Transform interferometers. Recently, BL4U has become operational, which is equipped with a scanning transmission soft X-ray microscope (STXM).

I will introduce the current status of the UVSOR beam-lines.

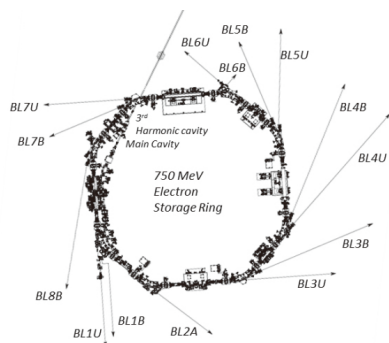


Fig. 1. Layout of the beam-lines in the UVSOR facility

Beamline	Monochromator / Spectrometer	Energy Range	Targets	Techniques
BL1U	Free electron laser	1.6 - 13.9 eV		
BL1B	Martin-Puplett FT-IR	0.5 - 30 meV	Solid	Reflection Absorption
BL2A	Double crystal	585 eV - 4 keV	Solid	Reflection Absorption
BL3U*	Varied-line-spacing plane grating (Monk-Gillieson)	60 - 800 eV	Gas Liquid Solid	Photoemission Photon-emission
BL3B	2.5-m off-plane Eagle	1.7 - 30 eV	Solid	Reflection Absorption
BL4U	Varied-line-spacing plane grating (Monk-Gillieson)	130 - 700 eV	Gas Liquid Solid	Absorption (Microscopy)
BL4B	Varied-line-spacing plane grating (Monk-Gillieson)	25 eV - 1 keV	Gas Solid	Photoionization Photodissociation Photoemission
BL5U	Spherical grating (SGM-TRAIN*)	5 - 250 eV	Solid	Photoemission
BL5B	Plane grating	6 - 600 eV	Solid	Calibration Absorption
BL6U*	Variable-included-angle varied-line-spacing plane grating	30 - 500 eV	Gas Solid	Photoionization Photodissociation Photoemission
BL6B	Michelson FT-IR	3 meV - 2.5 eV	Solid	Reflection Absorption
BL7U	10-m normal incidence (modified Wadsworth)	6 - 40 eV	Solid	Photoemission
BL7B	3-m normal incidence	1.2 - 25 eV	Solid	Reflection Absorption
BL8B	Plane grating	1.9 - 150 eV	Solid	Photoemission

Table 1. List of the beam-lines in the UVSOR facility

A Floor Deformation of SACLA Building

Hiroaki KIMURA

Noriyoshi AZUMI, Jun KIUCHI, Tomoya KAI, Sakuo MATSUI

RIKEN SPring-8 Center, 1-1-1, Kouto, Sayo-cyo, Hyogo 679-5148, Japan

JASRI, 1-1-1, Kouto, Sayo-cyo, Hyogo 679-5198, Japan

Generally, it is known that SPring-8 site is located on the very good ground, which is very stable and rigid bedrock. In contrast, the area of SACLA building is not rigid enough. Figure 1(a) shows schematic cross-section view of understructure of SACLA building and geological layers. The figure shows that the bedrock area (cutting area) is only 1/5 of the building and 4/5 of the building is located on the overlapping area. The maximum thickness of embankment is over 50 m.

The SACLA building consists of a light source building and an accelerator building. The light source building, where undulator section is installed, requires to being stable especially. For this building, a direct foundation on the bedrock and an artificial layer replaced with crusher stone were adopted for this building. The maximum thickness of that is 18 m. A civil engineering designer anticipated that its subsidence is less than 2 mm/10 years. On the other hand, for the accelerator building, pillar foundation was adopted. Total number of the pillar is 136, their diameters are 1.5 m, and maximum of their length is 52 m. The designer anticipated that its subsidence is 15 mm/ 10 years at 52 m pillar.

The building was completed at March 2009. From construction phase of the building, the deformation of the floor is being measured. Figure 1(b) shows history of floor subsidence from August 2008. Recent maximum subsidence is 1 mm/year. This value is within the prediction. The shape of the subsidence data is very similar to that of embankment. Then subsidence is proportional to the thickness of embankment, not to the length of pillar.

We will present the data of vertical and horizontal deformation of the floor and show a relationship between the deformation and the structure of SACLA building.

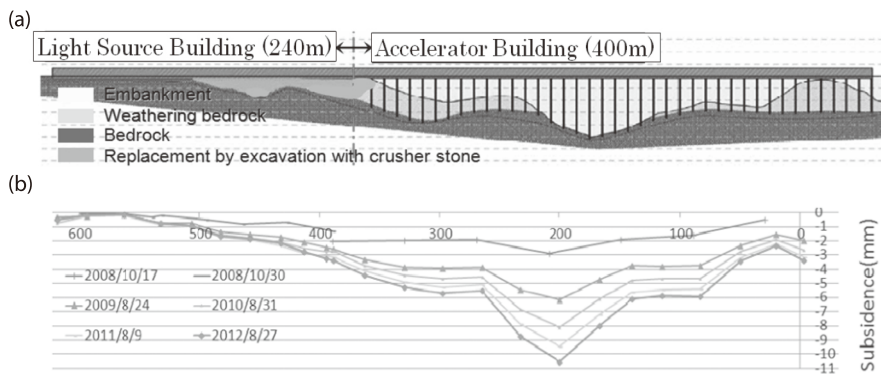


Figure 1: (a) Schematic view of understructure of SACLA building and geological layers.
(b) History of subsidence of the floor from August 2008.



Optical design of an undulator based ARPES beamline on Indus-2

Kiran Baraik, Soma Banik, Tapas Ganguli, G.S. Lodha, S. K. Deb

Indus Synchrotron Utilization Division, Raja Ramanna Centre for Advance Technology, Indore-452013

The design of an undulator based Angle Resolved Photoelectron Spectroscopy (ARPES) beamline is presented here, which is proposed to be installed in Indus-2 (2.5 GeV, 300 mA) synchrotron radiation source. The undulator proposed for this beamline is a planer Pure Permanent Magnet (PPM) type undulator which has 23 periods and a period length of 93 mm. The ARPES experimental station is proposed to have a five axis sample manipulator with sample temperature down to $\sim 30\text{K}$. The beamline is designed to cover the energy range of 30-1000 eV and is expected to give resolving power of about 12000-3000 for the energy range with moderated flux. It consists of three types of optical elements: two toroidal mirrors, two spherical mirrors, four Varied Line Spacing Plane Gratings (VLS-PG). The two toroidal mirrors have been used as pre and post focusing mirrors. In the monochromator section spherical mirror and VLS-PG are mounted in Monk-Gillieson configuration [1]. In order to

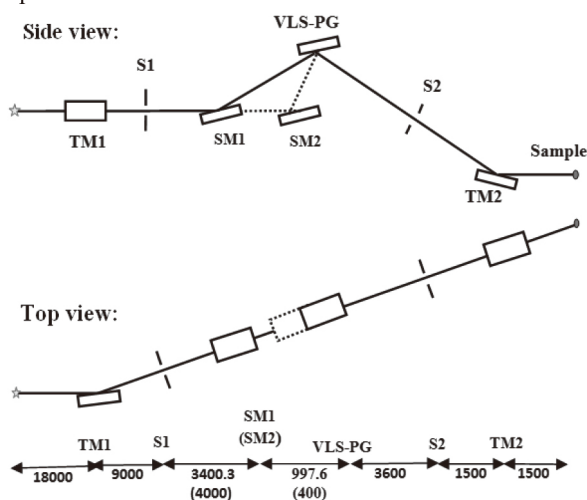


Fig. 1. Optical layout of the beamline

cover the energy range of interest, two interchangeable spherical mirrors and four interchangeable VLS-PGs have been used in the monochromator section. The VLS-PGM operates in two constant included angle configurations to cover two photon energy ranges of 30-270 eV and 215-1000 eV. The output beam from last optical element of the beamline is horizontal at a height of $\sim 1100\text{ mm}$ so as to be compatible to the proposed experimental station. The overall performance of the beamline has been evaluated by carrying out ray tracing simulation with SHADOWvui [2]. SPECTRA [3] has been used to study the characteristics of the undulator radiation and to determine the size of an aperture at a distance of 10 m from the centre of the undulator. The ultimate resolution and photon flux at 30 eV from ray tracing simulation are 5 meV and 2.5×10^{12} photons/s/0.1 % BW, respectively, with the spot size (FWHM) of $\sim 300\text{ }\mu\text{m}$ (H) $\times 110\text{ }\mu\text{m}$ (V) at the sample.

[1] K. Amemiya et al., Journal of Synchrotron Radiation, **3**,282-288, (1996)

[2] F. Cerrina et al., SHADOWvui, Centre for X-ray Lithography, University of Wisconsin

[3] T. Tanaka and H. Kitamura, Journal of Synchrotron Radiation **8**, 1221, (2001)

Low-cost, high-performance electrocatalysts for polymer electrolyte membrane fuel cells

Kug-Seung Lee

Pohang Accelerator Laboratory, Pohang, 790-784, Republic of Korea

Pt-based electrocatalysts offer good performance when applied to low-temperature fuel cells, including polymer electrolyte membrane fuel cells (PEMFCs) and direct methanol fuel cells (DMFCs). However, the use of Pt makes these fuel cells expensive to produce. Many attempts have been made to reduce the amount of Pt used in fuel cell electrodes. One method involving the alloying Pt with transition metals has been extensively studied with the objective of enhancing electrocatalytic activity and reducing the Pt content in catalysts. Such alloying methods, however, have not satisfactorily reduced the Pt loading. Reports on the use of non-noble catalysts such as transition metal chalcogenides, oxides, and macrocycles as alternatives to Pt have shown that their electrocatalytic activities are much lower than Pt. The surface modification of metal nanoparticles has been suggested to be a promising candidate for minimizing the amount of Pt used and such modification has been realized by the formation of core/shell structures using chemical, electrochemical, and surface-segregation methods. In this presentation, syntheses of core/shell structured catalysts formed by using chemical and surface-segregation methods and their electrochemical activities will be covered. Au or Ir elements have been used as core materials while Pt or Pt alloys have been used as shell materials.

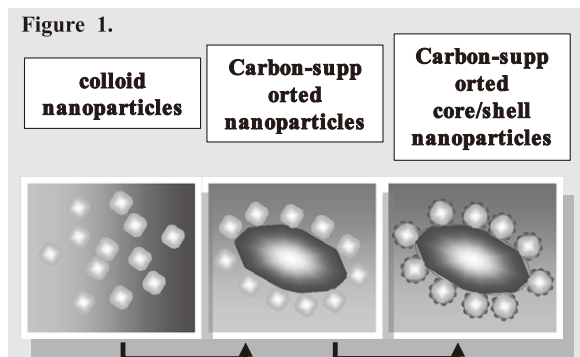


Fig. 1. A simple description of chemical reduction procedure for the formation of the core/shell structure.

A chemical reduction method that has been used for the formation of the core/shell structure is described in Figure 1.

- [1] K.-S. Lee, I.-S. Park, H.-Y. Park, T.-Y. Jeon, Y.-H. Cho, Y.-E. Sung, *J. Electrochem.Soc.* **156**(10), B1150 (2009).
- [2] K.-S. Lee, I.-S. Park, H.-Y. Park, T.-Y. Jeon, Y.-E. Sung, *Catal. Today* **146**(1-2), 20 (2009).
- [3] K.-S. Lee, S. J. Yoo, D. Ahn, T.-Y. Jeon, K. H. Choi, I.-S. Park, Y.-E. Sung, *Langmuir* **27**(6), 3128 (2011).
- [4] K.-S. Lee, Y.-H. Cho, T.-Y. Jeon, S. J. Yoo, H.-Y. Park, J. H. Jang, Y.-E. Sung, *ACS Catalysis*, **2**(5), 739 (2012).
- [5] K.-S. Lee, H.-Y. Park, H. C. Ham, S. J. Yoo, H. J. Kim, E. Cho, A. Manthiram, J. H. Jang, *J. Phys. Chem C* **117**, 9164 (2013)



Capacitive coupled RF discharge plasma for cleaning of carbon contaminated Optics

P. K Yadav¹, M. Kumar², J. A. Chakera², S. K. Rai¹, P. A. Naik², G. S. Lodha¹

¹*X ray Optics Section, Indus Synchrotrons Utilization Division*
²*Laser Plasma Laboratory, Laser Plasma Division*

Raja Ramanna Centre for Advanced Technology, Indore 452 013, M.P., India

The deposition of carbon layer on optics surfaces due to prolonged use in synchrotron light sources and lasers is a severe problem that reduces the efficiency of the optics dramatically. Low pressure plasma glow discharge has been considered as a cost effective way in the optics cleaning compared to recoating the surfaces. A capacitively coupled RF glow discharge plasma based optics cleaning setup is installed and optimized for carbon contamination removal rate from optics surfaces by varying process parameters like feed power, process gas pressure and exposure time. The removal rate of deposited carbon coating is estimated using x-ray reflectivity measurements (XRR). At low feed power (10 watts) carbon removal rate about 0.6 nm/min at 0.04 mbar argon pressure is observed. The over exposure of optics to plasma damage the reflecting surfaces also. Some optics used in laser applications such as VLS, Compressive Optics and Off Axis Parabola Mirror also cleaned by this system. The integrated reflectivity of these optics is regained from 60% to 95% of the fresh optics. Uncleaned and cleaned VLS grating shown in fig-1. Experimental and theoretical curve of reflectivity for Carbon capped Mo film treated and untreated by RF plasma is shown in fig. 2.



Fig. 1. Integrated reflectivity of compressive grating reduces to 65% at $(800 \pm 10 \text{ nm})$ due to contamination (left). After cleaning at 10 watts and 0.04 mbar Ar pressure integrated reflectivity improve up-to 95% (Right). Reflectivity is measured by calorimetric technique.

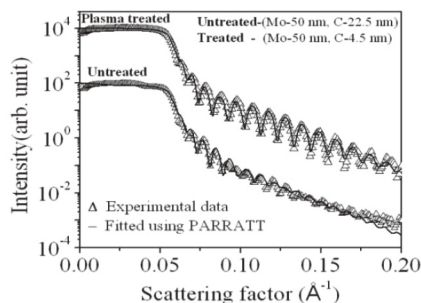


Fig. 2. An experimental and theoretical fitted curve of the samples treated and untreated by RF plasma.



Fabrication of OSAKA MIRROR for Synchrotron Application

Shota Matsuyama

JTEC Corporation (Japan)

*Research Center: Saito Bio-Incubator 7-7-15 Saito-Asagi,
Ibaraki-shi Osaka JAPAN*

Email: shota.matsuyama@j-tec.co.jp

At JTEC Corporation we have been fabricating OSAKA MIRROR using EEM, nano-fabrication, and RADSI and MSI, nano-measurement, of Osaka University. We will explain our production technology, our potentiality and the mirrors we have delivered. For your further understanding of OSAKA MIRROR, we'll show our procedure from design process to fabrication and necessary points. In addition, we report on the development of our production technology and the recent delivery.



MeV-Ion Beam Analysis of Atomic Layer-Deposition Ultra-Thin Oxide Films

Teerasak Kamwanna^{1,2}, Anumust Deachana³, Liangdeng Yu⁴, Dheerawan Boonyawan^{4,5}, Paul K Chu⁶, Somsorn Singkarat^{4,5}

¹*Integrated Nanotechnology Research Center, Khon Kaen University, Khon Kaen 40002, Thailand.*

²*Department of Physics, Faculty of Science, Khon Kaen University, Khon Kaen 40002, Thailand.*

³*Physics and General Science, Faculty of Science and Technology, Songkhla Rajabhat University, Songkhla 90000, Thailand.*

⁴*Thailand Center of Excellence in Physics, Commission on Higher Education, 328 Si Ayutthaya Road, Bangkok 10400, Thailand.*

⁵*Plasma and Beam Physics Research Facility, Department of Physics and Materials Science, Faculty of Science, Chiang Mai University, Chiang Mai 50200, Thailand.*

⁶*Plasma Laboratory, Department of Applied Physics, City University of Hong Kong, Tat Chee Avenue, Kowloon, Hong Kong, China.*

Ultra-thin aluminum oxide (Al_2O_3) film is currently being explored as a high dielectric constant gate dielectric for the next generation CMOS and related devices. Among many methods to produce such a film, atomic layer deposition (ALD) is a very attractive technique in the sense that it enables deposition of ultra-thin layers on the substrate with monolayer control. In this work, the Al_2O_3 film was deposited using ALD technique on a single crystalline silicon (100) substrate with a plasma grown silicon dioxide (SiO_2) layer sandwiched in between as a buffer interface. The total oxide layered structure was characterized by Rutherford backscattering spectrometry (RBS) in the channeling mode with MeV He^{2+} -ions as the analyzing probe. The RBS/channeling analysis detects O, Al and Si atoms in the ultra-thin oxide layers with clear separation from their Si substrate. Our evaluation was compared with results obtained by other standard technique, such as x-ray photoelectron spectroscopy (XPS).

Corresponding author. E-mail: teekam@kku.ac.th

STUDIES OF PHOTONUCLEAR REACTIONS INDUCED BY BREMSSTRAHLUNGS WITH END-POINT ENERGIES ABOVE THE DIPOLE RESONANCE REGION

Kim Tien Thanh

*Institute of Physics, Vietnam Academy of Science and Technology
No. 10, Daotian, Thule, Badinh, Hanoi.*

Abstract Nuclear reactions have become powerful tools for studying properties and characteristics of nuclei. The use of different particles, for example, proton, neutron, gamma and so on as projectiles was able to determine a series of general properties of nuclei as well as parameters of their levels and nuclear reaction mechanism involved. The study of nuclear reactions at bremsstrahlung photon beams has definite advantages. In this work we would like to present the results of our study of photonuclear reactions induced by bremsstrahlung with end-point energies above the giant dipole resonance region, namely:

- Study of the isomeric ratios in photonuclear reactions induced by bremsstrahlungs with end-point energies above the dipole resonance region /1,2,6-8/.
- Study of photonuclear reactions with multiparticle emission induced by 2.5 GeV bremsstrahlung /3-6/.

The studies have been carried out at the linear electron accelerators and the synchrotron of Pohang accelerator center, Pohang University of Science and Technology (POSTECH), Pohang, South Korea.

References

- [1]. Van Do Nguyen, Duc Khue Pham, Tien Thanh Kim, Duc Thiep Tran, Van Duan Phung, Young Seok Lee, Guinyun Kim, Youngdo Oh, Hee-Seock Lee, Hengsik Kang, Moo-Hyun Cho, In Soo Ko and Won Namkung, Journal of the Korean Physical Society, 50 (2007) 417-425.
- [2]. Nguyen Van Do, Pham Duc Khue, Kim Tien Thanh, Bui Van Loat, Guinyun Kim, Youngdo Oh, Hee-Seock Lee and Won Namkung, Communications in Physics, Vol. 18, No. 4 (2008) 240-249.
- [3]. Nguyen Van Do, Pham Duc Khue, Kim Tien Thanh, Le Truong Son, Md. Shakilur Rahman, Kyung-Sook Kim, Manwoo Lee, Guinyun Kim, Youngdo Oh, Hee-Seock Lee, Moo-Huyn Cho, In Soo Ko, Won Namkung, Nucl. Instr. and Meth. B 266(2008)5080-5086.
- [4]. Kim Tien Thanh, Pham Duc Khue and Nguyen Van Do, Communications in Physics, Vol.19, Special Issue (2009), pp. 167-175
- [5]. Nguyen Van Do, Pham Duc Khue, Kim Tien Thanh, Nguyen Thi Thanh Van, Communications in Physics, Vol.19, Special Issue (2009), pp. 177-187
- [6]. Van Do Nguyen, Duc Khue Pham, Tien Thanh Kim, Md. Shakilur Radman, Kyung-Sook Kim, Guinyun Kim, Hee-Seock Lee, Moo-Hyun Cho, In Soo Ko, Won Namkung, Tae-Ik Ro, J Radioanal Nucl Chem Vol. 283 (2010) 683-690.
- [7]. Nguyen Van Do, Pham Duc Khue, Kim Tien Thanh, Tran Hoai Nam, Md. Shakilur Rahman, Kyung-Sook Kim, Manwoo Lee, Guinyun Kim, Hee-Seock Lee, Moo-Huyn Choo, In Soo Ko, Won Namkung, J Radioanal Nucl Chem Vol. 287 (2011) 813-820.
- [8]. Nguyen Van Do, Pham Duc Khue, Kim Tien Thanh, Guinyun Kim, Manwoo Lee, Kyung-Sook Kim, Sun-Chul Yang, Eunae Kim, Moo-Huyn Cho, Won Namkung, Nucl. Instr. and Meth. B 283(2012)40-45.

Monitoring Arsenic in Particulate Matter

Travis Ancelet, Perry Davy, Bill Trompetter, Andreas Markwitz

GNS Science, 30 Gracefield Road, PO Box 31312, Lower Hutt 5040, New Zealand

GNS Science has applied ion beam analysis techniques for the determination of elemental concentrations in air particulate matter for a number of years in an effort to understand and better inform regulatory authorities of the sources contributing to particulate matter pollution [1]. A surprising result from a number of studies around New Zealand was that arsenic concentrations increased significantly during the winter, likely as a result of the combustion of copper chrome arsenate-treated timber. Unfortunately, the filters typically used for particle collection produce a poor limit of detection ($20\text{--}30\text{ ng m}^{-3}$) for arsenic, making it difficult to accurately quantify arsenic concentrations and use arsenic in receptor models for source apportionment purposes. The use of thinner filters and different filter materials results in a significant improvement in the limit of detection for arsenic. In this work we present an overview of the experimental beam-line setup and provide examples of research results from various polluted urban locations where different filters have been employed.

[1] W. J. Trompetter, A. Markwitz and P. K. Davy, Int. J. PIXE **15**, 249 (2005).

Metal sulfides-catalyzed hydrodeoxygenation of phenol and triglycerides

Vorranutch Itthibenchapong

Pongtanawat Khemthong, Kajornsak Faungnawakij

Nanomaterials for Energy and Catalysis Laboratory,

National Nanotechnology Center (NANOTEC),

National Science and Technology Development Agency (NSTDA)

*111 Thailand Science Park, Phahonyothin Road, Khlong Nueng, Khlong Luang,
Pathum Thani 12120, Thailand*

As high demands of alternative fuels due to the scarcity of fossil fuels, biofuels e.g. biodiesel, biooil, biogas have been employed over 10 years through the conversion of biomass [1] by suitable catalytic reactions. Among of them, hydrodeoxygenation (HDO) has been used in various applications such as biomass upgrading into valuable chemicals, biodiesel quality improvement, and bio-hydrotreated diesel (BHD) production. HDO catalysts involve with metal, metal oxides, and metal sulfides on supports e.g. γ - Al_2O_3 , SiO_2 , graphite. Co, Ni, Cu, Mo, and their oxides or sulfides are conventional catalysts aside from noble metals e.g. Pt, Pd, Ru, Rh.

Metal sulfide catalysts for HDO reaction are typically synthesized through the sulfurization with H_2S . However, H_2S is a severely toxic gas and high cost in comparison to other industrial gases, thus special equipment and handling are necessary. Therefore, the use of low cost and water-soluble sulfiding agent provides some advantages such as encouraging sulfurization with metal salt solution, simple scaling up, and lower cost production. Moreover, the presulfurization is not required when performing continuous reactor system. In our work, we used thiourea ($\text{CS}(\text{NH}_2)_2$) as the sulfur source to prepare unsupported MoS_2 , $\text{MoS}_2/\gamma\text{-Al}_2\text{O}_3$, unsupported sulfided NiMo, and sulfided NiMo/ $\gamma\text{-Al}_2\text{O}_3$. The synthesis approach required low temperature in a range of 250-500 °C in air. The higher purity and crystallinity of samples could be achieved if the calcination was performed at higher 350 °C under inert or vacuum atmosphere. As-synthesized catalysts were characterized by XRD, FT-IR, SEM, and N_2 adsorption-desorption. The catalytic activities have been studied on 2 reactants. The HDO of phenol, a model compound of lignin, leads to cyclohexane as the final product, while palm oil (triglycerides) as the reactant yields long chain C15-C18 alkanes (BHD).

Structural details of as-synthesized catalysts, i.e. local structure of metal cations, active sites, have been planned to study by XAS at the Synchrotron Light Research Institute (Public Organization), Thailand. The data fitting to model structures will be performed on Athena and Artemis [2]. Besides the metal sulfides, nanostructured copper phosphates have been developed for potential catalysts in HDO process, and analyzed by XAFS spectroscopy [3]. We expect the better understanding of physical, chemical and catalytic properties of MoS_2 and sulfided NiMo system along with other related catalysts on HDO reaction to design, optimize, and develop novel catalysts for HDO and related reactions in the future works.

[1] D. M. Alonso, S. G. Wettstein, J. A. Dumesic, Chem. Soc. Rev. **41**, 8075 (2012).

[2] B. Ravel, M. Newville, J. Synchrotron Rad. **12**, 537 (2005).

[3] P. Khemthong, P. Daorattanachai, N. Laosiripojana, K. Faungnawakij, Catal Commun. **29**, 96 (2012).

EXHIBITORS/
EXHIBIT & POSTER FLOOR PLAN

7th Asia Oceania Forum for Synchrotron Radiation Research (AOFSSRR 2013) Vendor Exhibition

Date & Time: September 22nd (Sunday), 2013, 9:30 – 17:00

Venue: Egret Himeji B1 Exhibition Gallery

Booth	Company Name / Address / Contact Person	Exhibit Items
1	PMAC-Japan Co., Ltd. http://www.pmac-japan.co.jp/ 1-8-3 Ningyo-cho, Nihombashi, Chuo-ku, Tokyo 103-0013, Japan <u>Junji TACHIBANA</u> / Director / Sales Department Phone: (81) 3-3665-6421 Fax: (81) 3-3665-6888	<1-axis slider demonstration unit> · Brick Controller (Motion controller) · Stepper motor · Absolute linear scale <Motion Controller> · Geo Brick-LV NSLS-II
2	Niki Glass Co., Ltd. http://www.nikiglass.co.jp/ 3-9-7 Mita, Minato-ku, Tokyo 108-0073, Japan <u>Masanori YAMADA</u> / Tokyo Branch Phone: (81) 3-3456-4700 Fax: (81) 3-3456-3423	· Panel · MCA · Goniometerhead
3	Rigaku Corporation http://www.rigaku.co.jp/ 3-9-12 Matsubara-cho, Akishima, Tokyo 196-8666, Japan <u>Masataka AOKI</u> / Manager / Marketing & Communications Phone: (81) 42-545-8111 Fax: (81) 42-544-9795	· Poster: High speed x-ray detector · Poster: X-ray diffraction related products
4	MELEC Incorporated http://www.melec-inc.com 516-10, Higashiasakawa-machi, Hachioji, Tokyo 193-0834, Japan <u>Ryuichi NAGAI</u> / Manager / Control Equipment Sales Dept. Phone: (81) 42-664-5384 Fax: (81) 42-666-5664	· 2-Axis 5phase Stepping Motor Driver · 2-Axis Motion Contoller and Driver · Cable between a driver and the motor · Shelf board for exclusive use of the driver

Booth	Company Name / Address / Contact Person	Exhibit Items
5	JTEC Corporation http://www.j-tec.co.jp SaitoBio-Incubator7-7-15 Saito-Asagi, Ibaraki, Osaka 567-0085, Japan <u>Megumi KIYOMOTO</u> Phone: (81) 72-643-2292 Fax: (81) 72-643-2391	<ul style="list-style-type: none"> · X-ray focusing system: JM1000 · X-ray mirrors
6	NEOMAX ENGINEERING Co., Ltd. http://www.nxe.co.jp/ Seavance North 1-2-1 Shibaura, Minato-ku, Tokyo 105-8614, Japan <u>Masanobu FUJISAWA</u> / Manager / Sales Dept. Phone: (81) 3-5765-4250 Fax: (81) 3-5765-4457	<ul style="list-style-type: none"> · 3 posters about undulators
7	TOYAMA Co., Ltd. http://www.toyama-en.com/ 4-13-16, Hibarigaoka, Zama, Kanagawa 252-0003, Japan <u>Hisataka TAKENAKA</u> / Manager / X-ray optical system TF Phone: (81) 46-253-1411 Fax: (81) 46-253-1412	<ul style="list-style-type: none"> · Catalogues <ol style="list-style-type: none"> 1) An Introduction to TOYAMA 2) VLSPGM Monochromator 3) Beamline components for XFEL 4) Real-time Multi-component Mass Spectrometer 5) XY-Manipulator · 2 Posters
8	Candox Systems, Inc. http://www.candox.co.jp/ 15-21, Oshiage-cho, Gyoda, Saitama 361-0045, Japan <u>Shigeo YAGAMI</u> / Sales Manager / Sales Dept. Phone: (81) 48-564-0500 Fax: (81) 48-564-0501 NIPPON SOKKI CO., LTD. http://www.nippon-sokki.co.jp/ Center Bldg, 2723 Kitazaike, Kakogawa-cho, Kakogawa, Hyogo 675-0031, Japan <u>Kazunori SHIMIZU</u> / Chief Phone: (81) 79-425-7111 Fax: (81) 79-425-7119	<ul style="list-style-type: none"> · Trigger & Clock Delay Module Model: 84DgR5C01 · ADVANTEST Cross Domain Analyzer · Tektronix Mixed Domain Oscilloscope



direction of castle



Poster Presentation & Vendor Exhibition

Date: September 22nd (Sunday), 2013

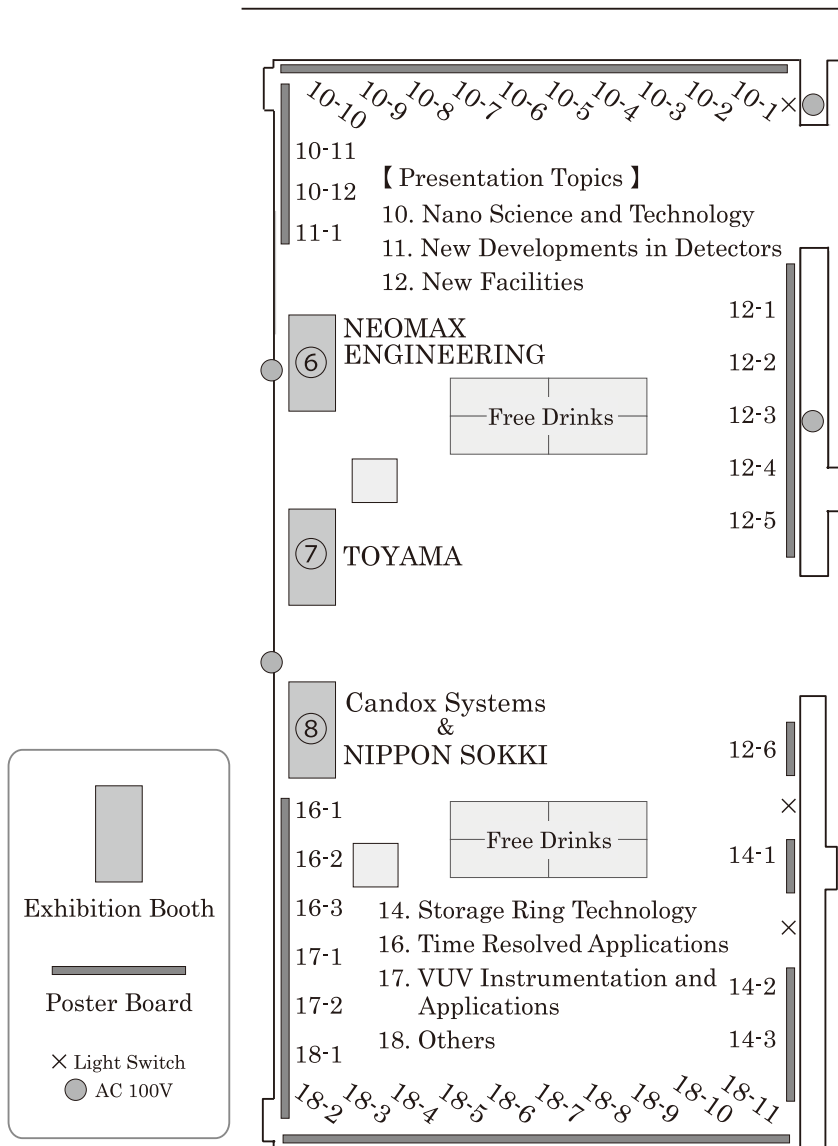
Poster Presentation: 12:30 - 16:00 / Vendor Exhibition: 9:30 - 17:00

Venue: Egret Himeji B1 Exhibition Gallery

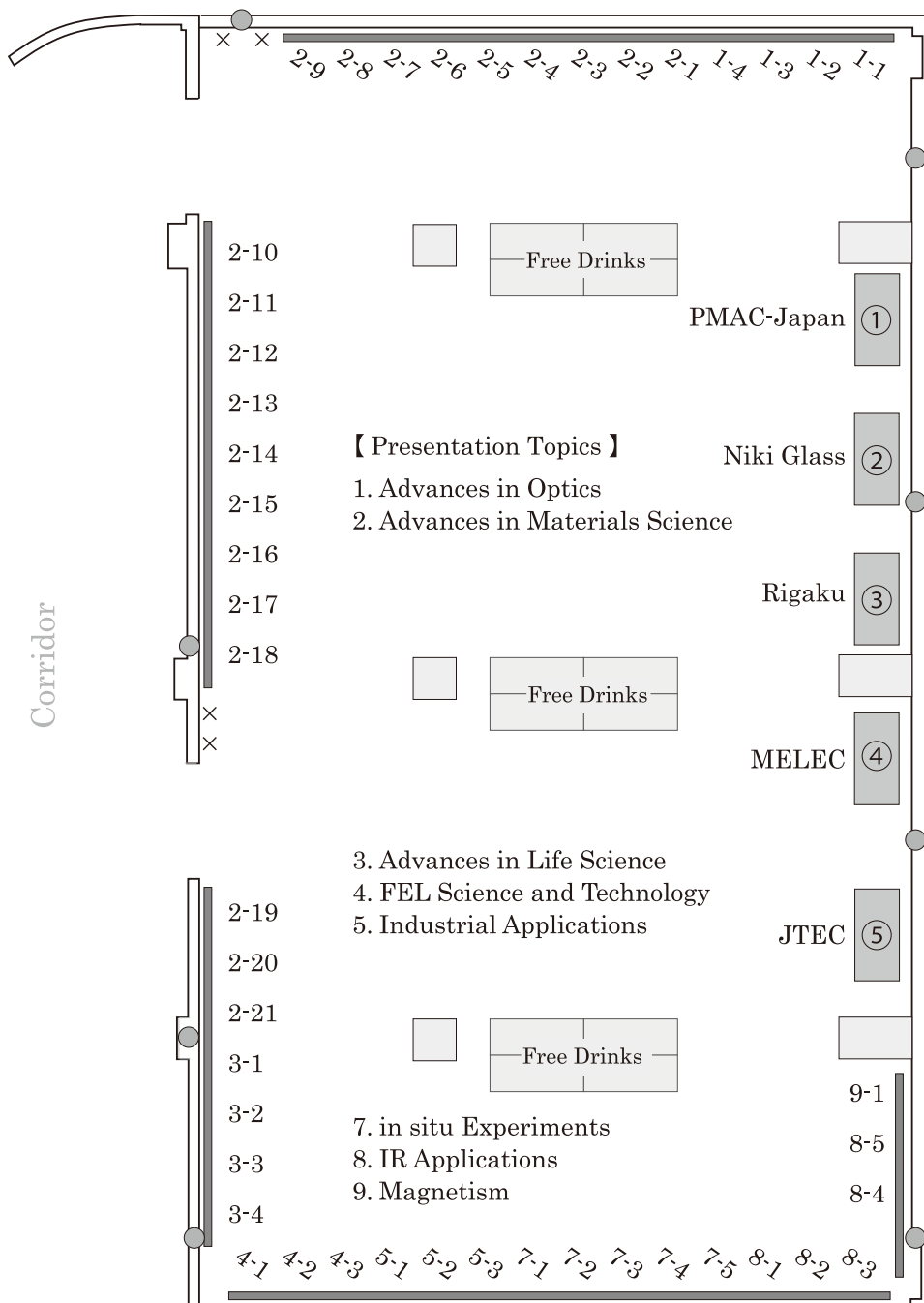
Basement Lobby



Corridor



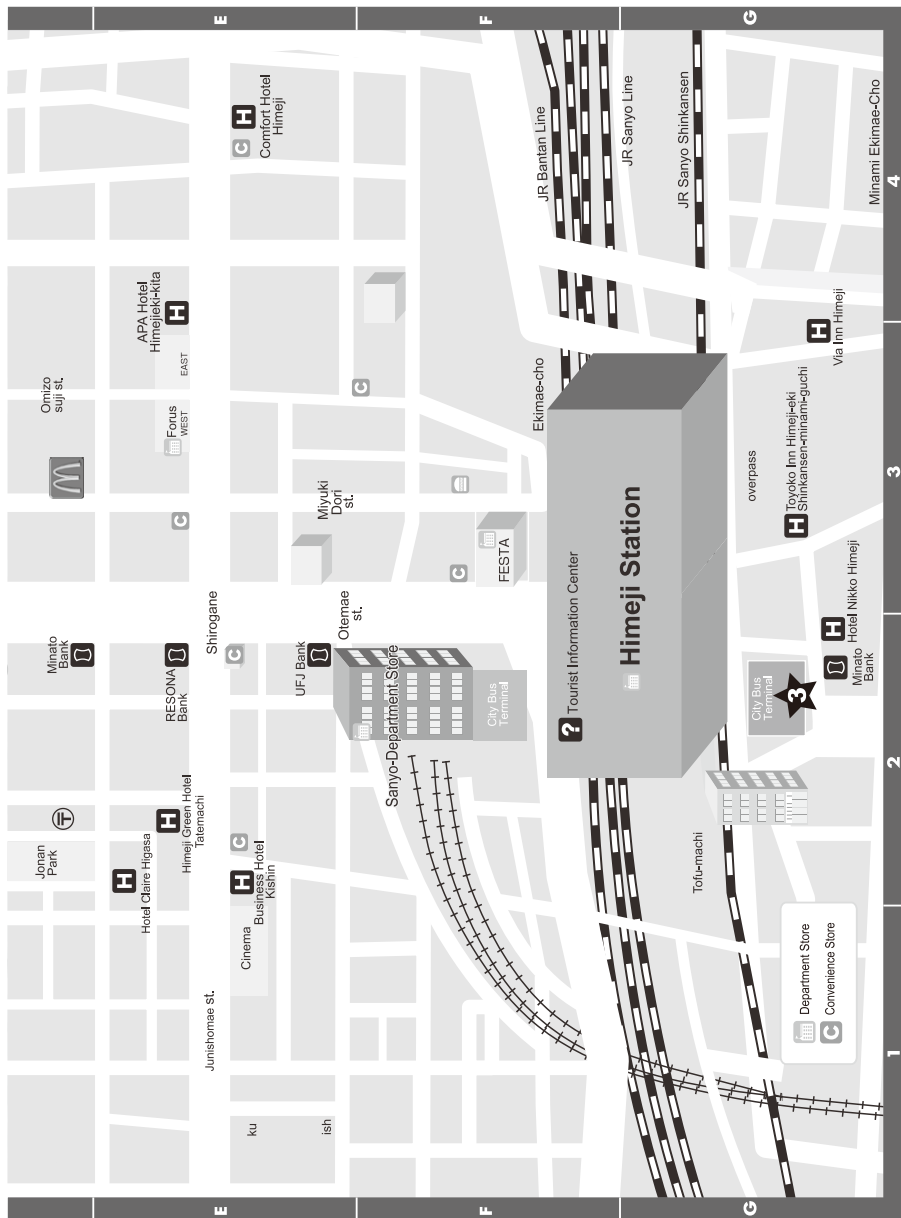
Poster Presentation & Vendor Exhibition



INFORMATION

MAP





- ★ Conference Venue: Egret Himeji
- ★ Welcome Party Venue: Koukoen
- ★ Location to gather for SPring-8/SACLA Site Tour

PHOTON IS OUR BUSINESS

60th
Anniversary

60th
Anniversary Celebrating 60 Years in Photonics



PHOTON FAIR 2013

60th Anniversary

60th anniversary
HAMAMATSU PHOTONICS K.K.
Exhibition

2013. 11/7-8-9

VENUE : ACT CITY HAMAMATSU

Leading with Light: From Hamamatsu to the World

In celebration of our 60 years in photonics, Hamamatsu Photonics K.K. will host the PHOTON FAIR 2013 exhibition in Hamamatsu City, Japan. We will present our latest technology as well as our concepts for future development, which we expect will contribute to many fields including industry, academic research, and medicine.

www.photonfair.jp/en/

HAMAMATSU PHOTONICS K.K.

325-6, Sunayama-cho, Naka-ku, Hamamatsu City, Shizuoka Pref., 430-8587, Japan
Phone:(81)53-452-2141 Fax:(81)53-456-7889 **www.hamamatsu.com**



Himeji Convention & Visitors Bureau
Tsutomu Nakauchi Foundation